DYNAMIC VARIATIONAL ASYMPTOTIC PROCEDURE FOR LAMINATED COMPOSITE SHELLS

A Thesis
Presented to
The Academic Faculty

by

Chang-Yong Lee

In Partial Fulfillment
of the Requirements for the Degree
Doctor of Philosophy in the
School of Aerospace Engineering

Georgia Institute of Technology
August 2007

DYNAMIC VARIATIONAL ASYMPTOTIC PROCEDURE FOR LAMINATED COMPOSITE SHELLS

Approved by:

Professor Dewey H. Hodges, Advisor
School of Aerospace Engineering
Georgia Institute of Technology

Professor Olivier A. Bauchau
School of Aerospace Engineering
Georgia Institute of Technology

Professor Donald W. White
School of Civil and Environmental Engineering
Georgia Institute of Technology

Professor Massimo Ruzzene
School of Aerospace Engineering
Georgia Institute of Technology

Professor Vitali V. Volovoi
School of Aerospace Engineering
Georgia Institute of Technology

Date Approved: 21 June 2007

To

My father Jeom-Dong Lee

My mother Ok-Ja Ha

ACKNOWLEDGEMENTS

I would like to express my deep appreciation to Dr. Dewey H. Hodges, my advisor, for his invaluable guidance and deep consideration throughout this work. His remarkable personal conduct and professional ethic will serve as great examples in my own life.

I would also like to thank the other members of my thesis advisory committee, Drs. Olivier A. Bauchau, Massimo Ruzzene and Vitali V. Volovoi for their valuable suggestions about key research points. In addition, I thank Dr. Donald W. White for serving on my thesis reading committee.

Special thanks go to Dr. Victor L. Berdichevksy for allowing me an opportunity to look at his book before its publication to better understand the details of variational methods.

I am specially indebted to Drs. Yong-Soo Pyo and Seon-Jin Kim for their unreserved encouragement and endless concern during the graduate study.

Thank to Dr. Seung Oh Lee and Mr. Samer A. Tawfik for their friendship to share their knowledge and time in enlightening discussion during the graduate study.

I am greatly grateful toward my father, Jeom-Dong, my mother, Ok-Ja Ha, my sister, Hyun-Jung Lee, and my brother, Chang-Woo Lee, for their love and emotional support in every moment of my life.

I would like to express my profound gratitude to my wife, Hyun-Ju Park, whose love, tenderness and inspiration surround me all the time. I also thank my sons Bryan Lee and Nathan Lee whose smile have relaxed me greatly during hard times.

TABLE OF CONTENTS

LIST OF TABLES

LIST OF FIGURES

SUMMARY

In this work, we rigorously investigate new analytical and numerical approaches of constructing asymptotically correct laminated shell models that are accurate over a wide range of frequencies. The work is based on three essential theoretical foundations: (a) the concept of decomposition of the rotation tensor, (b) the variational asymptotic method and (c) hyperbolic short-wavelength extrapolation. Based on these, the Dynamic Variational Asymptotic Plate and Shell Analysis (DVAPAS) has been developed as part of the present study.

Unlike published shell theories, the main two parts of this thesis are devoted to the asymptotic construction of a refined theory for composite laminated shells valid over a wide range of frequencies. The resulting theory is applicable to shells each layer of which is made of materials with monoclinic symmetry. Both analytical and finite-element-based approaches are developed using quite similar procedures. The main objective of the analytical development is to provide insight and guidance for development of finite-element-based shell modeling; the main objective of the second part is to create a practical procedure for modeling layered shells.

First, the dynamic, three-dimensional, elasticity problem is compactly and elegantly formulated in intrinsic form considering the complex geometry of shell structures. Then the Variational Asymptotic Method is used to rigorously split this three-dimensional problem into a linear, one-dimensional, through-the-thickness analysis and a nonlinear, two-dimensional, surface analysis with the aid of the small parameters inherent in the structure. However, there is one important physical parameter in dynamics that is not present in statics. With respect to the characteristic "length" associated with the change of deformation with respect to time, the Variational Asymptotic Method also allows us to completely decouple the problem in terms of a low-frequency vibration analysis and a high-frequency

vibration analysis, both in the long-wavelength regime. The one-dimensional through-the-thickness analysis for the low- and high-frequency vibration approximations is solved by a one-dimensional finite element method in which the warping displacement field is discretized along the normal line. From results obtained, a total energy functional valid over the wide range of frequency has been constructed from the one-dimensional through-the-thickness analysis. One more step is then performed to complete the analysis. To ensure that the resulting strain energy is positive definite and sufficiently simple for all wavelengths, another logically independent step, called hyperbolic short-wavelength extrapolation, is used in the present work. An asymptotically correct energy functional for all wave lengths and frequency regimes up to the first approximation is first derived. This then provides a two-dimensional constitutive law in terms of matrices of inertia and stiffness coefficients and becomes suitable for input into the corresponding two-dimensional surface analysis, as well as for three-dimensional recovery relations to asymptotically represent three-dimensional displacement, strain and stress fields in terms of variables obtained from solving the equations of the shell analysis. The engineering software, DVAPAS, is developed based on the present shell model. It is a standard one-dimensional finite element code. The beginning step of the validation process is chosen to compare our numerical results with published analytical solutions, and the excellent agreement proves that the present model is capable of analyzing dynamic structural responses over a wide range of frequencies and wavelengths.

In a word, in the literature there is not to be found such a consistent and general approach, whether analytical or numerical. The associated computer program DVAPAS has the potential to have many applications in industry for analyzing composite structures that are subjected to various forms of dynamic disturbances.

CHAPTER I

INTRODUCTION

1.1 Motivation

As composite materials were introduced into the world, the initial impetus for using them was their high strength-to-weight and stiffness-to-weight ratios, along with very significant improvement in fatigue life and damage tolerance compared to most metallic materials. Furthermore, when composite materials are used to tailor a structure, they provide excellent opportunities for design flexibility and potential optimization of design criteria by controlling their directional natures to achieve certain performance goals or eliminate undesirable instabilities.

In general, many engineering structures made of composite materials are subjected to various forms of dynamic disturbances which may arise from either mechanical or environmental sources. The various excitation sources that act on a structure can be broadly classified as i) low-frequency ii) medium-frequency and iii) high-frequency disturbances. There is no absolute frequency range associated with each of these regimes, as much depends upon the structure itself; however, the main characteristics of the three types of excitation are the same for all structures and can be summarized briefly as follows [1].

1. Low-frequency disturbance: In this case the lowest modes of vibration of the structure are excited, just as in statics. The characteristic wavelength of the structural deformation is much longer than the smallest dimension of structures, and the characteristic timescale of the vibrations is linked to other dimensions of structure.

2. Medium-frequency disturbance: This involves excitation of the higher modes of vibration, but still the characteristic wavelength of the structure isn't much less than other dimensions of the structures.

3. High-frequency disturbance: In this case the highest modes of vibration are excited.

Indeed, the characteristic wavelength of the structural deformation is much less than or equal to the smallest dimension of structure. Moreover, the vibrations the characteristic timescale of which is linked to the smallest dimension of structures.

Referring to physical behavior and the existing literature, the dynamic response to low-frequency disturbances leads essentially to mechanical vibration of the whole structure. However, medium- to high-frequency excitation may be lead to unacceptable noise and vibration. In particular, excessive vibration maybe create large fluctuations of mechanical loads and stress, which leads to fatigue failure of structural components, loosening of threaded connections, friction and wear, and damage of electronic and other delicate components. Therefore, there is clearly a need for prediction and control of vibration over a wide range frequencies at the structural design stage. However, one can immediately surmise from reviewing the literature that established methods for design of ideal and simple structures made of isotropic materials and subjected to low-frequency disturbances are not suitable for analyzing realistic and complex composite structures over a wide range frequencies. This in turn requires the availability of new analytical methods that are able to predict the structural dynamic response of composite materials subjected to various forms of dynamic disturbances.

Because laminated composite shells are increasingly being used in various engineering applications that are very sensitive to excessive structural noise and vibration, research covering the dynamic behavior of composite shells has received considerable attention in the past three decades. This research spans aerospace, mechanical, marine, and automotive engineering. Tracking the history of new developments of approximate shell and plate theories, one can easily observe there are two main competing methods, namely asymptotic [2] and variational ones [3]. With the help of these two methods, there have been many attempts to develop dynamic models valid over a wide range of frequencies. First, in order to use variational methods, one needs an *a priori* kinematic assumption for the distribution of displacements as functions of the in-plane coordinates. Substituting this assumption into the three-dimensional (3-D) energy functional, one can derive the equations determining the dependency of the displacement field upon the thickness coordinate by varying the

functional obtained after the averaging procedure. The main disadvantage of the variational method is the necessity of having kinematic assumption for the displacements, while simplicity and brevity are its advantages.

On the other hand in asymptotic methods one expands the displacements in an asymptotic series (so there are no *ad hoc* kinematic assumptions). Indeed, the asymptotic method needs no *a priori* assumptions; however, it is very cumbersome and restricted from both geometric and material points of view [4, 5, 6]. Although there are many new theories based on elaborate mathematics or bound up with the phenomenal power of computers in the literature, none of the theories resolve satisfactorily all the above disadvantages at the same time. This is partly because there are many new models that are constructed for specific problems without generalization in mind (variational method case), partly due to some models being too complicated to be used in a design process (asymptotic method case). Simple yet efficient and generalized methods of analysis are still needed to predict the structural dynamic response over a wide range of frequencies.

Berdichevsky [7, 8, 3] first proposed the synthesis of these two methods, called the Variational Asymptotic Method (VAM), which seems to avoid the disadvantages of both methods described above. It also has proved to be very effective and accurate in formulating theories for isotropic elastic beams, plates and shells for both low- and high-frequency vibrations. At least some asymptotic methods give results similar to VAM, but they are more difficult to apply, more awkward in the series substitution into the equations of the 3-D theory, and more problematic as far as the subsequent asymptotic derivation of the recurrent system of equations for corresponding terms of the series. VAM is a powerful and systematic mathematical method. It can be used to split an original nonlinear 3-D elasticity problem into a linear analysis over the less important dimension(s) and a nonlinear analysis over the remaining dimension(s). For example, for a shell, VAM will decouple the elasticity problem into a linear 1-D analysis through the thickness which is called through-the-thickness analysis and nonlinear 2-D analysis over the reference surface. The main motivation of this study is to apply VAM to construct asymptotically correct models for shells made of composite laminated materials, which are valid over a wide range of wavelengths and frequencies.

1.2 Reviews of Previous Work

A shell is a thin 3-D body bounded by two, relatively close, curved surfaces where the thickness (i.e. the distance between the two curved surfaces) is relatively small compared to dimensions of the surfaces. In general, two fundamental restrictions are characteristic of approximate shell and plate theories. They impose limits on wavelengths and timescales in question. That is, to analyze the structural dynamic responses of shell and plate can be broadly classified into three approximations ranges due to various forms of dynamic disturbances – i) long-wave, low-frequency approximations (for a low-frequency disturbance) ii) long-wave, high-frequency ones (for a medium-frequency disturbance) and iii) short-wave, high-frequency ones (for a high-frequency disturbance). The short-wave, low-frequency approximations are not of great interest in dynamics because they are used to determine quasi-static boundary layers localized near the edges of the shell, whereas the other approximations describe disturbances which extend over the entire shell. It is essential that the range of applicability of the short-wave, high-frequency approximations and those of the long-wavelength approximations overlap [4]. Moreover, because the short-wavelength problem is essentially 3-D and does not admit a two-dimensional (2-D) description, we can only expect that applying 2-D theory to this field obtains only qualitative correspondence [9]. Referring the existing literature, there is a tremendous amount of work done on using approximate shell models for the prediction and control of structural dynamic responses under low-frequency vibration areas [10, 11, 12, 13, 14, 15]. Most of the existing literature focuses on applying approximate theories based on the first range with various numerical methods. However, for the second and third approximations there is little work being done on shells and plates [16, 17, 18, 19]. Refs. [1] and [20] presented an extensive review describing all well-known numerical methods, their advantages and disadvantages. The literature survey of previous work here is not intended to enumerate all approximate shell/plate theories, but it focuses on reviewing the main theories that have appeared in the past and are applicable to the whole excitation regime. Before proceeding, almost all shell theories are the direct or indirect extension of plate theories. Although one model working very well for plates might not be suitable for shells, it is still a common practice to derive shell theories

by using a similar technique for deriving in plate theories.

For vibration of plates and shells, the correct 2-D equation of small flexural vibrations of plates was first proposed by Sophie Germain in 1811. However, her choice of boundary condition proved to be incorrect. As early as 1828, Poisson and Cauchy both considered this problem from the point of view of 3-D elasticity; they started with full expansions in infinite series of powers of the thickness-coordinates, and then exercised great ingenuity in discarding higher powers and combining what was left so as to reach the desired equations. They had before them the ingredients of the higher-order equations, but there was no interest in high-frequency vibrations as that time. Poisson's work again produced Sophie Germain's equation. However, much controversy arose concerning Poisson's boundary conditions. These said that the resultant forces and moments applied at the edge of the plate must be equal to the internal forces and moments arising from the strain. Not long afterwards, Kirchhoff was the first to show that these conditions are too numerous and cannot in general be satisfied. He introduced energy considerations and integral theorems into the theory of the plates, which have remained in use until today. Similar to the rod theory based on Saint-Venant's principle, Kirchhoff's reasoning was based on two assumptions [21]:

1. The straight fibres of a plate which are perpendicular to the middle surface before deformation remain so after deformation.

2. All the elements of the middle-surface remain unstretched.

However, he too was interested only in low frequencies and included just enough terms of the series for his immediate purpose. Much later Rayleigh and Lamb found the dispersion equation for waves in an infinite plate according to 3-D elasticity. Also, Gazis derived and studied dispersion equations for waves in circular cylindrical shells of infinite length [22, 23]. A similar situation exists in regard to the classical 1-D equation of motion of elastic rods as compared with the exact 3-D elasticity studied by Pochhammer and Chree. One can show that the classical 2-D equations of motion of elastic plates and shells can be used to describe their vibrations in the low-frequency, long-wavelength range. However, numerical analysis of Rayleigh-Lamb's and Pochhammer-Chree's dispersion equations shows that, as

the frequency increases, many new branches of the dispersion curve arise. These branches are connected to each other in the complex wave-number plane, signifying complicated interactions between waves associated with the different branches near a free edge of a plate or shell. As the wave number and the frequency increase, the velocities in the 3-D theory have upper limits for all branches, in contrast to the classical 2-D theory. Hence the latter cannot be expected to give good results for the frequencies of modes of vibration of high-order.

In recent years there has been much interest in higher-order theories of plates and shells. Timoshenko [24] was the first to include the effect of transverse shear deformation and rotatory inertia to derive a 1-D theory of flexural motions of bars, which gives more satisfactory results for vibration modes with short wavelengths and high frequencies. Based on Timoshenko's investigation, Reissner and Mindlin developed a corresponding 2-D theory of elastic plates and shells called first-order shear deformation theory. Reissner [25] assumed that stresses are distributed linearly through the thickness in static behavior, while Mindlin [26] assumed that the 3-D displacement fields can be represented as a linear combination of unknown functions of the in-plane coordinates and given functions of the thickness coordinate.

According to Ref. [27], let the plate coordinates be x_1, x_2, x_3 with x_3 being the thickness coordinate and the x_1–x_2 plane being the middle-plane of the plate throughout this chapter. The plate thickness is h. Assume that the displacements u_1^{3d}, u_2^{3d}, u_3^{3d} may be expanded in terms of the power series of the thickness coordinate x_3 as

$$u_i^{3d}\left(x_1, x_2, x_3, t\right) = \sum_{n=0}^{\infty} x_3^n u_i^{2d(n)}\left(x_1, x_2, t\right) \tag{1}$$

Here note that a superscript enclosed in parentheses is not a power, but only indicates the order of the term to which it is attached. For example, the generalized 2-D displacements ($u_1^{2d(0)}$, $u_2^{2d(0)}$, $u_3^{2d(0)}$, $u_1^{2d(1)}$, $u_2^{2d(1)}$) have the same physical meaning as in the first-order shear deformation theory (FSDT) [25, 26], and $u_3^{2d(1)}$ describes elongation or contraction of the normal line element [28, 29, 19]. The simplest plate theory is the so-called classical plate theory (CPT), in which $u_1^{2d(1)}$ and $u_2^{2d(1)}$ are represented by the partial derivatives

of $u_3^{2d(0)}$ with respect to in-plane coordinates. In Fig. 1, the first three orders of x_3 are illustrated for the linear isotropic, elastic case.

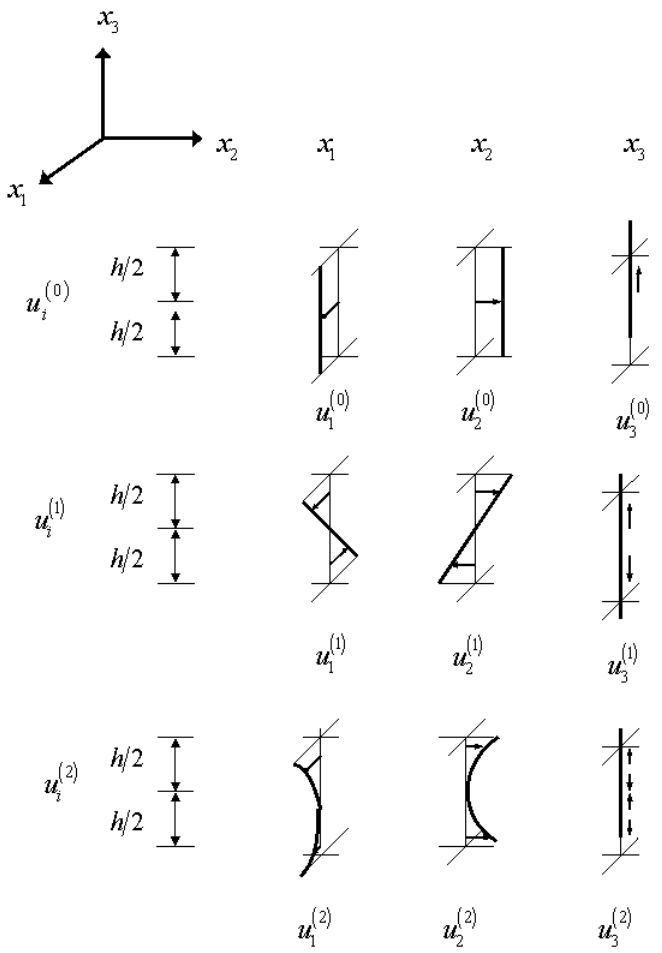

Figure 1: Components of displacement of orders zeros, one and two

However, Timoshenko's beam theory and its generalizations for plates and shells (Reissner-Mindlin's, and later Berdichevsky's, refined shell theories [8, 3]) have the shortcoming that they cannot satisfactorily predict the cut-off frequency (corresponding to zero wave number) and the long-wavelength asymptotes of the first branch of thickness vibrations. In particular, there are other expansions to do a more exact analysis. It was Mindlin and Medick [29] who succeeded in deriving 2-D equations of motion for plates that give satisfactory results for dispersion curves of both low-frequency and high-frequency branches. Unlike Mindlin's previous works, the 3-D displacement distributions are expressed by series

expansions in terms of Legendre polynomials in the thickness coordinate (instead of the thickness coordinate itself), so that

$$u_i^{3d} = \sum_{n=0}^{\infty} P_n(\zeta)\, u_i^{2d(n)}(x_1, x_2, t) \tag{2}$$

where $\zeta = x_3/h$, and the first few polynomials are

$$P_0(\zeta) = 1,\ P_1(\zeta) = \zeta,\ P_2(\zeta) = \left(3\zeta^2 - 1\right)/2,\ P_3(\zeta) = \left(5\zeta^3 - 3\zeta\right)/2, \tag{3}$$

$$P_n(\zeta) = \frac{1}{2^n n!}\frac{d^n\left(\zeta^2 - 1\right)^n}{d\zeta^n} \tag{4}$$

The reason for expanding in $P(\zeta)$ instead of ζ itself was given by Mindlin and Medick as follows. Expansions in ζ raised to second and higher powers leads to awkward mathematical forms owing to the lack of orthogonality of the terms of a power series. Although similarly awkward forms occur using the Legendre polynomials, they generally do not occur until third-order terms are reached. Fig. 2 illustrates the different distributions of displacements through the thickness from ones based on a power series.

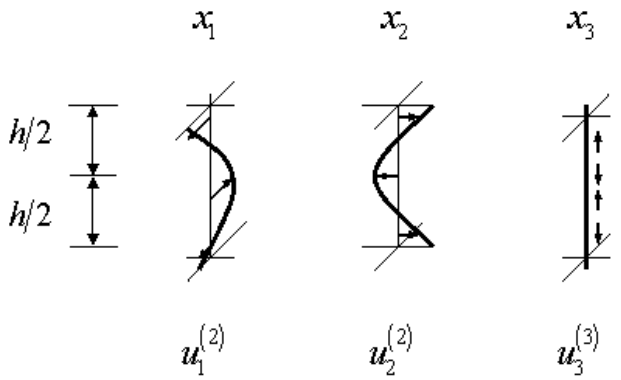

Figure 2: Symmetric components of displacements

According to Refs. [29] and [30], these series expressions are substituted into the 3-D energy functional, integrated over the thickness coordinate, and then some terms are truncated to produce the required order of approximation. However, since neither power series nor Legendre polynomials represent eigenvectors of the branches of thickness vibrations exactly, the 2-D theories thus obtained cannot predict exact cut-off frequencies and long-wavelength

asymptotes of those branches. Later, to avoid encountering complex mathematical forms due to Legendre polynomials and to resolve the above problems, Lee and Nikodem [31] used a different type of series and obtained the equations for anti-symmetric and symmetric vibrations up to fourth-order approximations:

$$u_i^{3d} = \sum_{n=0}^{\infty} \cos\left[\frac{n\pi}{2}(1-\zeta)\right] u_i^{2d(n)}(x_1, x_2, t) \tag{5}$$

However, certain "correction coefficients" are still needed to improve the match between the frequency spectra of an infinite plate as obtained from the approximate and exact equations.

Although theories of Mindlin and his co-workers have been successfully applied in many engineering problems, their introduction of the "shear correction factors" remains a little mysterious. Berdichevsky was the first to show that a long-wavelength asymptotic analysis can be applied for branches of high-frequency vibrations of elastic plates near the cut-off frequencies (corresponding to zero wave numbers) [32]. Based on VAM he found distributions of the displacements and derived the equations of high-frequency, long-wavelength vibrations for all thickness branches. This method was also applied to beams [33] and shells [34]. Later work by Kaplunov [35] confirms the results for plates, but displays some arithmetic mistakes in the calculation of the coefficients for the equations of shells, the correction of which leads to the full agreement of the results from VAM.

Although Berdichevsky obtained asymptotically correct equations that describe correctly the low- and high-frequency vibrations of plates and shells in the long-wavelength ranges near the cut-off frequencies, when these equations without any modification are directly applied for a wide range of wavelengths, they show an unsatisfactory description of the dispersion curves and the group velocities in the short-wavelength range. Moreover, the formulation of boundary-value problems is associated with the behavior of the corresponding differential operators at short wavelengths. Thus, even asymptotically exact equations in the long-wavelength range may lead to an ill-posed boundary-value problem [7]. Therefore, construction of the theory of plates and shells involves not only the derivation of equations in the long-wavelength range, but also another logically independent step – the extrapolation of those equations to the short wavelength regime. It is possible to carry

out either trivial extrapolations, when the system of equations derived for long waves is applied to short waves without any changes, or non-trivial extrapolations, when terms that are small in the long-wavelength range but appreciable for short waves are introduced (or removed). For shells in the short-wavelength range it is impossible to describe the 3-D stress state exactly using a 2-D theory, and only a qualitative agreement can at best be expected. For this reason, different 2-D equations are allowed in the theory of shells. However, it is natural to demand an asymptotic equivalence in the long-wavelength range of different short-wavelength extrapolations.

The hyperbolic short-wavelength extrapolation for a shell made of an elastic material was first proposed by Berdichevsky and Le [36, 16]. This involves the classical (low-frequency) branches and several thickness (high-frequency) branches of vibrations; it takes into account their cross-terms at short wavelengths. The structure of the equations is similar to that of Mindlin for plates; but, in contrast to his theory, this one is asymptotically exact in the low-frequency regime, and some of the first high-frequency branches of vibrations for the long-wavelength approximations are determined by the asymptotic analysis and not by introduction of "shear correction factors" based on ad hoc assumptions.

This brings additional advantages:

1. Problems for which exact dispersion equations are unknown or unavailable (for instance, shell vibrations) can also be analyzed;

2. The asymptotically exact 3-D stress and strain state can be recovered from the 2-D integral characteristics.

The application of the 2-D theory to various problems, such as the dispersion of waves or the frequency spectra of plates or shells, shows that it enables one not only to predict the asymptotically correct distributions of the stress and displacement fields in the long-wavelength range, but also to describe qualitatively correctly their behaviour in the short-wavelength range. The construction of the approximate theory by VAM is then generalized for beams [37, 9], sandwich plates [38], piezoelectric shells [39, 40], plates [41], and a dynamic version of Saint-Venant's principle [42, 43].

This approach is extended to model composite plates by Lee [44] and composite beams by Cesnik [45] for statics, and for dynamics of composite beams by Volovoi [46] for dynamics. They introduced new "degrees of freedom" into the 3-D displacement field. According to the eigenfunction approach introduced by Sutyrin [47], they developed so-called "alternative theories" to treat transverse shear effects. However, these theories themselves are not asymptotically correct, nor were they claimed to be. To the best of the author's knowledge this type of development, for laminated composite shells valid for vibrations over a wide range of frequencies, does not appear in the literature.

1.3 Present Work

As reviewed in the above section, most published 2-D shell models are restricted to only analyze structural dynamic responses within the long-wave, low-frequency vibration area. Moreover, under the established models many extended and modified theories are developed and introduced to overcome two fundamental restrictions – wavelengths and timescales. However, contrary to their developers' intentions these theories suffer from other drawbacks, such as an *ad hoc* kinematic assumption for the displacements, specific limitations on geometry and materials, etc. Also there are the similar drawbacks on the numerical procedures such as excessive dependence on computer performance and limited representations for general geometries.

The approach introduced in the present research is thus new and powerful. The compact and elegant representation of the dynamic intrinsic formulation [48], the rigorous dimensional reduction procedure of VAM, and the non-trivial, hyperbolic, short-wavelength extrapolation procedure [3] have all been combined to construct an asymptotically correct shell model. It enables one to analyze shell dynamic responses within both low-frequency, and high-frequency, long-wavelength vibration regimes. It also leads to energy functionals that are both positive definiteness and of sufficient simplicity for all wavelengths.

The procedure can be summarized as follows: We first transform the original 3-D dynamic elasticity problem into an intrinsic form so that the developed theory is applicable for arbitrarily large displacement and global rotation subject only to the assumption that

the strain is small. The main advantage using the dynamic intrinsic formulation is also a compact and elegant representation without the unnecessary complexities of a purely mathematical description. And then for plates and shells within the long-wavelength regime, a 1-D linear through-the-thickness analysis and a 2-D nonlinear surface analysis can be decoupled using VAM with the aid of small geometrical parameters inherent in the structure. Unlike the corresponding static analysis, however, there is one more important physical parameter in dynamics, called the characteristic timescale associated with the change of the deformation with respect to time. It is used to rigorously split the original 3-D dynamic problem into low- and high-frequency vibration regimes. The 1-D through-the-thickness analysis yields a generalized 2-D constitutive law represented by mass and stiffness matrices, M_{2d} and K_{2d}, respectively, and a load-related column matrix F_{2d}. Again, asymptotically exact approximations of the original 3-D solutions can be recovered using global deformation from the corresponding 2-D surface analysis together with results from the 1-D through-the-thickness analysis. This whole procedure was first performed analytically. From the insight gained from that procedure, a finite element version of the analysis was then developed; and a corresponding computer program, Dynamic Variational Asymptotic Plate and Shell Analysis (DVAPAS), was developed. DVAPAS can obtain the generalized 2-D constitutive law and recover accurately the 3-D results for stress and strain in composite shells.

Before proceeding to a detailed derivation of the present theory, it must be emphasized that there is no previous work known to the author that has been done toward variational-asymptotic modeling of composite laminated shells for accurate prediction of dynamic behavior over a wide range of frequencies. Moreover, the present work represents the first attempt to develop a corresponding finite element-based procedure, which makes more the problem tractable in practice. A difficulty is met when one tries to validate our results obtained from DVAPAS, because most of those published are restricted to homogeneous and isotropic shell cases. Even though there are a few published works to investigate composite cases, it is very difficult to compare our results directly in terms of the mass and stiffness matrices. So some independent works will be needed to develop the corresponding 2-D surface analysis associated with the present theory and to continue towards full verification

and validation of the present process by comparison with available published works. Fortunately, mass and stiffness matrices for homogeneous and isotropic plates/shells are directly provided by Refs. [16] and [9], which shows very good agreement with 3-D numerical results by Gazis [22, 23]. In addition, all results calculated are also summarized well. For this reason, we choose Le's analytic solutions in the validation process to check our analytic and numerical procedures in detail. As it will be demonstrated, the present theory shows excellent agreement with his analytic solutions for the whole process.

CHAPTER II

ANALYTICAL PROCEDURE

In the theory of plates and shells, dimensional reduction from the dynamic equations of 3-D elasticity to the approximate 2-D equations is possible if the displacements change little in the in-plane directions over distances of the order of the plate/shell thickness h within the long-wavelength approximation $h/l \to 0$. Here l is a characteristic length scale associated with the variation of the deformation of the reference surface, often referred to as the "wavelength" of in-plane deformation. In statics, this condition leads, in the first approximation, to the constancy of displacements along the thickness coordinate. However, in dynamics, for stress states that change slowly in the in-plane directions, an infinite variety of displacement distributions along the plate/shell thickness (branches) is possible. Each branch is characterized by some specific frequency ω. According to Ref. [32] it turned out that, for problems with zero displacement at the edge, the branches have the splendid quality that they are orthogonal with respect to kinetic and strain energies. This makes it possible to independently investigate vibrations corresponding to different branches. Therefore, classical theories of plates and shells, such as Kirchhoff-Love theory, describe low-frequency vibrations, for which the displacements are, to a first approximation, constant through the thickness. However, for high frequencies the above generalizations that published shell theories have almost universally used are not suitable for analyzing complicated high-frequency effects because the displacements rapidly oscillate along the thickness coordinate. In addition, within short wave range $h/l \to \infty$ because it is very difficult to represent the 3-D stress state exactly by the 2-D theory, and only a qualitative agreement can at best be expected it is more natural that we should apply the other operator into the equations of the theory of plates and shells - the hyperbolic short-wave extrapolation procedure.

In this chapter, an asymptotically correct dynamic shell theory valid over a wide range of frequencies is proposed. The theory is applicable to shells in which each layer is made with

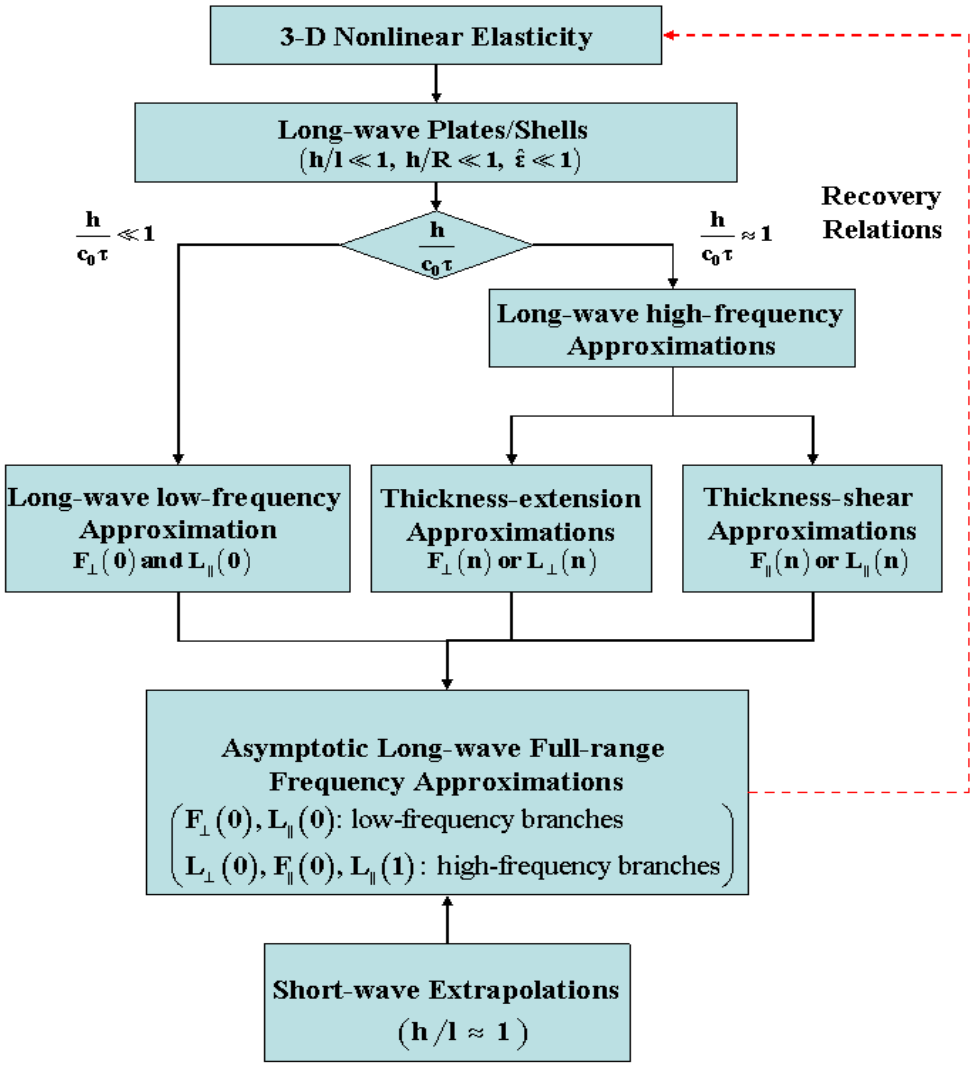

Figure 3: Overview of dynamic shell analysis

monoclinic material. Unlike most of established shell theories that are limited to the low-frequency, long-wavelength regime, the present theory describes in an asymptotically correct manner not only the low-frequency regime but also some of the first high-frequency branches of vibrations of the shell in the long-wavelength regime. Moreover, to allow recovery of the 3-D stress state in the short-wavelength regime, we introduce hyperbolic, short-wavelength extrapolation procedure pioneered by Berdichevsky and Le [34]. The present theory will be obtained using four steps. First, the dynamic 3-D elasticity problem is formulated in an intrinsic form considering the complex geometry of shell structures (Sections 2.1 and 2.2). Then the VAM is used to rigorously split this 3-D problem into a linear 1-D through-the-thickness analysis and a nonlinear 2-D shell analysis, taking into account the full range of frequencies. This means that we construct the asymptotically correct energy functional in the low- and high-frequency, long-wavelength regime up to terms of the order $h/R \ll 1$ and $h/l \ll 1$ within the first approximations, where R is the characteristic radius of curvature of the shell reference surface and l the characteristic wavelength in the in-plane directions (Section 2.3 and 2.4). Unlike most published plate and shell theories, another logically independent step – hyperbolic short-wavelength extrapolation is used in the present approach to describe the 3-D stress state qualitatively (Section 2.5). Finally, the resulting theory provides recovery relations to approximately express the 3-D displacement, strain and stress fields (Section 2.6). Fig. 3 shows a flowchart for the overall process.

Note that here and throughout the rest of the shell development, Greek indices assume values 1 and 2 while Latin indices assume 1, 2, and 3. Repeated indices are summed over their range except where explicitly mentioned.

2.1 Shell Kinematics

A shell may be considered geometrically as a smooth 2-D surface S surrounded by a layer of matter with thickness h to form a 3-D body with one dimension much smaller than the other two. Let S be called the reference surface of the 3-D body, bounded by a smooth closed curve ∂S and mathematically represented by a set of arbitrary curvilinear coordinates, x_α. However, without loss of generality, one may choose the lines of curvature to be the

curvilinear coordinates to simplify the formulation. In addition, for representing the 3-D medium uniquely and following a very natural choice generally, the third coordinate is specified as $x_3 = h\zeta$, the coordinate normal to the reference surface. Throughout the analysis, a non-dimensional coordinate through the thickness is used $-1/2 \leq \zeta \leq 1/2$. In fact, almost all published shell theories are based on this choice. Note that a plate is a special case of a shell whose middle surface is planar. As sketched in Fig. 4, letting

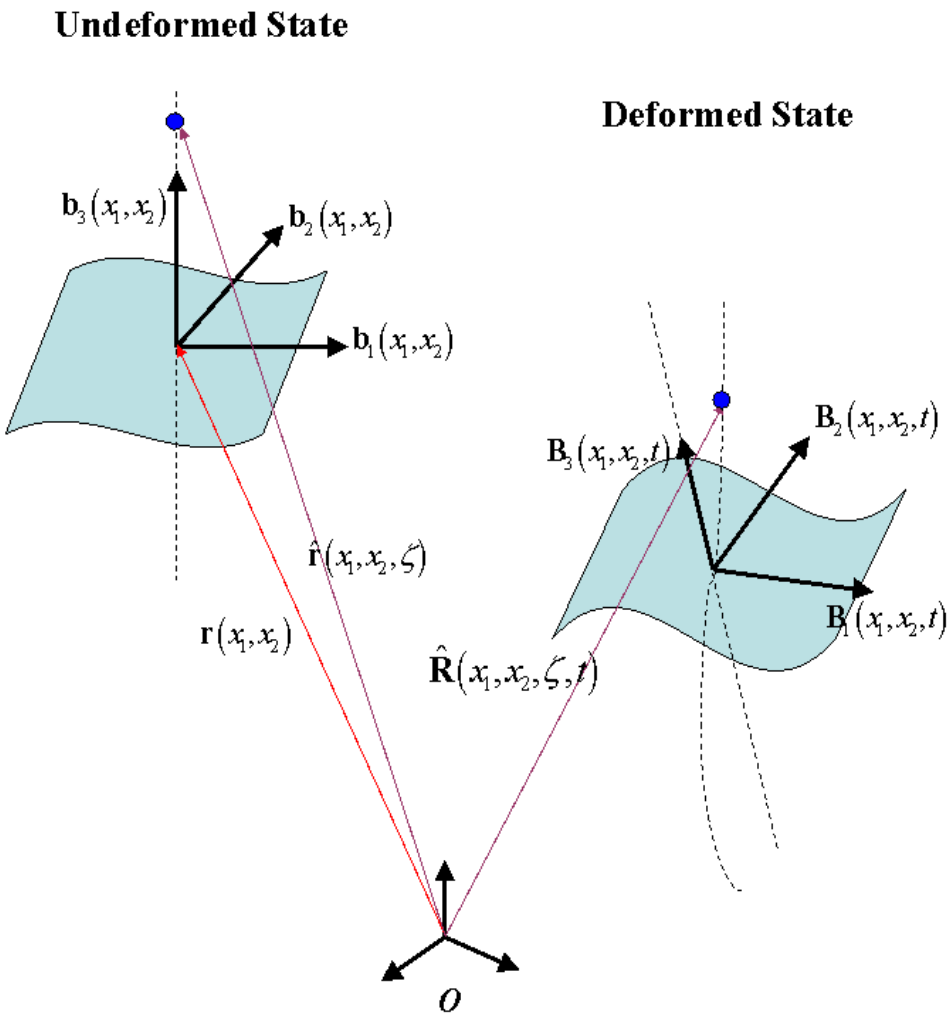

Figure 4: Schematic of shell deformation

$\mathbf{b}_3(x_1, x_2)$ denote the unit vector normal to the reference surface, one can then describe the position of any material point in the stress-free, undeformed configuration by its position

vector $\hat{\mathbf{r}}$ relative to an inertially fixed point O, such that

$$\hat{\mathbf{r}}\left(x_1, x_2, \zeta\right) = \mathbf{r}\left(x_1, x_2\right) + h\zeta \mathbf{b}_3\left(x_1, x_2\right) \tag{6}$$

where $\mathbf{r}$ is the position vector from O to the point located by x_α on the reference surface.

When the reference surface of the undeformed shell coincides with its middle surface, it naturally follows that

$$\langle \hat{\mathbf{r}}\left(x_1, x_2, \zeta\right) \rangle = \mathbf{r}\left(x_1, x_2\right) \tag{7}$$

where the angle-brackets $\langle \bullet \rangle$ denote the definite integral through the thickness of the shell $\zeta \in [-1/2, 1/2]$ and will be used throughout the rest of the development for shells.

Typically, let 2-D base vectors $\mathbf{a}_\alpha$ associated with x_α be defined as:

$$\mathbf{a}_\alpha\left(x_1, x_2\right) = \mathbf{r}_{,\alpha} \tag{8}$$

From henceforth, for simplicity, we will avoid including the independent variables on which a function depends unless it is not obvious for the reader to determine what they are. From Eq. (8) one can define the so-called Lamé parameters as:

$$A_\alpha\left(x_1, x_2\right) = \sqrt{\mathbf{a}_\alpha \cdot \mathbf{a}_\alpha} \tag{9}$$

Let us mention that in Eq. (9), the summation convention is not applied because α is not a dummy index. The same rule will apply to the rest of development without repeating the same statement. Then, for the computational procedures used later, the 2-D unit base vectors $\mathbf{b}_i$ constitute an orthogonal triad system such that

$$\begin{aligned} \mathbf{b}_\alpha\left(x_1, x_2\right) &= \frac{\mathbf{a}_\alpha}{A_\alpha} \\ \mathbf{b}_3 = \mathbf{b}_1 \times \mathbf{b}_2 &= \frac{\mathbf{a}_1 \times \mathbf{a}_2}{|\mathbf{a}_1 \times \mathbf{a}_2|} \end{aligned} \tag{10}$$

Now by taking the partial derivatives of Eq. (6) with respect to x_α, it is easy to see that the covariant 3-D base vectors $\mathbf{g}_i$ associated with the chosen coordinate system are given by:

$$\begin{aligned} \mathbf{g}_1 &= \mathbf{a}_1 + h\zeta \mathbf{b}_{3,1} \\ \mathbf{g}_2 &= \mathbf{a}_2 + h\zeta \mathbf{b}_{3,2} \\ \mathbf{g}_3 &= \mathbf{b}_3 \end{aligned} \tag{11}$$

From the differential geometry of the surface and with the help of Refs. [49] and [50] one can express the derivative of 2-D unit base vectors $\mathbf{b}_{i,\alpha}$ as follows:

$$\mathbf{b}_{i,\alpha} = A_\alpha \mathbf{k}_\alpha \times \mathbf{b}_i \tag{12}$$

with

$$\mathbf{k}_\alpha = (-k_{\alpha 2}\mathbf{b}_1 + k_{\alpha 1}\mathbf{b}_2 + k_{\alpha 3}\mathbf{b}_3) \tag{13}$$

where $\mathbf{k}_\alpha$ is the curvature vector measured in $\mathbf{b}_i$ in which $k_{\alpha\beta}$ refers to out-of-plane curvatures. We note that $k_{12} = k_{21} = 0$ because the coordinates are defined to be the lines of curvatures. However, the geodesic curvatures $k_{\alpha 3}$ do not necessarily vanish for the chosen coordinate system, and they can be expressed in terms of the Lamé parameters as:

$$k_{13} = -\frac{A_{1,2}}{A_1 A_2}, \quad k_{23} = \frac{A_{2,1}}{A_1 A_2} \tag{14}$$

As we are interested in the interior solution with geometrical and shear refinements for regular shells, we assume that the initial curvatures k_{ij} and Lamé parameters A_α are slowly varying or constant. This assumption will result in the neglect of all the derivatives of these quantities with respect to in-plane coordinates x_α in the formulation.

Using Eqs. (12) and (13) one can rewrite the expression for the covariant 3-D base vectors from Eq. (11) as:

$$\begin{aligned} \mathbf{g}_1 &= A_1 \left(1 + h\zeta k_{11}\right) \mathbf{b}_1 \\ \mathbf{g}_2 &= A_2 \left(1 + h\zeta k_{22}\right) \mathbf{b}_2 \\ \mathbf{g}_3 &= \mathbf{b}_3 \end{aligned} \tag{15}$$

By the standard definition [49], the contravariant base vectors are given by

$$\mathbf{g}^i \left(x_l\right) = \frac{1}{2\sqrt{g}} e_{ijk} \mathbf{g}_j \times \mathbf{g}_k \tag{16}$$

where $g = \det\left(\mathbf{g}_i \cdot \mathbf{g}_j\right)$ is the determinant of the metric tensor for the undeformed configuration, and e_{ijk} are the components of the permutation tensor in a Cartesian coordinate system. Thus, one can define the contravariant 3-D base vectors $\mathbf{g}^i$ as

$$\begin{aligned} \mathbf{g}^1 &= \frac{\mathbf{b}_1}{A_1 \left(1 + h\zeta k_{11}\right)} \\ \mathbf{g}^2 &= \frac{\mathbf{b}_2}{A_2 \left(1 + h\zeta k_{22}\right)} \\ \mathbf{g}_3 &= \mathbf{b}_3 \end{aligned} \tag{17}$$

When the shell is deformed, the particle that had position vector $\hat{\mathbf{r}}(x_1, x_2, \zeta)$ in the undeformed state now has the position vector $\hat{\mathbf{R}}(x_1, x_2, \zeta, t)$ in the deformed configuration. The latter can be uniquely determined by the deformation of the 3-D body. A new triad $\mathbf{B}_i(x_1, x_2, \zeta, t)$ is introduced for the deformed shell. Note that the $\mathbf{B}_i$ unit vectors are just tools to enable one to express vectors and tensors in their component form during the derivation. They are not necessarily tangent to the coordinates of the deformed shell. The relation between $\mathbf{B}_i$ and $\mathbf{b}_i$ can be specified by an arbitrarily large rotation specified in terms of the matrix of direction cosines $C(x_1, x_2, t)$, so that

$$\begin{aligned} \mathbf{B}_i &= C_{ij}\mathbf{b}_j \\ C_{ij} &= \mathbf{B}_i \cdot \mathbf{b}_j \end{aligned} \tag{18}$$

subject to the requirement that $\mathbf{B}_i$ is coincident with $\mathbf{b}_i$ when the structure is undeformed. Without loss of generality, the position vector $\hat{\mathbf{R}}$ can be defined as:

$$\hat{\mathbf{R}}(x_1, x_2, \zeta, t) = P_i(x_1, x_2, \zeta, t)\,\mathbf{B}_i(x_1, x_2, t) \tag{19}$$

where P_i are unknown arbitrary 3-D functions to be determined independently at each frequency regime.

Before closing this section, definitions of the 2-D generalized curvature and inertial angular velocity measures are introduced for the purpose of formulating this problem in dynamic intrinsic form. Following Refs. [50, 51] and [52], they can be defined as:

$$\begin{aligned} \mathbf{B}_{i,\alpha} &= A_\alpha\left(-K_{\alpha 2}\mathbf{B}_1 + K_{\alpha 1}\mathbf{B}_2 + K_{\alpha 3}\mathbf{B}_3\right) \times \mathbf{B}_i \\ \dot{\mathbf{B}}_i &= \Omega_j \mathbf{B}_j \times \mathbf{B}_i \end{aligned} \tag{20}$$

where K_{ij} are the curvatures of the deformed surface, which are the summation of curvatures of undeformed geometry k_{ij} and curvatures introduced by the deformation κ_{ij} and of which the order is denoted by $O(\hat{\varepsilon}/h)$. In addition, Ω_i are the inertial angular velocity measures of the deformed shell reference surface, of which the order is denoted by $O(c\hat{\varepsilon}/l)$, where $\hat{\varepsilon}$ is the order of the maximum strain in the plate/shell, and c the order of the characteristic velocity of plane waves c_0 in the composite material under consideration.

2.2 3-D Formulation

Following [53], the Jauman-Biot-Cauchy strain components for small local rotation are given by

$$\Gamma_{ij} = \frac{1}{2}\left(F_{ij} + F_{ji}\right) - \delta_{ij} \tag{21}$$

where δ_{ij} is the Kronecker symbol, and F_{ij} the mixed-basis component of the deformation gradient tensor such that

$$F_{ij} = \mathbf{B}_i \cdot \mathbf{G}_k \mathbf{g}^k \cdot \mathbf{b}_j \tag{22}$$

Here $\mathbf{G}_i = \partial\hat{\mathbf{R}} \Big/ \partial x_i$ is the 3-D covariant basis vector of the deformed configuration. With the help of Eqs. (17), (20), (21) and (22), one can obtain the 3-D strain and velocity fields as:

$$\begin{aligned}
\Gamma_{11} &= \frac{P_{1;1} - \kappa_{13}P_2 + \left(k_{11} + \kappa_{11}\right)P_3}{1 + h\zeta k_{11}} - 1 \\
2\Gamma_{12} &= \frac{P_{1;2} - \kappa_{23}P_2 + \kappa_{21}P_3}{1 + h\zeta k_{22}} + \frac{P_{2;1} + \kappa_{13}P_1 + \kappa_{12}P_3}{1 + h\zeta k_{11}} \\
\Gamma_{22} &= \frac{P_{2;2} + \kappa_{23}P_1 + \left(k_{22} + \kappa_{22}\right)P_3}{1 + h\zeta k_{22}} - 1 \\
2\Gamma_{13} &= \frac{1}{h}P_{1|\zeta} + \frac{P_{3;1} - \left(k_{11} + \kappa_{11}\right)P_1 - \kappa_{12}P_2}{1 + h\zeta k_{11}} \\
2\Gamma_{23} &= \frac{1}{h}P_{2|\zeta} + \frac{P_{3;2} - \kappa_{21}P_1 - \left(k_{22} + \kappa_{22}\right)P_2}{1 + h\zeta k_{22}} \\
\Gamma_{33} &= \frac{1}{h}P_{3|\zeta} - 1
\end{aligned} \tag{23}$$

and

$$\begin{aligned}
\Lambda_1 &= \dot{P}_1 - \Omega_3 P_2 + \Omega_2 P_3 \\
\Lambda_2 &= \dot{P}_2 + \Omega_3 P_1 - \Omega_1 P_3 \\
\Lambda_3 &= \dot{P}_3 - \Omega_2 P_1 + \Omega_1 P_2
\end{aligned} \tag{24}$$

where $(\bullet)_{;\alpha} = 1/A_\alpha \partial\left(\bullet\right)/\partial x_\alpha$, $(\bullet)_{|\zeta} = \partial\left(\bullet\right)/\partial\zeta$ and $(\dot{\bullet}) = \partial\left(\bullet\right)/\partial t$. Note that unlike most published 2-D shell theories, the order of unknown 3-D functions P_i is not assumed *a priori* to derive Eqs. (23) and (24), but rather it is obtained as a result of the minimization procedure in the primary approximation for each range of frequency vibrations. For convenience $\hat{q}$ denotes the order of P_i.

Until now, we have been trying to be general except for the small strain approximation. However, to make the problem more manageable, we have to make some inevitable approximations that published shell theories have almost universally used. There are several small parameters in most engineering structures, and the existence of small parameters brings about a great variety of possibilities for application of asymptotic methods. In the shell problem considered, three possible small parameters exist: the maximum strain $\hat{\varepsilon}$, the geometric parameter h/R and the thickness-to-wavelength parameter h/l. To apply the third parameter to our procedure, this means that our problem is in the long-wavelength regime. Therein the smallest wavelength l of the deformation pattern associated with the in-plane coordinates is considerably greater than the shell thickness h. Moreover, we will introduce one more important physical parameter for a dynamical shell theory:

$$\frac{h}{c_0\tau} \tag{25}$$

where c_0 is the characteristic velocity of shear waves in the composite material under consideration and τ is the characteristic timescale of the change of the deformation with respect to time. Following to Ref. [3], if one limits the consideration to low-frequency vibration of the shell, then τ can be linked to l as

$$\frac{h}{c_0\tau} \ll 1 \Rightarrow \tau \sim O\left(\frac{l}{c_0}\right) \tag{26}$$

On the other hand, for the high-frequency (thickness) vibrations case

$$\frac{h}{c_0\tau} \gg 1 \Rightarrow \tau \sim O\left(\frac{h}{c_0}\right) \tag{27}$$

Therefore, generally speaking, there are three independent small parameters: h/l, h/R and $\hat{\varepsilon}$. Note that the wavelength of the high-frequency vibrations along the thickness coordinate of the 3-D shell is usually smaller than h, but this fact is not an obstacle for the application of the VAM, which is based on the smallness of h/l.

Following to Refs. [50] and [51], Hamilton's principle for the surface can now be constructed as:

$$\int_{t_1}^{t_2}\int_S \left[\delta\overline{\mathcal{L}} + \overline{\delta\mathcal{W}}\right] dS dt = \overline{\delta\mathcal{A}} \tag{28}$$

where t_α are arbitrary fixed times, S denotes the undeformed reference surface, $\overline{\mathcal{L}}$ is the Lagragian density per unit area, $\overline{\delta\mathcal{W}}$ is the virtual work of the applied loads per unit area, and $\overline{\delta\mathcal{A}}$ is the virtual action at the boundary of shell and at the ends of the time interval. Furthermore, $\overline{\mathcal{L}}$ can be written as

$$\overline{\mathcal{L}} = \overline{\mathcal{K}} - \overline{\mathcal{U}} \tag{29}$$

By definition, $\overline{\mathcal{K}}$ and $\overline{\mathcal{U}}$ are the 3-D kinetic energy and strain energy densities per unit area, respectively, of the form

$$\overline{\mathcal{K}} = \frac{1}{2}\left\langle \rho\left[\Lambda_e^T\Lambda_e + \Lambda_t^2\right]\eta\right\rangle \tag{30}$$

and

$$\overline{\mathcal{U}} = \frac{1}{2}\left\langle \begin{Bmatrix} \Gamma_e \\ 2\Gamma_s \\ \Gamma_t \end{Bmatrix}^T \begin{bmatrix} D_e & D_{es} & D_{et} \\ D_{es}^T & D_s & D_{st} \\ D_{et}^T & D_{st}^T & D_t \end{bmatrix} \begin{Bmatrix} \Gamma_e \\ 2\Gamma_s \\ \Gamma_t \end{Bmatrix}\eta \right\rangle \tag{31}$$

where

$$\begin{aligned} \Gamma_e &= \lfloor \Gamma_{11} \;\; 2\Gamma_{12} \;\; \Gamma_{22} \rfloor^T \\ 2\Gamma_s &= \lfloor 2\Gamma_{13} \;\; 2\Gamma_{23} \rfloor^T \\ \Gamma_t &= \Gamma_{33} \\ \Lambda_e &= \lfloor \Lambda_1 \;\; \Lambda_2 \rfloor^T \\ \Lambda_t &= \Lambda_3 \end{aligned} \tag{32}$$

with

$$\eta = \frac{\mathbf{g}_1 \times \mathbf{g}_2 \cdot \mathbf{g}_3}{|\mathbf{a}_1 \times \mathbf{a}_2|} = 1 + 2h\zeta H + (h\zeta)^2 K \tag{33}$$

Here $H = (k_{11} + k_{22})/2$ and $K = k_{11}k_{22}$ are called the mean and the Gaussian curvatures of the surface, respectively. Here $\rho(\zeta)$ is the mass density of a 3-D body and $D(\zeta)$ is the 3-D 6×6 material matrix, which comes from the fourth-order elasticity tensor expressed in the $\mathbf{b}_i$ basis. This matrix is in general fully populated. However, if it is desired to model laminated composite shells in which each lamina exhibits a monoclinic symmetry about its own mid-plane (for which the material matrix is determined by 13 constants instead of 21) and rotated about the local normal to be a layer in the composite laminated shell, then D_{es}

and D_{st} will always vanish no matter what the layup angle is. Considering this, we can simplify the strain energy expression Eq. (31) to the following form:

$$\overline{\mathcal{U}} = \frac{1}{2}\left\langle \left[\Gamma_e^T D_e \Gamma_e + 2\Gamma_e^T D_{et}\Gamma_t + 2\Gamma_s^T D_s\left(2\Gamma_s\right) + D_t\Gamma_t^2\right]\eta\right\rangle \tag{34}$$

Following the methodology introduced by Yu *et al.* [54], the loading can be assumed to be of order h/l and h/R, which is acceptable for our level of approximation.

Now, the complete statement of the problem can be presented in terms of the principle of virtual work, such that

$$\delta\overline{\mathcal{K}} - \delta\overline{\mathcal{U}} + \overline{\delta\mathcal{W}} = 0 \tag{35}$$

In spite of the possibility of accounting for nonconservative forces, in the above, the problem that governs the 3-D unknown functions is conservative. Thus, one can pose the problem that governs the functions as the minimization of a total energy functional, viz.,

$$\overline{\mathcal{L}} = \overline{\mathcal{K}} - \overline{\mathcal{P}} \tag{36}$$

with $\overline{\mathcal{P}} = \overline{\mathcal{U}} + \overline{\mathcal{V}}$, so that

$$\delta\overline{\mathcal{L}} = 0 \tag{37}$$

where $\overline{\mathcal{V}}$ is the work done by applied loads. Below, for simplicity of terminology, we will refer to $\overline{\mathcal{P}}$ as the total potential energy, or the total potential. Here and throughout the rest of the shell development, we assume the mass density to be a constant to make our problem more tractable and procedure simpler. Introducing non-dimensional quantities $\rho/\rho_0 = 1$ and $D^* = D/\mu_0$ into Eqs. (30) and (34), the total energy functional can be non-dimensionalized, so that

$$2\overline{\mathcal{K}} = \rho_0\left\langle \left[\Lambda_e^T\Lambda_e + \Lambda_t^2\right]\eta\right\rangle \tag{38}$$

and

$$2\overline{\mathcal{U}} = \mu_0\left\langle \left[\Gamma_e^T D_e^*\Gamma_e + 2\Gamma_e^T D_{et}^*\Gamma_t + 2\Gamma_s^T D_s^*\left(2\Gamma_s\right) + D_t^*\Gamma_t^2\right]\eta\right\rangle \tag{39}$$

Here ρ_0 and μ_0 are characteristic values of mass density and material constants in the material under consideration (all of which are assumed to be of the same order). Therefore, $c_0 = \sqrt{\mu_0/\rho_0}$. Up to this point, this is simply an alternative formulation of the original

3-D elasticity problem. If we attempt to solve this problem directly, we will meet the same difficulty as solving any full 3-D elasticity problem. Fortunately, as shown below, VAM can be used to calculate the 3-D unknown functions asymptotically.

2.3 Low-frequency, Long-wavelength Vibration Approximations

In this section we derive the 2-D equations for vibrations of a monoclinic laminated composite shell under low-frequency, long-wavelength approximations.

2.3.1 Primary approximation

The dimensional reduction from 3-D to 2-D cannot be done exactly. The best one can do is to accomplish it asymptotically taking advantage of the smallness of h/l, h/R and $\hat{\varepsilon}$. Now, with the help of an additional small parameter, Eq. (26), we are ready to determine the constraints and the orders of the undetermined function for low-frequency vibrations. At the primary step of VAM, the entire kinetic energy density can be neglected in the asymptotic sense, and only the total potential retained as the formally leading terms in Eq. (39). Therefore, from Eq. (36) we obtain the following functional

$$2\overline{\mathcal{L}} = -\mu_0 \left\langle \frac{1}{h^2} P_{\|\|\zeta}^T D_s^* P_{\|\|\zeta} + \frac{1}{h^2} D_t^* P_{3|\zeta}^2 \right\rangle \tag{40}$$

with $(\bullet)_{\|} = \lfloor (\bullet)_1 \quad (\bullet)_2 \rfloor^T$. It is obvious that the above Eq. (40) is negative definite; its maximum is equal to zero and is reached for functions $\mathbf{R}$ that are independent of ζ, *i.e.*,

$$\hat{\mathbf{R}}\left(x_1, x_2, \zeta, t\right) = \mathbf{R}\left(x_1, x_2, t\right) \tag{41}$$

where R_α and R_3 are arbitrary functions of x_α and t.

Now, in accordance with the variational-asymptotic scheme, the position vector Eq. (19) in the deformed configuration can be redefined in the form

$$\hat{\mathbf{R}}\left(x_1, x_2, \zeta, t\right) = \mathbf{R}\left(x_1, x_2, t\right) + \bar{P}_i\left(x_1, x_2, \zeta, t\right) \mathbf{B}_i\left(x_1, x_2, t\right) \tag{42}$$

where $\bar{P}_i$ are unknown 3-D functions to be determined later. The formulation in Eq. (42) is six times redundant because of the way unknown functions are introduced; six constraints are needed to make it unique. The redundancy can be removed by choosing appropriate

definitions of $\mathbf{R}$ and $\mathbf{B}_i$. The first three constraints can be chosen such that the average of each function through the thickness vanishes. Following Refs. [3] and [9], if we define $\hat{\mathbf{R}}$ similarly as Eq. (7) to be average position through the thickness of the deformed configuration, from it follows that the undetermined functions satisfy the three constraints:

$$\left\langle \bar{P}_\alpha \left(x_1, x_2, \zeta, t\right) \right\rangle = 0, \quad \left\langle \bar{P}_3 \left(x_1, x_2, \zeta, t\right) \right\rangle = 0 \tag{43}$$

According to Eqs. (43), $\mathbf{R}$ describes the position vector from point O to the point on the reference surface of the deformed shell. *i.e.*,

$$\mathbf{R}\left(x_1, x_2, t\right) = \mathbf{r}\left(x_1, x_2\right) + \mathbf{u}\left(x_1, x_2, t\right) \tag{44}$$

where $\mathbf{u}\left(x_1, x_2, t\right)$ denote the average shell displacement vector.

Another two constraints can be specified by taking $\mathbf{B}_3$ as the normal to the reference surface of the deformed shell. It is pointed out that this choice is only for convenience in the derivation and has nothing to do with the Kirchhoff assumption.

Definitions of the 2-D generalized strain and inertial velocity measures are needed for calculating the undetermined functions asymptotically. Following Refs. [50, 51] and [52], they can be defined as:

$$\begin{aligned} \mathbf{R}_{,\alpha} &= A_\alpha \left(\mathbf{B}_\alpha + \varepsilon_{\alpha\beta}\mathbf{B}_\beta\right) \\ \dot{\mathbf{R}} &= V_i \mathbf{B}_i \end{aligned} \tag{45}$$

where $\varepsilon_{\alpha\beta}$ are the 2-D in-plane strains and of which the order is denoted by $O(\hat{\varepsilon})$ and V_i are the inertial velocity measures of any material point on the shell reference surface, the order of which is denoted by $O(c\hat{\varepsilon})$. Both $\varepsilon_{\alpha\beta}$ and $\kappa_{\alpha\beta}$ are termed as 2-D generalized strains. On the other hand, both V_i and Ω_α are termed as 2-D inertial generalized velocities. Here one is free to set $\varepsilon_{12} = \varepsilon_{21}$, *i.e.*

$$\frac{\mathbf{B}_1 \cdot \mathbf{R}_{,2}}{A_2} = \frac{\mathbf{B}_2 \cdot \mathbf{R}_{,1}}{A_1} \tag{46}$$

which can serve as another constraint to specify the global rotation of the triad $\mathbf{B}_i$ and make the formulation in Eq. (42) unique.

In accordance with the variational-asymptotic scheme, we substitute Eqs. (42) again into the total energy functional and neglect all small terms containing $\bar{P}_\alpha$ and $\bar{P}_3$ in the

asymptotic sense. Due to the low-frequency assumption Eq. (26), the time derivatives of $\bar{P}_\alpha$ and $\bar{P}_3$ can be removed in the kinetic energy density again. As the result of the foregoing procedure the total potential can be retained as the formally dominant terms in the form

$$2\overline{\mathcal{L}} = -\mu_0 \left\langle \frac{1}{h^2} \bar{P}_{\|\|\zeta}^T D_s^* \bar{P}_{\|\|\zeta} + 2\varepsilon^T D_{et}^* \left(\frac{1}{h} \bar{P}_{3|\zeta} - 1 \right) + D_t^* \left(\frac{1}{h} \bar{P}_{3|\zeta} - 1 \right)^2 \right\rangle \tag{47}$$

where

$$\varepsilon = \lfloor \varepsilon_{11} \;\; 2\varepsilon_{12} \;\; \varepsilon_{22} \rfloor^T$$

The unknown function that maximizes the energy functional expression of Eq. (47), subject to constraint Eqs. (43), can be obtained by applying the usual procedure of the calculus of variations with the aid of Lagrange multipliers. The final result is

$$\begin{aligned} \bar{P}_\alpha &= 0 \\ \bar{P}_3 &= h\zeta \end{aligned} \tag{48}$$

Finally, as a result of the primary step under the low-frequency, long-wavelength approximations, the position vector $\hat{\mathbf{R}}$ can be expressed as

$$\hat{\mathbf{R}}\left(x_1, x_2, \zeta, t\right) = \mathbf{R}\left(x_1, x_2, t\right) + h\zeta \mathbf{B}_3\left(x_1, x_2, t\right) + w_i\left(x_1, x_2, \zeta, t\right) \mathbf{B}_i\left(x_1, x_2, t\right) \tag{49}$$

where the unknown 3-D functions w_i represent the general warping displacement of an arbitrary point on the normal line of the deformed shell, consisting of both in- and out-of-plane components so that all possible deformations are considered (see Fig. 5). According to Eq. (49), the 3-D displacement distributions now can be expressed as a series with respect to $h\zeta$ in the case of low-frequency vibration approximations, just as in statics. However, Eq. (49) are the very beginning point assumptions on which most published shell theories are exclusively developed.

Before proceeding to the first approximation in the next section, it is convenient to redefine corresponding 3-D strain and velocity fields associated with Eq. (49):

$$\begin{aligned} \Gamma_e &= \left[\varepsilon + \zeta\left(h\kappa\right)\right] + I_\alpha w_{\|;\alpha} + C_R^e w_3 + h\zeta \bar{C}_R^e \left[\varepsilon + \zeta\left(h\kappa\right)\right] \\ &\quad + h\zeta \left(H_\alpha w_{\|;\alpha} + \tilde{C}_R^e w_3 \right) \\ 2\Gamma_s &= \frac{1}{h} w_{\|\|\zeta} + e_\alpha w_{3;\alpha} + C_R^s w_\| + h\zeta C_R^s \left(e_\alpha w_{3;\alpha} - C_R^s w_\| \right) \\ \Gamma_t &= \frac{1}{h} w_{3|\zeta} \end{aligned} \tag{50}$$

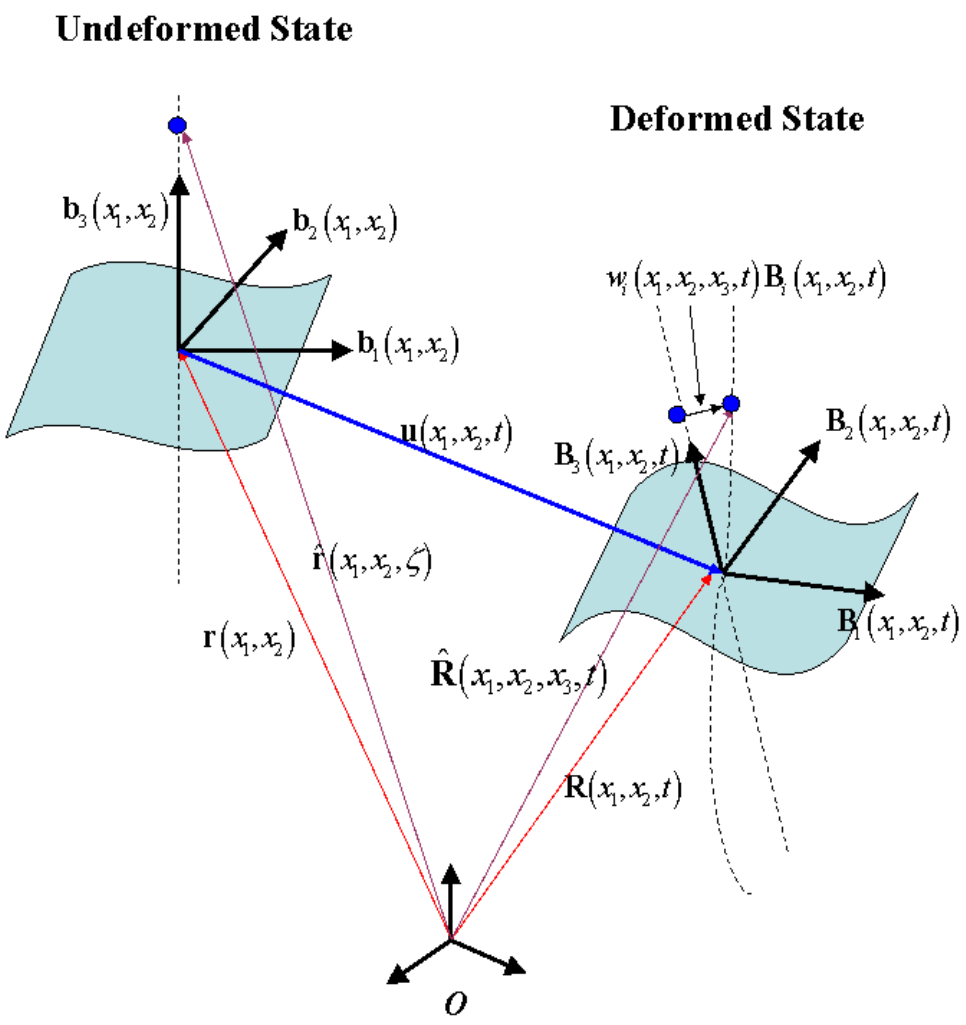

Figure 5: Schematic of shell deformation under the low-frequency vibration area

and

$$\begin{aligned}\Lambda_e &= V_{\|} + \xi\left(h\Omega_{\|}\right) + \dot{w}_{\|} \\ \Lambda_t &= V_3 + \dot{w}_3\end{aligned} \tag{51}$$

with

$$\begin{aligned}\varepsilon &= \lfloor \varepsilon_{11} \;\; 2\varepsilon_{12} \;\; \varepsilon_{22} \rfloor^T \\ h\kappa &= \lfloor h\kappa_{11} \;\; h\left(\kappa_{12} + \kappa_{21}\right) \;\; h\kappa_{22} \rfloor^T\end{aligned} \tag{52}$$

All the operators are defined as:

$$\xi = \begin{bmatrix} 0 & -\zeta \\ \zeta & 0 \end{bmatrix} \tag{53}$$

$$I_1 = \begin{bmatrix} 1 & 0 & 0 \\ 0 & 1 & 0 \end{bmatrix}^T \qquad I_2 = \begin{bmatrix} 0 & 1 & 0 \\ 0 & 0 & 1 \end{bmatrix}^T \tag{54}$$

$$e_1 = \lfloor 1 \;\; 0 \rfloor^T \quad e_2 = \lfloor 0 \;\; 1 \rfloor^T \tag{55}$$

and

$$H_1 = \begin{bmatrix} -k_{11} & 0 & 0 \\ 0 & -k_{11} & 0 \end{bmatrix}^T \qquad H_2 = \begin{bmatrix} 0 & -k_{22} & 0 \\ 0 & 0 & -k_{22} \end{bmatrix}^T \tag{56}$$

$$\bar{C}_R^e = \begin{bmatrix} -k_{11} & 0 & 0 \\ 0 & -k_{11} & 0 \\ 0 & -k_{22} & 0 \\ 0 & 0 & -k_{22} \end{bmatrix}^T \qquad C_R^s = \begin{bmatrix} -k_{11} & 0 \\ 0 & -k_{22} \end{bmatrix}^T \tag{57}$$

$$C_R^e = \lfloor k_{11} \;\; 0 \;\; k_{22} \rfloor^T \qquad \tilde{C}_R^e = \lfloor k_{11}^2 \;\; 0 \;\; k_{22}^2 \rfloor^T \tag{58}$$

With the helps of Yu's methodology [54], one can construct the work done by applied loads in the following way. The virtual displacement is taken as the Lagrangean variation of the displacement field, such that

$$\delta\hat{\mathbf{R}} = \overline{\delta q}_{B_i}\mathbf{B}_i + h\zeta\overline{\delta\psi}_{B_i}\mathbf{B}_i \times \mathbf{B}_3 + \delta w_i\mathbf{B}_i + \overline{\delta\psi}_{B_i}\mathbf{B}_i \times w_j\mathbf{B}_j \tag{59}$$

where the virtual displacement of the reference surface is given by

$$\overline{\delta q}_{B_i} = \delta\mathbf{u} \cdot \mathbf{B}_i \tag{60}$$

and the virtual rotation of the reference surface is defined such that

$$\delta \mathbf{B}_i = \overline{\delta\psi}_{B_j} \mathbf{B}_j \times \mathbf{B}_i \tag{61}$$

The bars in Eq. (59) indicate that these quantities are not necessarily variations of functions. Since the strain is small, one may safely ignore products of the warping and the loading in the virtual rotation term. Then, the work done through a virtual displacement due to the applied loads $\alpha_i \mathbf{B}_i$ on the top surface and $\beta_i \mathbf{B}_i$ at the bottom surface and body force $\phi_i \mathbf{B}_i$ through the thickness is

$$\begin{aligned} \overline{\delta\mathcal{W}} &= \alpha_i \mathbf{B}_i \cdot \delta \mathbf{R}^+ + \beta_i \mathbf{B}_i \cdot \delta \mathbf{R}^- + \langle \phi_i \mathbf{B}_i \cdot \delta \mathbf{R} \rangle \\ &= (\alpha_i + \beta_i + \langle \phi_i \rangle) \, \overline{\delta q}_{B_i} - \delta\psi_{B_i} e_{3ij} \left[\frac{h}{2} (\alpha_j - \beta_j) + \langle x_3 \phi_j \rangle \right] \\ &+ \delta \left(\alpha_i w_i^+ + \beta_i w_i^- + \langle \phi_i w_i \rangle \right) \end{aligned} \tag{62}$$

where α_i, β_i and ϕ_i are taken to be independent of the deformation, $(\bullet)^+ = (\bullet)|_{\zeta=1/2}$, and $(\bullet)^- = (\bullet)|_{\zeta=-1/2}$. By introducing column matrices $\overline{\delta q}$, $\overline{\delta\psi}$, α, β, and ϕ which are formed by stacking the three elements associated with indexed symbols of the same names, and using Eqs. (6) and (19) one may write the virtual work in a matrix form, so that

$$\overline{\delta\mathcal{W}} = \overline{\delta q}^T f + \overline{\delta\psi}^T m + \delta \left(\alpha^T w^+ + \beta^T w^- + \left\langle \phi^T w \right\rangle \right) \tag{63}$$

where

$$\begin{aligned} f &= \alpha + \beta + \langle \phi \rangle \\ m &= \tilde{e}_3 \left[\frac{1}{2} (\alpha - \beta) + \langle \zeta \phi \rangle \right] \end{aligned} \tag{64}$$

with

$$\tilde{e}_3 = \begin{bmatrix} 0 & -1 & 0 \\ 1 & 0 & 0 \\ 0 & 0 & 0 \end{bmatrix} \tag{65}$$

Thus, the work done by applied loads is

$$\overline{\mathcal{V}} = -\alpha_\parallel^T w_\parallel^+ - \alpha_3 w_3^+ - \beta_\parallel^T w_\parallel^- - \beta_3 w_3^- - \left\langle \phi_\parallel^T w_\parallel \right\rangle - \langle \phi_3 w_3 \rangle \tag{66}$$

in which only the warping displacement is varied, subject to the constraints Eqs. (43). Using Eqs. (23), (24) and (66), Eq. (36) can be rewritten as a low-frequency approximation of the

non-dimensional energy functional in terms of

$$
\begin{aligned}
2\overline{\mathcal{K}} = \rho_0 \Big\langle \Big\{ & \left[V_\parallel + \xi\left(h\Omega_\parallel\right) + \dot{w}_\parallel\right]^T \left[V_\parallel + \xi\left(h\Omega_\parallel\right) + \dot{w}_\parallel\right] \\
& + \left[V_3 + \dot{w}_3\right]^2 \Big\} \eta \Big\rangle
\end{aligned}
\tag{67}
$$

and

$$
\begin{aligned}
2\overline{\mathcal{P}} = \mu_0 \Bigg\langle \Bigg\{ & \left[\frac{1}{h} w_{\parallel|\zeta} + e_\alpha w_{3;\alpha} - C_R^s w_\parallel + h\zeta C_R^s \left(e_\alpha w_{3;\alpha} - C_R^s w_\parallel\right)\right]^T D_s^* \\
& \left[\frac{1}{h} w_{\parallel|\zeta} + e_\alpha w_{3;\alpha} + C_R^s w_\parallel + h\zeta C_R^s \left(e_\alpha w_{3;\alpha} + C_R^s w_\parallel\right)\right] + \frac{1}{h^2} D_t^* \left(w_{3|\zeta}\right)^2 \\
& + \frac{2}{h}\left[\varepsilon + \zeta\left(h\kappa\right) + I_\alpha w_{\parallel;\alpha} + C_R^e w_3 + h\zeta\left(H_\alpha w_{\parallel;\alpha} + \tilde{C}_R^e w_3\right)\right]^T D_{et}^* w_{3|\zeta} \\
& + \Big[\varepsilon + \zeta\left(h\kappa\right) + I_\alpha w_{\parallel;\alpha} + C_R^e w_3 + h\zeta \bar{C}_R^e \left(\varepsilon + \zeta\left(h\kappa\right)\right) \\
& + h\zeta\left(H_\alpha w_{\parallel;\alpha} + \tilde{C}_R^e w_3\right)\Big]^T D_e^* \Big[\varepsilon + \zeta\left(h\kappa\right) + I_\alpha w_{\parallel;\alpha} + C_R^e w_3 \\
& + h\zeta \bar{C}_R^e \left(\varepsilon + \zeta\left(h\kappa\right)\right) + h\zeta\left(H_\alpha w_{\parallel;\alpha} + \tilde{C}_R^e w_3\right)\Big]\Bigg\} \eta\Bigg\rangle - \alpha_\parallel^T w_\parallel^+ - \alpha_3 w_3^+ \\
& - \beta_\parallel^T w_\parallel^- - \beta_3 w_3^- - \left\langle \phi_\parallel^T w_\parallel \right\rangle - \left\langle \phi_3 w_3 \right\rangle
\end{aligned}
\tag{68}
$$

Now one is ready to use the VAM to solve the unknown warping field asymptotically.

2.3.2 First approximation (First-order warping field)

The VAM requires one to find the leading terms of the functional according to the different orders. The total energy functional consists of quadratic expressions involving both warping and 2-D generalized strains and velocities. In addition, there are terms that involve the loading along with interaction terms between the warping and the both of the other types of quantities. Since only the warping is varied, one needs the leading terms that involve warping only and the leading terms that involve the warping and other quantities (*i.e.* the generalized strain and velocity, and loading). Following Refs. [3] and [55], one can

summarize the orders of the interested quantities:

$$\begin{aligned} V_i &\sim O\left(c\hat{\varepsilon}\right) \\ \Omega_\alpha &\sim O\left(c\hat{\varepsilon}/l\right) \\ \varepsilon_{\alpha\beta} \sim h\kappa_{\alpha\beta} &\sim O\left(\hat{\varepsilon}\right) \\ f_3 &\sim O\left(\mu\left(h/l\right)^2\hat{\varepsilon}\right) \\ f_\alpha &\sim O\left(\mu\left(h/l\right)\hat{\varepsilon}\right) \\ m_\alpha &\sim O\left(\mu h^2\hat{\varepsilon}/l\right) \end{aligned} \tag{69}$$

where μ is the order of the material constants.

Therefore, the leading terms of Eq. (36) for the first approximation are given by

$$2\overline{\mathcal{L}} = -\mu_0 \left\langle \frac{1}{h^2}\left(w_{|||\zeta}^T D_s^* w_{|||\zeta} + D_t^* w_{3|\zeta}^2\right) + \frac{2}{h}\left[\varepsilon + \zeta\left(h\kappa\right)\right]^T D_{et}^* w_{3|\zeta} \right\rangle \tag{70}$$

The warping field that maximizes the energy functional expression of Eq. (70), subject to constraint Eqs. (43), can be obtained by applying the usual procedure of the calculus of variations with the aid of Lagrange multipliers. The resulting warping is

$$\begin{aligned} w_\alpha &= 0 \\ w_3 &= h\bar{D}_1\varepsilon + h\bar{D}_2\left(h\kappa\right) \end{aligned} \tag{71}$$

where

$$\bar{D}_{1|\zeta} = -D_{et}^{*T}/D_t^*, \quad \bar{D}_{2|\zeta} = -\zeta D_{et}^{*T}/D_t^* \tag{72}$$

with

$$\langle \bar{D}_1 \rangle = 0, \quad \langle \bar{D}_2 \rangle = 0 \tag{73}$$

Note that inter-lamina continuity of $\bar{D}_1$ and $\bar{D}_2$ must be maintained because of the continuity of warping functions that are needed, in turn, to produce a continuous displacement field. This solution is the same as that derived by the VAM in Refs. [44, 56].

2.3.3 Total energy functional for low-frequency vibrations

Before closing in this section for performing short-wave extrapolation it is convenient to find the total energy functional of low-frequency vibrations in the long-wavelength regime.

Substituting Eq. (71) back into the total energy functional Eq. (36), one can obtain the total energy functional asymptotically correct up to the zeroth-order approximation as

$$\overline{\mathcal{L}} = \frac{1}{2}\rho_0 \left\langle \left(V_\parallel^T V_\parallel + V_3^2 \right) \right\rangle - \frac{1}{2}\mu_0 \left\langle \left[\varepsilon + \zeta \left(h\kappa \right) \right]^T D_c^* \left[\varepsilon + \zeta \left(h\kappa \right) \right] \right\rangle \tag{74}$$

where

$$D_c^* = D_e^* - D_{et}^* D_{et}^{*T} / D_t^* \tag{75}$$

The energy functional of this approximation coincides with classical laminated shell theories, just as in statics.

2.4 High-frequency, Long-wavelength Vibration Approximations

In the classical theory of low-frequency vibrations, the 2-D total energy functional Eq. (74) relies only on the three functions $\mathbf{u}$, which describe the average displacement field of the shell, just as in statics. Following the terminology introduced by Le [9], these functions will subsequently be called "*external*" degrees of freedom, since their characteristics totally depend on the kinematics of the reference surface of the deformed shell. As the frequency increases, it is obvious to assume that some "*internal*" degrees of freedom associated with branches of the shell high-frequency vibrations will be took effect and have more and more influence over a total energy functional, so that we should figure out the general way how to obtain those fields corresponding to the internal degrees of freedom and then how to include those as variables in the 2-D kinetic and potential energy densities without introducing any mystic assumptions. To do so the variational-asymptotic procedure will be used. Let us analyze the vibrations of monoclinic laminated composite shells under high-frequency, long-wavelength approximations.

2.4.1 Primary approximation

Now, we are ready to determine the constraints and the orders of the yet-to-be-determined displacement field of a shell undergoing high-frequency, long-wavelength vibrations. In contrast to the case of low-frequency vibrations, the kinetic energy density must now be retained in the primary step of the variational-asymptotic procedure since the frequencies

are no longer small due to Eq. (27). Therefore, from Eq. (36) we obtain the functional

$$2\overline{\mathcal{L}} = \rho_0 \left\langle \left(\dot{P}_{\|}^T \dot{P}_{\|} + \dot{P}_3^2 \right) \right\rangle - \mu_0 \left\langle \frac{1}{h^2} P_{\|\|\zeta}^T D_s^* P_{\|\|\zeta} + \frac{1}{h^2} D_t^* P_{3|\zeta}^2 \right\rangle \tag{76}$$

Calculating the variation of Eq. (76) and setting the variations of P_α, P_3 at t_1 and t_2 equal to zero, the stationary points of the energy functional fall into two classes: i) the out-of-plane displacement P_3 is much greater than the in-plane displacements P_α and ii) the in-plane displacements P_α are much greater than the out-of-plane P_3. These correspond to four series of vibrations as will be seen presently. Following the terminology introduced by Mindlin [27], one class is the series of thickness-extension vibrations characterized by

$$P_\alpha \left(x_1, x_2, \zeta, t \right) = 0, \quad P_3 \left(x_1, x_2, \zeta, t \right) = q \left(\zeta \right) \psi_3 \left(x_1, x_2, t \right) \tag{77}$$

where $q\left(\zeta\right)$ corresponds to the odd and even solutions of the following 1-D through-thickness variational problem

$$\left\langle D_t^* q_{|\zeta} \, \delta q_{|\zeta} - \beta_{t0}^2 q \delta q \right\rangle = 0 \tag{78}$$

with

$$\beta_{t0} = \beta_{30} = \frac{\omega_3 h}{c_0}$$

The series with odd solutions is denoted by $L_\perp$ (symmetric thickness-extension vibrations), and that with even solutions by $F_\perp$ (anti-symmetric thickness-extension vibrations). For the case of homogeneous and isotropic material,

$$\begin{aligned} L_\perp(n): &\quad q(\zeta) = \sin \alpha\zeta \qquad \alpha = \pi(2n+1) \\ F_\perp(n): &\quad q(\zeta) = \cos \beta\zeta \qquad \beta = 2\pi n \end{aligned} \tag{79}$$

As expected, the branch $F_\perp(0)$ corresponds to low-frequency vibration. Fig. 6 shows graphs of $L_\perp(0)$, $F_\perp(1)$ and $L_\perp(1)$ through the thickness of the shell. Another class is the series of thickness-shear vibrations characterized by

$$P_\alpha \left(x_1, x_2, \zeta, t \right) = p_{\alpha\beta} \left(\zeta \right) v_\beta \left(x_1, x_2, t \right), \quad P_3 \left(x_1, x_2, \zeta, t \right) = 0 \tag{80}$$

where $p_{\alpha\beta}\left(\zeta\right)$ correspond to the odd or even solutions of the following 1-D variational problems

$$\left\langle \mathrm{p}_{|\zeta}^T D_s^* \delta \mathrm{p}_{|\zeta} - \beta_{s0}^2 \mathrm{p}^T \delta \mathrm{p} \right\rangle = 0 \tag{81}$$

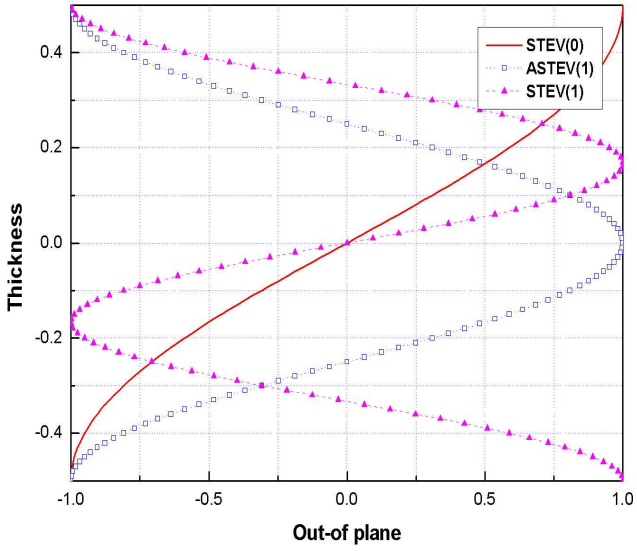

Figure 6: Eigenvectors of $L_\perp(0)$, $F_\perp(1)$ and $L_\perp(1)$

where

$$\beta_{s0} = \begin{bmatrix} \beta_{10} & 0 \\ 0 & \beta_{20} \end{bmatrix} = \begin{bmatrix} \dfrac{\omega_1 h}{c_0} & 0 \\ 0 & \dfrac{\omega_2 h}{c_0} \end{bmatrix}$$

and $\mathrm{p}\,(\zeta)$ is the 2×2 matrix, the components of which are $p_{\alpha\beta}$. Similar to the thickness-extension branches, the series with the odd solutions is denoted by $F_\parallel$ (asymmetric thickness-shear vibrations), and that with even solutions by $L_\parallel$ (symmetric thickness-shear vibrations). For elastic shells made of homogeneous and isotropic material, $F_\parallel$ and $L_\parallel$ can be expressed as:

$$\begin{aligned} F_\parallel(n): &\quad p_{11}(\zeta) = \sin\alpha\zeta \qquad \alpha = \pi(2n+1) \\ L_\parallel(n): &\quad p_{11}(\zeta) = \cos\beta\zeta \qquad \beta = 2\pi n \end{aligned} \tag{82}$$

Analogously, the branch $L_\parallel(0)$ corresponds to the low-frequency vibration. Fig. 7 shows graphs of $F_\parallel(0)$, $L_\parallel(1)$ and $F_\parallel(1)$ through the thickness of the shell.

The characteristic eigenvalues β_{t0}^2 and β_{s0}^2 run through a countable set of values; however, indices are attached neither to them nor to the corresponding eigenvectors in order to avoid complicating the notation. Since $q\,(\zeta)$ and $p_{\alpha\beta}\,(\zeta)$ are determined uniquely up to a constant

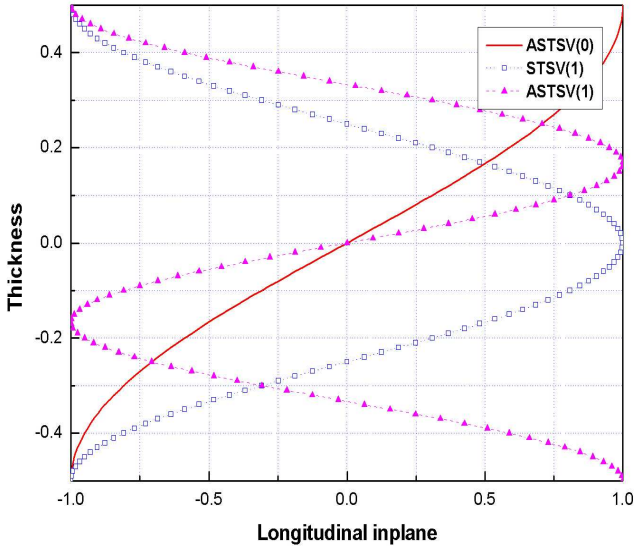

Figure 7: Eigenvectors of $F_{\|}(0)$, $L_{\|}(1)$ and $F_{\|}(1)$

from Eqs. (78) and (81), the following normalization conditions can be imposed

$$\langle q^2 \rangle = 1, \quad \langle \mathrm{p}^T \mathrm{p} \rangle = \mathrm{I} \tag{83}$$

where I is the 2×2 identity matrix. The constants are chosen so as to simplify later the changes of variable (see Section 2.5). Furthermore, in each particular solution the functions ψ_3, v_α are dependent arbitrarily on the in-plane coordinates x_α and harmonically on t with frequencies ω_3, ω_α determined from the appropriate values of β_3 and β_α, respectively, according to

$$\omega_3 = \frac{\beta_3 c_3}{h} = \frac{\beta_{30} c_0}{h}, \quad \omega_\alpha = \frac{\beta_\alpha c_\alpha}{h} = \frac{\beta_{\alpha 0} c_0}{h} \tag{84}$$

where in Eqs. (84), the summation convention is not applied because α is not a dummy index. (For homogeneous, isotropic materials, $c_3 = \sqrt{\lambda + 2\mu/\rho}$ and $c_\alpha = \sqrt{\mu/\rho}$ are the velocities of dilatational and shear waves, respectively). On the other hand, for functions ψ_3, v_α independent of in-plane coordinates x_α, each of the solutions given above represents an exact solution of 3-D dynamic equations of elasticity for an infinite plate and correspond to synchronized vibrations of transverse fibres along the plate (with the zero in-plane wave

number). The frequencies of Eqs. (84) are called cut-off frequencies. As expected, for vibrations whose amplitude and frequency vary slowly in the in-plane coordinates, Eqs. (78) and (81) can be regarded as the primary approximation. Eqs. (77) and (80) can be considered as the leading terms in a certain asymptotic expansion in which ψ_3, v_α are functions of x_α and t, so that

$$\ddot{\psi}_3 \approx -\omega_3^2 \psi_3, \quad \ddot{v}_\alpha \approx -\omega_\alpha^2 v_\alpha \tag{85}$$

The values of ω_α and ω_3 in these estimations are taken for the same branch as the corresponding function, with the exception of $F_\perp(0)$ and $L_\parallel(0)$, for which it is assumed that $\dot{\psi}_3 \sim c_0 \psi_3 / l$, $\dot{v}_\alpha \sim c_0 v_\alpha / l$, where l is the smallest wavelength of the deformation patterns. As expected, the branches $F_\perp(0)$ and $L_\parallel(0)$ correspond to the low-frequency vibrations in Eq. (26). The independence of the displacements in these branches from $h\zeta$ in the zeroth approximation is an aspect of the Kirchhoff-Love hypothesis. On the other hand, all the remaining branches correspond to high-frequency vibrations with Eq. (27). Therefore, since $\omega_3,\ \omega_\alpha \to \infty$ as $h \to 0$, the corresponding vibrations are naturally called high-frequency (thickness) vibrations. Finally, using the results of the previous section, the position vector $\hat{\mathbf{R}}$ can be represented as

$$\begin{aligned} \hat{\mathbf{R}}(x_1, x_2, \zeta, t) &= \mathbf{R}(x_1, x_2, t) + h\zeta \mathbf{B}_3(x_1, x_2, t) + q(\zeta)\, \psi_3(x_1, x_2, t)\, \mathbf{B}_3(x_1, x_2, t) \\ &\quad + p_{\alpha\beta}(\zeta)\, v_\beta(x_1, x_2, t)\, \mathbf{B}_\beta(x_1, x_2, t) + w_i(x_1, x_2, \zeta, t)\, \mathbf{B}_i(x_1, x_2, t) \\ &= \mathbf{R}(x_1, x_2, t) + h\zeta \mathbf{B}_3(x_1, x_2, t) + P_i(x_1, x_2, \zeta, t)\, \mathbf{B}_i(x_1, x_2, t) \end{aligned} \tag{86}$$

where

$$\begin{aligned} \mathbf{P}(x_1, x_2, \zeta, t) &= q(\zeta)\, \psi_3(x_1, x_2, t)\, \mathbf{B}_3(x_1, x_2, t) + p_{\alpha\beta}(\zeta)\, v_\beta(x_1, x_2, t)\, \mathbf{B}_\beta(x_1, x_2, t) \\ &\quad + w_i(x_1, x_2, \zeta, t)\, \mathbf{B}_i(x_1, x_2, t) \end{aligned} \tag{87}$$

Here w_i are the unknown 3-D warping functions for the high-frequency vibration approximations. Unlike the three constraints used in the low-frequency vibrations, the three new constraints may be needed to calculate w_i, which will be discussed in detail in the next section.

According to Ref. [36], the propagation time for a perturbation through the thickness for these branches of vibrations is of the same order as the period of vibrations. Therefore,

for most published plate and shell theories it is impossible to assume the displacements to be only polynomials in $h\zeta$ even in a primary approximation (see Eq. (86)). For instance, the lowest branch of the thickness-shear vibrations $F_{\|}(0)$ is associated with vibrations for which a shift of the transverse fiber into the half-wave of a sinusoid occurs. Generalized Reissner-Mindlin plate/shell theories are representative of this type of theories that take this kind of vibration into account. However, utilization of a linear displacement field over the thickness instead of the correct sinusoid in a generalized Reissner-Mindlin plate/shell theory does not lead to a satisfactory quantitative prediction of the actual behavior.

Analogously, having made the above approximations, using Eq. (86) instead of Eq. (49) and eliminating the effects of the low-frequency vibrations from Eqs. (23), (24) and (66), Eq. (36) can be rewritten as a non-dimensional, high-frequency energy functional in terms of

$$2\overline{\mathcal{K}} = \rho_0 \left\langle \left(\dot{P}_{\|}^T \dot{P}_{\|} + \dot{P}_3^2 \right) \eta \right\rangle \tag{88}$$

and

$$\begin{aligned} 2\overline{\mathcal{P}} = \mu_0 \Bigg\langle \Bigg\{ & \left[\frac{1}{h} P_{\|\|\zeta} + e_\alpha P_{3;\alpha} - C_R^s P_{\|} + h\zeta C_R^s \left(e_\alpha P_{3;\alpha} - C_R^s P_{\|} \right) \right]^T D_s^* \left[\frac{1}{h} P_{\|\|\zeta} + e_\alpha P_{3;\alpha} \right. \\ & \left. + C_R^s P_{\|} + h\zeta C_R^s \left(e_\alpha P_{3;\alpha} + C_R^s P_{\|} \right) \right] + \frac{1}{h^2} D_t^* \left(p_{3|\zeta} \right)^2 + \frac{2}{h} \left[I_\alpha P_{\|;\alpha} + C_R^e P_3 \right. \\ & \left. + h\zeta \left(H_\alpha P_{\|;\alpha} + \tilde{C}_R^e P_3 \right) \right]^T D_{et}^* P_{3|\zeta} + \left[I_\alpha P_{\|;\alpha} + C_R^e P_3 + h\zeta \left(H_\alpha P_{\|;\alpha} + \tilde{C}_R^e P_3 \right) \right]^T \\ & D_e^* \left[I_\alpha P_{\|;\alpha} + C_R^e P_3 + h\zeta \left(H_\alpha P_{\|;\alpha} + \tilde{C}_R^e P_3 \right) \right] \Bigg\} \eta \Bigg\rangle - \alpha_{\|}^T P_{\|}^+ - \alpha_3 P_3^+ \\ & - \beta_{\|}^T P_{\|}^- - \beta_3 P_3^- - \left\langle \phi_{\|}^T P_{\|} \right\rangle - \langle \phi_3 P_3 \rangle \end{aligned} \tag{89}$$

Now one is ready to use the VAM to solve the unknown warping field for high-frequency vibrations asymptotically.

2.4.2 First approximation (First-order warping field)

According to Ref. [32], it turns out that the branches possess a remarkable property: they are orthogonal in the kinetic and strain energy densities in the first approximation. This means that in a first approximation vibrations of one type do not interact with vibrations of other types, and the possibility appears for investigating the vibrations of one branch

independently of the vibrations of the others (except for the classical branches describing low-frequency vibrations). As before, the variations of v_α, ψ_3 should vanish at t_1, t_2, just as in the case of low-frequency vibrations. Concerning the boundary conditions at the shell edge, we first consider the clamped edge, for which

$$p_{\alpha\beta}v_\beta = 0 \qquad q\psi_3 = 0 \quad \text{at}, \quad \partial S \times (-1/2 \quad 1/2) \tag{90}$$

Based on the above fact, we can find the next refinement for the warping fields in the branches associated with the thickness-extension vibrations (the series $L_\perp$ or $F_\perp$). At this step we seek the stationary w_i of Eq. (36) in the form

$$\begin{aligned} P_\alpha &= w_\alpha\left(x_1, x_2, \zeta, t\right) \\ P_3 &= q\left(\zeta\right)\psi_3\left(x_1, x_2, t\right) + w_3\left(x_1, x_2, \zeta, t\right) \\ &= P_{30} + w_3\left(x_1, x_2, \zeta, t\right) \end{aligned} \tag{91}$$

where ψ_3 is regarded as one branch of this series as a given function of x_α and t satisfying the condition due to Eq. (90), namely

$$\psi_3 = 0 \quad \text{at} \quad \partial S \tag{92}$$

while w_α and w_3 are unknown functions that should be determined by the variational-asymptotic procedure. Without any loss of generality, the following constraint can be imposed on $\overline{w}_3$:

$$\left\langle q\left(\zeta\right) w_3 \right\rangle = 0 \tag{93}$$

which corresponds to the assumption that $\psi_3 = \left\langle q\left(\zeta\right) P_3 \right\rangle$. Let us substitute Eqs. (91) into the non-dimensional kinetic and potential energies per unit area as Eqs. (88) and (89), and then the total energy functional Eq. (36). With the help of VAM and keeping the leading terms that depend on w_i and the leading cross terms in Eq. (36), we obtain the functional

$$\begin{aligned} 2\overline{\mathcal{L}} = \rho_0 &\left\langle \left[\dot{w}_\parallel^T\dot{w}_\parallel + \dot{w}_3^2 + \underline{2\dot{P}_{30}\dot{w}_3} + 4H\zeta w_3\dot{w}_3\right]\right\rangle \\ &- \mu_0\left\langle \frac{1}{h^2}\left[w_{\parallel\vert\zeta}^T D_s^* w_{\parallel\vert\zeta} + D_t^* w_{3\vert\zeta}^2 + \underline{2D_t^* P_{30\vert\zeta} w_{3\vert\zeta}}\right]\right. \\ &+ \frac{2}{h}\left[w_{\parallel\vert\zeta}^T D_s^* e_\alpha P_{30;\alpha} - \underline{\underline{w_\parallel^T I_\alpha^T D_{et}^* P_{30\vert\zeta\,;\alpha}}} + 2H D_t^*\zeta P_{30} w_{3\vert\zeta}\right. \\ &\left.\left. + w_{3\vert\zeta}^T D_{et}^{*T} C_R^e P_{30} + w_3 C_R^{eT} D_{et}^* P_{30\vert\zeta}\right]\right\rangle \end{aligned} \tag{94}$$

Here the underlined terms will cancel out each other because of Eq. (78). The double-underlined term was obtained using integration by parts, and the terms evaluated at the boundary vanish due to Eq. (92). Thus, the above 3-D problem can be reduced to a 1-D through-the-thickness problem that does not depend on partial derivatives of w_α and w_3 with respect to x_α and t, and the last ζ enters in only as a parameter. First, the stationary points w_α of Eq. (94) are easily found to be

$$w_\alpha = hs_{\alpha\beta}\left(\zeta\right)\psi_{3;\beta} \tag{95}$$

where $s_{\alpha\beta}\left(\zeta\right)$ are solutions of the variational problems

$$\left\langle \mathrm{s}^T_{\alpha|\zeta} D^*_s \delta\mathrm{s}_{\beta|\zeta} + qe^T_\alpha D^*_s \delta\mathrm{s}_{\beta|\zeta} - q_{|\zeta} D^{*T}_{et} I_\alpha \delta\mathrm{s}_\beta - \beta^2_{t0}\mathrm{s}^T_\alpha \delta\mathrm{s}_\beta \right\rangle = 0 \tag{96}$$

where s_α are the 2×1 matrices, components of which are $s_{\alpha\beta}$. Next, let us seek the correction w_3 to P_3, which has the form

$$w_3 = h\tau_R\left(\zeta\right)\psi_3 \tag{97}$$

where $\tau_R\left(\zeta\right)$ is the solution of the variational problem

$$\begin{aligned}&\left\langle D^*_t \tau_{R|\zeta}\,\delta\tau_{R|\zeta} + 2H\zeta D^*_t q_{|\zeta}\;\delta\tau_{R|\zeta} + qC^{eT}_R D^*_{et}\delta\tau_{R|\zeta} + q_{|\zeta} D^{*T}_{et} C^e_R \delta\tau_R \right.\\ &\left. -\beta^2_{t0}\left[\tau_R\delta\tau_R + 2H\zeta q\delta\tau_R\right]\right\rangle = 0\end{aligned} \tag{98}$$

subject to the constraint

$$\left\langle q\tau_R\right\rangle = 0 \tag{99}$$

As expected, the in-plane warping functions turn out to be much smaller than the out-of-plane displacement in the long-wavelength regime and are $O\left(h\hat{q}/l\right)$, and the refinement w_3 to the original out-of-plane displacement is of the order $O\left(h\hat{q}/R\right)$ when the out-of-plane displacement is $O\left(\hat{q}\right)$. Summarizing, we have the following distribution of the warping fields over the thickness in the series of thickness-extension vibrations (in the first approximation):

$$\begin{aligned}P_\alpha &= hs_{\alpha\beta}\left(\zeta\right)\psi_{3;\beta}\\ P_3 &= q\left(\zeta\right)\psi_3 + h\tau_R\left(\zeta\right)\psi_3\end{aligned} \tag{100}$$

Analogously, we also find the next refinement for the warping fields in the branches associated with the thickness-shear vibrations (the series $L_\parallel$ or $F_\parallel$). Given v_α, we seek w_α

and w_3 in the first approximation for one branch of this series:

$$\begin{aligned} P_\alpha(x_1,x_2,\zeta,t) &= p_{\alpha\beta}(\zeta)\, v_\alpha(x_1,x_2,t) + w_\alpha(x_1,x_2,\zeta,t) \\ &= P_{\alpha 0} + w_\alpha(x_1,x_2,\zeta,t) \\ P_3(x_1,x_2,\zeta,t) &= w_3(x_1,x_2,\zeta,t) \end{aligned} \tag{101}$$

in which, without any loss of generality, v_α are regarded as one branch of this series as given functions of x_α and t, satisfying the following condition due to Eq. (90):

$$v_\alpha = 0 \quad \text{at} \quad \partial S \tag{102}$$

Here w_α and w_3 should be determined by the variational-asymptotic procedure and satisfy the constraints

$$\langle p_{\alpha\beta}(\zeta)\, w_\beta \rangle = 0 \tag{103}$$

Discarding the small terms of w_3 and the small cross terms, we obtain the functional

$$\begin{aligned} 2\overline{\mathcal{L}} = {} & \rho_0 \left\langle \left[\dot{w}_3^2 + \dot{w}_\parallel^T \dot{w}_\parallel + \underline{2\dot{w}_\parallel^T \dot{P}_{\parallel 0}} + 4H\dot{w}_\parallel^T \zeta \dot{P}_{\parallel 0} \right] \right\rangle \\ & - \mu_0 \left\langle \frac{1}{h^2} \left[D_t^* w_{3|\zeta}^2 + w_{|||\zeta}^T D_s^* w_{|||\zeta} + \underline{2 w_{|||\zeta}^T D_s^* P_{\parallel 0|\zeta}} \right] \right. \\ & + \frac{2}{h} \left[w_{3|\zeta} D_{et}^{*T} I_\alpha P_{\parallel 0;\alpha} - \underline{\underline{w_3 e_\alpha^T D_s^* P_{\parallel 0|\zeta;\alpha}}} + 2H w_{|||\zeta}^T D_s^* \zeta P_{\parallel 0|\zeta} \right. \\ & \left. \left. + w_\parallel^T C_R^{sT} D_s^* P_{\parallel 0|\zeta} + w_{|||\zeta}^T D_s^* C_R^s P_{\parallel 0} \right] \right\rangle \end{aligned} \tag{104}$$

Following the same procedure as in the previous step, the cross (underlined) terms of the order h^{-2} in Eq. (104) vanish due to Eq. (81), and for the double-underlined term, integration by parts was performed taking into account that $v_\alpha = 0$ at the boundary due to Eq. (103). The stationary point w_3 is easily found to have the form

$$w_3 = h r_{\alpha\beta}(\zeta)\, v_{\alpha;\beta} \tag{105}$$

where $r_{\alpha\beta}(\zeta)$ are the solutions of the following variational problems

$$\left\langle \mathrm{r}_{\alpha|\zeta}^T D_t^* \delta \mathrm{r}_{\beta|\zeta} + \mathrm{p}^T I_\alpha^T D_{et}^* \delta \mathrm{r}_{\beta|\zeta} - \mathrm{p}_{|\zeta}^T D_s^* e_\alpha \delta \mathrm{r}_\beta - \beta_{s0}^2 \mathrm{r}_\alpha^T \delta \mathrm{r}_\beta \right\rangle = 0 \tag{106}$$

Here r_α are the 1×2 matrices, components of which are $r_{\alpha\beta}$. As before, for the thickness-shear vibrations, the out-of-plane warping function is much smaller than the in-plane displacements and is of the order $O(h\hat{q}/l)$. Again, the stationary point w_α is of the order

$O\left(h\hat{q}/R\right)$ and should have the form

$$w_\alpha = h\varphi_{R\alpha\beta}v_\beta \tag{107}$$

where $\varphi_{R\alpha\beta}\left(\zeta\right)$ are solutions of the variational problems

$$\begin{aligned}&\Big\langle\varphi_{R|\zeta}^T D_s^*\delta\varphi_{R|\zeta} + 2H\zeta \mathrm{p}_{|\zeta}^T D_s^*\delta\varphi_{R|\zeta} + \mathrm{p}_{|\zeta}^T D_s^* C_R^s\delta\varphi_R + \mathrm{p}^T C_R^{sT} D_s^*\delta\varphi_{R|\zeta}\\ &-\beta_{s0}^2\left[\varphi_R^T\delta\varphi_R + 2H\zeta\mathrm{p}^T\delta\varphi_R\right]\Big\rangle = 0\end{aligned} \tag{108}$$

where φ_R is the 2×2 matrix, each components of which is $\varphi_{R\alpha\beta}$. Thus, for the series of thickness-shear vibrations (within the first approximation) we have

$$\begin{aligned}P_\alpha &= p_{\alpha\beta}\left(\zeta\right)v_\beta + h\varphi_{R\alpha\beta}\left(\zeta\right)v_\beta\\ P_3 &= hr_{\alpha\beta}\left(\zeta\right)v_{\alpha;\beta}\end{aligned} \tag{109}$$

By continuing the iteration process, the next corrections to P_α and P_3 for each of the branches can be found. However, since they do not contribute to the total energy functional of the first approximation, we do not need to go any further.

2.4.3 Total energy functional for high-frequency vibrations

Before proceeding to hyperbolic short-wavelength extrapolation in the next section, it is convenient to find the total Lagrangean of each branch in the long-wavelength regime. Let the 3-D displacements P_α, P_3 be expressed by the infinite series of branches given above, where ψ_3, v_α are arbitrary functions in terms of x_α and t.

We first examine a branch in the series of thickness-extension vibrations, displacements of which are given by the asymptotic formulae in Eqs. (100). Substituting Eqs. (100) into Eqs. (88) and (89), keeping the leading quadratic terms and the leading cross terms, and using Eqs. (78), (96) and (98), we obtain the total energy functional $\overline{\mathcal{L}}_t$ defined as in Eq. (36) for thickness-extension vibrations within the first approximation:

$$\overline{\mathcal{L}}_t = \frac{1}{2}\rho_0\left[\dot{\psi}_3^2\right] - \frac{1}{2}\mu_0\left[\left(\frac{1}{h^2}\beta_{t0}^2 + \overline{\mathrm{I}}^t\right)\psi_3^2 + \overline{\mathrm{K}}_{\alpha\beta}^t\psi_{3;\alpha}\psi_{3;\beta}\right] + \overline{\mathrm{F}}^t\psi_3 \tag{110}$$

where the coefficients are of the form

$$\begin{aligned}
\overline{\mathrm{I}}^t &= \Big\langle C_R^{eT} D_e^* C_R^e q^2 + K D_t^* \left(\zeta q_{|\zeta}\right)^2 + 4H C_R^{eT} D_{et}^* \left(\zeta q q_{|\zeta}\right) \\
&\quad + 2\tilde{C}_R^{eT} D_{et}^* \left(\zeta q q_{|\zeta}\right) - D_t^* \tau_{R|\zeta}^2 + \beta_{t0}^2 \left[\tau_R^2 - K\left(\zeta q\right)^2\right] \Big\rangle \\
\overline{\mathrm{K}}_{\alpha\beta}^t &= \Big\langle e_\alpha^T D_s^* e_\beta q^2 + \mathrm{s}_{\alpha|\zeta}^T D_s^* e_\beta q - \mathrm{s}_\beta^T I_\alpha^T D_{et}^* q_{|\zeta} \Big\rangle \\
\overline{\mathrm{F}}^t &= \alpha_3 q^+ + \beta_3 q^- + \langle \phi_3 q \rangle
\end{aligned} \tag{111}$$

Analogously, we turn to a branch in the series of thickness-shear vibrations, displacements of which are given by the asymptotic formulae in Eqs. (109). Again substituting Eqs. (100) into Eq. (36), discarding the small quadratic terms and the small cross terms (i.e. of order h/R and h/l compared with unity), and using Eqs. (81), (106) and (108), we get the total energy functional $\overline{\mathcal{L}}_s$ defined as in Eq. (36) for thickness-shear vibrations:

$$\overline{\mathcal{L}}_s = \frac{1}{2}\rho_0 \left[\dot{v}_\parallel^T \dot{v}_\parallel\right] - \frac{1}{2}\mu_0 \left[v_\parallel^T \left(\frac{1}{h^2}\beta_{s0}^2 + \overline{\mathrm{I}}^s\right) v_\parallel + v_{\parallel;\alpha}^T \overline{\mathrm{K}}_{\alpha\beta}^s v_{\parallel;\beta}\right] + \overline{\mathrm{F}}^{sT} v_\parallel \tag{112}$$

where the coefficients are given by

$$\begin{aligned}
\overline{\mathrm{I}}^s &= \Big\langle \mathrm{p}^T C_R^{sT} D_s^* C_R^s \mathrm{p} + K\zeta^2 \mathrm{p}_{|\zeta}^T D_s^* \mathrm{p}_{|\zeta} + 4H\zeta \mathrm{p}_{|\zeta}^T D_s^* C_R^s \mathrm{p} \\
&\quad + 2\zeta \mathrm{p}_{|\zeta}^T D_s^* C_R^s C_R^s \mathrm{p} - \varphi_{R|\zeta}^T D_s^* \varphi_{R|\zeta} + \beta_{s0}^2 \left[\varphi_R^T \varphi_R - K\zeta^2 \mathrm{p}^T \mathrm{p}\right] \Big\rangle \\
\overline{\mathrm{K}}_{\alpha\beta}^s &= \Big\langle \mathrm{p}^T I_\alpha^T D_e^* I_\beta \mathrm{p} + \mathrm{p}^T I_\alpha^T D_{et}^* \mathrm{r}_{\beta|\zeta} - \mathrm{p}_{|\zeta}^T D_s^* e_\alpha \mathrm{r}_\beta \Big\rangle \\
\overline{\mathrm{F}}^s &= \alpha_\parallel^T \mathrm{p}_\parallel^+ + \beta_\parallel^T \mathrm{p}_\parallel^- + \Big\langle \phi_\parallel^T \mathrm{p}_\parallel \Big\rangle
\end{aligned} \tag{113}$$

Finally, we obtain the asymptotically correct, 2-D dynamical equations for the high-frequency, long-wavelength regime up to the first approximation, Eqs. (110) and (112). In addition to the leading terms containing the factor h^{-2} in the strain energy per unit area we also keep terms of the next order of smallness in the total energy functional, Eqs. (110) and (112), because, at the cut-off frequencies, the leading terms, though not small individually, almost cancel out each other. For the case of homogeneous and isotropic materials, Eqs. (110) and (112) coincide with those of Ref. [35] derived by the asymptotic method of Goldenveizer and of Ref. [16] derived by the VAM.

It is interesting to note that, following Ref. [9], even though Eqs. (110) and (112) are the correct equations in an asymptotic analysis, it does not always lead to a well-posed boundary

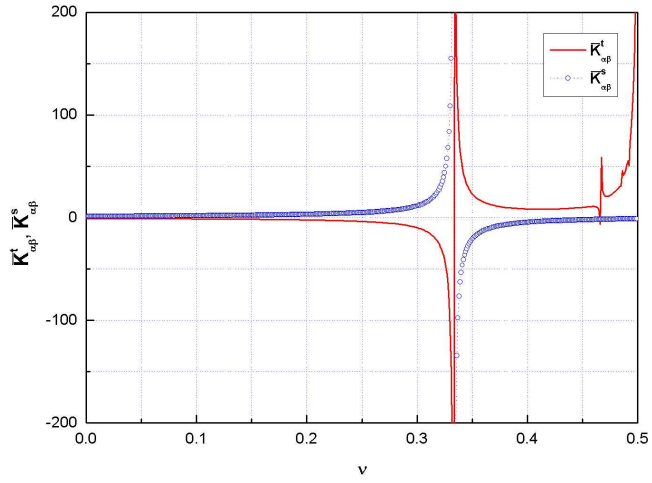

Figure 8: Graph of $\overline{\mathrm{K}}^t_{\alpha\beta}$ and $\overline{\mathrm{K}}^s_{\alpha\beta}$ as functions of ν

value problem. For instance, Fig. 8 shows graphs of $\overline{\mathrm{K}}^t_{\alpha\beta}$ and $\overline{\mathrm{K}}^s_{\alpha\beta}$ as functions of Poisson's ratio ν for the branch $L_\perp(0)$ and $L_\parallel(1)$ for homogeneous and isotropic materials. For example, as $\nu \to 0.33$ from below, the coefficient $\overline{\mathrm{K}}^t_{\alpha\beta} \to -\infty$. To address this anomaly we need an additional independent, logical process. The so-called hyperbolic, short-wavelength extrapolation is chosen for this step.

2.5 Hyperbolic Short-wavelength Extrapolation

The equations of the theory of laminated composite shells can be regarded as stemming from the equations of the 3-D theory of elasticity in the long-wavelength approximation $h/l \to 0$. By their structure the equations of shell theory have physical significance only for $h/l \ll 1$. On the other hand, the formulation of boundary-value problems is associated with behavior of the corresponding differential operator at short wavelengths ($h/l \to \infty$), so that formulation of the theory of shells involves not only the derivation of equations in the long-wavelength regime, but also another logically independent step – the extrapolation of those equations to the short-wavelength regime [3]. For shells in the short-wavelength regime it is impossible to describe the 3-D stress state exactly by the 2-D theory, and only a qualitative correspondence can be achieved. For this reason, it is possible to have differing

sets of asymptotically-exact 2-D equations in the theory of shells. Therefore, the question of how to implement short-wavelength extrapolation in the general case is still open to investigation. However, it is natural to demand asymptotic equivalence in the long-wave regime for various possible short-wave extrapolations.

Let us now consider vibrations of the composite laminated shell with either clamped or free boundary conditions at its edge. For convenience in the derivation, we assume that $\rho(\zeta)$ is a constant. Following [9], we assume that the vibrations we are going to describe can be regarded with sufficient accuracy as the superposition of the branches $F_\perp(0)$, $F_\parallel(0)$, $L_\parallel(0)$, $L_\perp(0)$ and $L_\parallel(1)$. The branches $F_\perp(0)$ and $L_\parallel(0)$ correspond to low-frequency vibrations, but the others to thickness (high-frequency) vibrations with the first branches. There are two main reasons to choose those branches. First, these branches possess the lowest cut-off frequencies, so that the dominant vibrational energy is concentrated in them. Second, the necessity of including also $L_\parallel(1)$ into the present theory is dictated by its strong interaction with the branch $L_\perp(0)$, and obviously $F_\parallel(0)$ is also strongly coupled with the branch $F_\perp(0)$ [27, 26]. Therefore, the dynamic equations contain eight unknown functions of the in-plane coordinates and time: $\bar{u}_\alpha^{2d}$, $\bar{u}_3^{2d}$, $\bar{\psi}_\alpha$, $\bar{\psi}_3$, $\bar{v}_\alpha$ (the symbols without the bar are reserved for the functions in the final equations), as are illustrated in Fig. 9 for the isotropic case [27, 31]. Thus, we can recover the 3-D displacements through the first approximation in a strict sense of asymptotic correctness in the following form

$$\begin{aligned}
\bar{U}_\alpha^{3d} &= \bar{u}_\alpha^{2d} + g_{\alpha\beta}(\zeta)\,\bar{\psi}_\beta + h\vartheta_{R\alpha\beta}(\zeta)\,\bar{\psi}_\alpha + p_{\alpha\beta}(\zeta)\,\bar{v}_\beta + h\varphi_{R\alpha\beta}(\zeta)\,\bar{v}_\beta + hs_{\alpha\beta}(\zeta)\,\bar{\psi}_{3;\beta} \\
\bar{U}_3^{3d} &= \bar{u}_3^{2d} + h\bar{D}_1(\zeta)\,\bar{\varepsilon} + h\bar{D}_2(\zeta)\,(h\bar{\kappa}) + q(\zeta)\,\bar{\psi}_3 + h\tau_R(\zeta)\,\bar{\psi}_3 \\
&\quad + hn_{\alpha\beta}(\zeta)\,\bar{\psi}_{\alpha;\beta} + hr_{\alpha\beta}(\zeta)\,\bar{v}_{\alpha;\beta}
\end{aligned} \tag{114}$$

As sketched in Fig. 9, the functions $\bar{u}_\alpha^{2d}$, $\bar{u}_3^{2d}$ describe shell displacements in the low-frequency branches, which have been studied in brief in Section 2.3. According to Ref. [51], the 2-D generalized strain and velocity fields are expressed in terms of $\bar{u}_\alpha^{2d}$ and $\bar{u}_3^{2d}$. The functions $\bar{D}_1$ and $\bar{D}_2$ can be calculated from Eq. (72), respectively. According to Ref. [27], the functions $\bar{\psi}_\alpha$ describe the thickness-shear branch $F_\parallel(0)$. The associated functions $g_{\alpha\beta}(\zeta)$ are the first

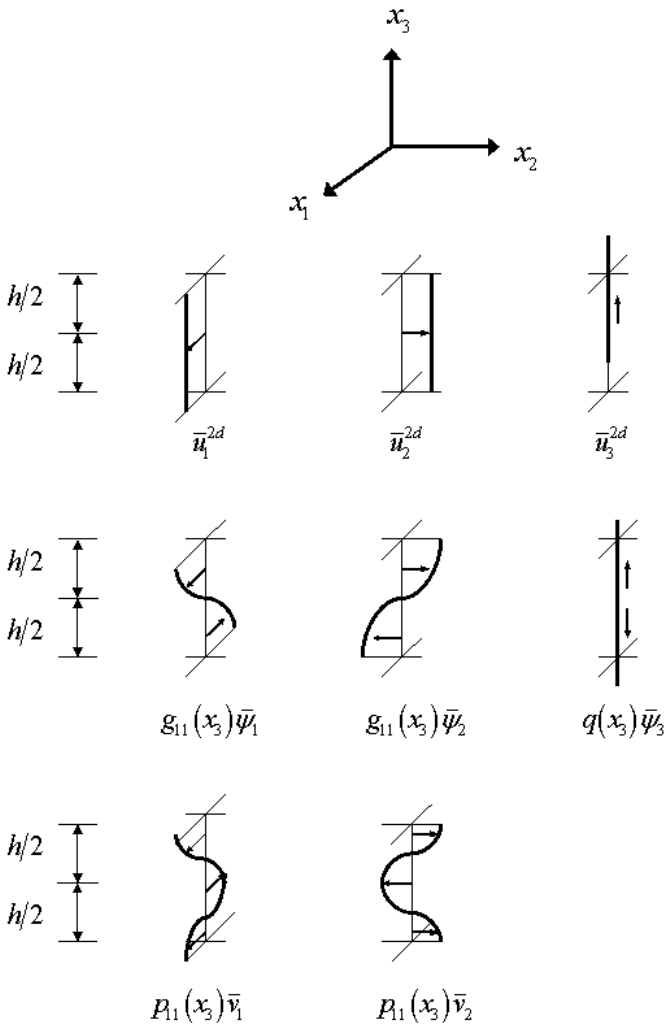

Figure 9: Components of 3-D displacements

odd solutions of the following variational equations

$$\left\langle \mathrm{g}_{|\zeta}^{T} D_s^{*} \delta \mathrm{g}_{|\zeta} - \beta_{s1}^{2} \mathrm{g}^{T} \delta \mathrm{g} \right\rangle = 0 \tag{115}$$

while $n_{\alpha\beta}$ and $\vartheta_{R\alpha\beta}$ are the solutions of Eqs. (106) and (108), respectively, in which p should be replaced by g. Moreover, we choose for $g_{\alpha\beta}(\zeta)$ another normalization condition to simplify the subsequent changes of variables as follows:

$$\frac{\langle \zeta g_{\alpha\beta} \rangle}{\langle \zeta^2 \rangle} = \mathrm{I} \tag{116}$$

Finally, the functions $\bar{\psi}_3$ and $\bar{\upsilon}_\alpha$ describe the thickness branches $L_\perp(0)$ and $L_\parallel(1)$, respectively, while the functions $q(\zeta)$ and $\tau_R(\zeta)$ are the solutions of Eqs. (96) and (98) derived for these branches previously in Section 2.4. We substitute Eqs. (114) into Eq. (36). Discarding small terms in the asymptotic sense and using the results of the previous sections, after lengthy but otherwise straightforward calculations, one obtains Eq. (36) with

$$\begin{aligned} 2\overline{\mathcal{K}} = \rho_0 \Big\{ & \bar{V}_\parallel^T \bar{V}_\parallel + \bar{V}_3^2 + \dot{\bar{\psi}}_\parallel^T \langle \mathrm{g}^T \mathrm{g} \rangle \dot{\bar{\psi}}_\parallel + \dot{\bar{\psi}}_3^2 + \dot{\bar{\upsilon}}_\parallel^T \dot{\bar{\upsilon}}_\parallel \\ & + 2 \left(h \bar{\Omega}_\parallel \right)^T \left[\langle \xi^T \mathrm{g} \rangle \dot{\bar{\psi}}_\parallel + \langle \xi^T \mathrm{p} \rangle \dot{\bar{\upsilon}}_\parallel \right] + 2h \Big[\bar{V}_\parallel^T \langle \mathrm{s}_\alpha \rangle \dot{\bar{\psi}}_{3;\alpha} + \bar{V}_3 \langle \mathrm{n}_\alpha \rangle \dot{\bar{\psi}}_{\parallel;\alpha} \\ & + \bar{V}_3 \langle \mathrm{r}_\alpha \rangle \dot{\bar{\upsilon}}_{\parallel;\alpha} + \dot{\bar{\psi}}_3 \langle q D_1 \rangle \dot{\bar{\varepsilon}} + \dot{\bar{\psi}}_3 \langle q D_2 \rangle (h \dot{\bar{\kappa}}) + \dot{\bar{\psi}}_3 \langle q \mathrm{n}_a \rangle \dot{\overline{\psi}}_{\parallel;\alpha} \\ & + \dot{\bar{\psi}}_3 \langle q \mathrm{r}_\alpha \rangle \dot{\bar{\upsilon}}_{\parallel;\alpha} + \dot{\bar{\psi}}_\parallel^T \langle \mathrm{g}^T \mathrm{s}_\alpha \rangle \dot{\bar{\psi}}_{3;\alpha} + \dot{\bar{\upsilon}}_\parallel^T \langle \mathrm{p}^T \mathrm{s}_\alpha \rangle \dot{\bar{\psi}}_{3;\alpha} \Big] \Big\} \end{aligned} \tag{117}$$

and

$$
\begin{aligned}
2\overline{\mathcal{P}} = \mu_0 \Bigg\{ & \left(\frac{1}{h}\right)^2 \left[\bar{\psi}_{\|}^T \left(\beta_1^2 \left\langle \mathrm{g}^T \mathrm{g}\right\rangle\right) \bar{\psi}_{\|} + \beta_2^2 \bar{\psi}_3^2 + \bar{v}_{\|}^T \left(\beta_3^2\right) \bar{v}_{\|}\right] + \bar{\psi}_{\|;\alpha}^T \overline{\mathrm{K}}_{\alpha\beta}^1 \bar{\psi}_{\|;\beta} \\
& + \overline{\mathrm{K}}_{\alpha\beta}^2 \bar{\psi}_{3;\alpha} \bar{\psi}_{3;\beta} + \bar{v}_{\|;\alpha}^T \overline{\mathrm{K}}_{\alpha\beta}^3 \bar{v}_{\|;\beta} + \bar{\psi}_{\|}^T \bar{\mathrm{I}}^1 \bar{\psi}_{\|} + \bar{\mathrm{I}}^2 \bar{\psi}_3^2 + \bar{v}_{\|}^T \bar{\mathrm{I}}^3 \bar{v}_{\|} \\
& + \bar{\varepsilon}^T \left\langle D_c^* \right\rangle \bar{\varepsilon} + 2\bar{\varepsilon}^T \left\langle \zeta D_c^* \right\rangle (h\bar{\kappa}) + (h\bar{\kappa})^T \left\langle \zeta^2 D_c^* \right\rangle (h\bar{\kappa}) \\
& + 2\left(\frac{1}{h}\right) \left[\bar{\psi}_{\|}^T \left\langle \mathrm{g}_{|\zeta}^T D_s^* \mathrm{s}_{\alpha|\zeta} \right\rangle \bar{\psi}_{3;\alpha} + \bar{v}_{\|}^T \left\langle \mathrm{p}_{|\zeta}^T D_s^* \mathrm{s}_{\alpha|\zeta} \right\rangle \bar{\psi}_{3;\alpha} + \bar{\psi}_3 \left\langle q_{|\zeta} D_t^* D_{1|\zeta} \right\rangle \bar{\varepsilon} \right. \\
& + \bar{\psi}_3 \left\langle q_{|\zeta} D_t^* D_{2|\zeta} \right\rangle (h\bar{\kappa}) + \bar{\psi}_3 \left\langle q_{|\zeta} D_t^* \mathrm{n}_{\alpha|\zeta} \right\rangle \bar{\psi}_{\|;\alpha} + \bar{\psi}_3 \left\langle q_{|\zeta} D_t^* \mathrm{r}_{\alpha|\zeta} \right\rangle \bar{v}_{\|;\alpha} \\
& + \bar{\varepsilon}^T \left\langle D_{et}^* q_{|\zeta} \right\rangle \bar{\psi}_3 + (h\bar{\kappa})^T \left\langle \zeta D_{et}^* q_{|\zeta} \right\rangle \bar{\psi}_3 + \bar{\psi}_3 \left\langle q_{|\zeta} D_{et}^{*T} I_\alpha \mathrm{g} \right\rangle \bar{\psi}_{\|;\alpha} \\
& \left. + \bar{\psi}_{\|}^T \left\langle \mathrm{g}_{|\zeta}^T D_s^* e_\alpha q \right\rangle \bar{\psi}_{3;\alpha} + \bar{\psi}_3 \left\langle q_{|\zeta} D_{et}^{*T} I_\alpha \mathrm{p} \right\rangle \bar{v}_{\|;\alpha} + \bar{v}_{\|}^T \left\langle \mathrm{p}_{|\zeta}^T D_s^* e_\alpha q \right\rangle \bar{\psi}_{3;\alpha} \right] \\
& + 2\left[\bar{\varepsilon}^T \left\langle D_{1|\zeta}^T D_{et}^{*T} I_\alpha \mathrm{g} + D_e^* I_\alpha \mathrm{g} \right\rangle \bar{\psi}_{\|;\alpha} + (\bar{\varepsilon})^T \left\langle D_{1|\zeta}^T D_t^* \mathrm{n}_{\alpha|\zeta} + D_{et}^* \mathrm{n}_{\alpha|\zeta} \right\rangle \bar{\psi}_{\|;\alpha} \right. \\
& + \bar{\varepsilon}^T \left\langle D_{1|\zeta}^T D_{et}^{*T} I_\alpha \mathrm{p} + D_e^* I_\alpha \mathrm{p} \right\rangle \bar{v}_{\|;\alpha} + (\bar{\varepsilon})^T \left\langle D_{1|\zeta}^T D_t^* \mathrm{r}_{\alpha|\zeta} + D_{et}^* \mathrm{r}_{\alpha|\zeta} \right\rangle \bar{v}_{\|;\alpha} \\
& + (h\bar{\kappa})^T \left\langle D_{2|\zeta}^T D_{et}^{*T} I_\alpha \mathrm{g} + \zeta D_e^* I_\alpha \mathrm{g} \right\rangle \bar{\psi}_{\|;\alpha} + (h\bar{\kappa})^T \left\langle D_{2|\zeta}^T D_t^* \mathrm{n}_{\alpha|\zeta} + \zeta D_{et}^* \mathrm{n}_{\alpha|\zeta} \right\rangle \bar{\psi}_{\|;\alpha} \\
& + (h\bar{\kappa})^T \left\langle D_{2|\zeta}^T D_{et}^{*T} I_\alpha \mathrm{p} + \zeta D_e^* I_\alpha \mathrm{p} \right\rangle \bar{v}_{\|;\alpha} + (h\bar{\kappa})^T \left\langle D_{2|\zeta}^T D_t^* \mathrm{r}_{\alpha|\zeta} + \zeta D_{et}^* \mathrm{r}_{\alpha|\zeta} \right\rangle \bar{v}_{\|;\alpha} \\
& + \bar{\psi}_{\|}^T \left\langle \mathrm{g}_{|\zeta}^T D_s^* e_\alpha D_1 \right\rangle \bar{\varepsilon}_{;\alpha} + \bar{\psi}_{\|}^T \left\langle \mathrm{g}_{|\zeta}^T D_s^* e_\alpha D_2 \right\rangle (h\bar{\kappa}_{;\alpha}) + \bar{v}_{\|}^T \left\langle \mathrm{p}_{|\zeta}^T D_s^* e_\alpha D_1 \right\rangle \bar{\varepsilon}_{;\alpha} \\
& \left. + \bar{v}_{\|}^T \left\langle \mathrm{p}_{|\zeta}^T D_s^* e_\alpha D_2 \right\rangle (h\bar{\kappa}_{;\alpha}) \right] \Bigg\} - \overline{\mathrm{F}}^{1T} \bar{\psi}_{\|} - \overline{\mathrm{F}}^2 \bar{\psi}_3 - \overline{\mathrm{F}}^{3T} \bar{v}_{\|}
\end{aligned}
\tag{118}
$$

In Eqs. (117) and (118), the coefficients β_1^2, β_2^2, β_3^2 are the eigenvalues of the variational problems for g, q and p, respectively; while $\overline{\mathrm{K}}_{\alpha\beta}^1$, $\overline{\mathrm{K}}_{\alpha\beta}^2$, $\overline{\mathrm{K}}_{\alpha\beta}^3$, $\bar{\mathrm{I}}^1$, $\bar{\mathrm{I}}^2$, $\bar{\mathrm{I}}^3$, $\overline{\mathrm{F}}^1$, $\overline{\mathrm{F}}^2$ and $\overline{\mathrm{F}}^3$ are

calculated from the corresponding coefficients according to Eqs. (111) and (113) as follows:

$$
\begin{aligned}
\overline{\mathrm{K}}^1_{\alpha\beta} &= \left\langle \mathrm{g}^T I^T_\alpha D^*_e I_\beta \mathrm{g} + \mathrm{g}^T I^T_\alpha D^*_{et} \mathrm{n}_{\beta|\zeta} - \mathrm{g}^T_{|\zeta} D^*_s e_\alpha \mathrm{n}_\beta \right\rangle \\
\overline{\mathrm{K}}^2_{\alpha\beta} &= \left\langle e^T_\alpha D^*_s e_\beta q^2 + \mathrm{s}^T_{\alpha|\zeta} D^*_s e_\beta q - \mathrm{s}^T_\beta I^T_\alpha D^*_{et} q_{|\zeta} \right\rangle \\
\overline{\mathrm{K}}^3_{\alpha\beta} &= \left\langle \mathrm{p}^T I^T_\alpha D^*_e I_\beta \mathrm{p} + \mathrm{p}^T I^T_\alpha D^*_{et} \mathrm{r}_{\beta|\zeta} - \mathrm{p}^T_{|\zeta} D^*_s e_\alpha \mathrm{r}_\beta \right\rangle \\
\bar{\mathrm{I}}^1 &= \Big\langle \mathrm{g}^T C^{sT}_R D^*_s C^s_R \mathrm{g} + K\zeta^2 \mathrm{g}^T_{|\zeta} D^*_s \mathrm{g}_{|\zeta} + 4H\zeta \mathrm{g}^T_{|\zeta} D^*_s C^s_R \mathrm{g} \\
&\quad + 2\zeta \mathrm{g}_{|\zeta} D^*_s C^s_R C^s_R \mathrm{g} - \vartheta^T_{R|\zeta} D^*_s \vartheta_{R|\zeta} + \beta_1^2 \left[\vartheta^T_R \vartheta_R - K\zeta^2 \mathrm{g}^T \mathrm{g} \right] \Big\rangle \\
\bar{\mathrm{I}}^2 &= \Big\langle C^{eT}_R D^*_e C^e_R q^2 + K D^*_t \left(\zeta q_{|\zeta} \right)^2 + 4H C^{eT}_R D^*_{et} \left(\zeta q q_{|\zeta} \right) \\
&\quad + 2\tilde{C}^{eT}_R D^*_{et} \left(\zeta q q_{|\zeta} \right) - D^*_t \tau^2_{R|\zeta} + \beta_2^2 \left[\tau^2_R - K \left(\zeta q \right)^2 \right] \Big\rangle \\
\bar{\mathrm{I}}^3 &= \Big\langle \mathrm{p}^T C^{sT}_R D^*_s C^s_R \mathrm{p} + K\zeta^2 \mathrm{p}^T_{|\zeta} D^*_s \mathrm{p}_{|\zeta} + 4H\zeta \mathrm{p}^T_{|\zeta} D^*_s C^s_R \mathrm{p} \\
&\quad + 2\zeta \mathrm{p}^T_{|\zeta} D^*_s C^s_R C^s_R \mathrm{p} - \varphi^T_{R|\zeta} D^*_s \varphi_{R|\zeta} + \beta_3^2 \left[\varphi^T_R \varphi_R - K\zeta^2 \mathrm{p}^T \mathrm{p} \right] \Big\rangle \\
\overline{\mathrm{F}}^1 &= \left\langle \phi^T_\parallel \mathrm{g} \right\rangle \\
\overline{\mathrm{F}}^2 &= \langle \phi_3 q \rangle \\
\overline{\mathrm{F}}^3 &= \alpha^T_\parallel \mathrm{p}^+ + \beta^T_\parallel \mathrm{p}^-
\end{aligned}
\tag{119}
$$

By using the normalization from Eqs. (83) and (116), one can derive the changes of variable in the following way: At first, the changes of variable for V_α, V_3, ψ_3 and υ_α can be

established for Eq. (117):

$$
\begin{aligned}
&\rho_0 \left\{ \bar{V}_{\parallel}^T \bar{V}_{\parallel} + 2h \bar{V}_{\parallel}^T \left\langle \mathrm{s}_\alpha \right\rangle \dot{\bar{\psi}}_{3;\alpha} \right\} \\
&= \rho_0 \left\{ \left[\bar{V}_{\parallel} + h \mathrm{a}_\alpha^1 \dot{\bar{\psi}}_{3;\alpha} \right]^T \left[\bar{V}_{\parallel} + h \mathrm{a}_\beta^1 \dot{\bar{\psi}}_{3;\beta} \right] \right\} - \rho_0 h^2 \left(\mathrm{a}_\alpha^{1T} \mathrm{a}_\beta^1 \right) \dot{\bar{\psi}}_{3;\alpha} \dot{\bar{\psi}}_{3;\beta} \\
&= \rho_0 \left\{ V_{\parallel}^T V_{\parallel} \right\} - \mu_0 \left\{ \beta_2^2 \left(\mathrm{a}_\alpha^{1T} \mathrm{a}_\beta^1 \right) \right\} \bar{\psi}_{3;\alpha} \bar{\psi}_{3;\beta} \\
&\rho_0 \left\{ \bar{V}_3^2 + 2h \bar{V}_3 \left(\left\langle \mathrm{n}_\alpha \right\rangle \dot{\bar{\psi}}_{\parallel;\alpha} + \left\langle \mathrm{r}_\alpha \right\rangle \dot{\bar{v}}_{\parallel;\alpha} \right) \right\} \\
&= \rho_0 \left\{ \left[\bar{V}_3 + h \left(\mathrm{a}_\alpha^5 \dot{\bar{\psi}}_{\parallel;\alpha} + \mathrm{b}_\alpha^1 \dot{\bar{v}}_{\parallel;\alpha} \right) \right]^2 \right\} \\
&- \rho_0 h^2 \left\{ \dot{\bar{\psi}}_{\parallel;\alpha}^T \left(\mathrm{a}_\alpha^{5T} \mathrm{a}_\beta^5 \right) \dot{\bar{\psi}}_{\parallel;\beta} + \dot{\bar{v}}_{\parallel;\alpha}^T \left(\mathrm{b}_\alpha^{1T} \mathrm{b}_\beta^1 \right) \dot{\bar{v}}_{\parallel;\beta} \right\} \\
&= \rho_0 \left\{ V_3^2 \right\} - \mu_0 \left\{ \bar{\psi}_{\parallel;\alpha}^T \left(\mathrm{a}_\alpha^{5T} \beta_1^2 \mathrm{a}_\beta^5 \right) \bar{\psi}_{\parallel;\beta} + \bar{v}_{\parallel;\alpha}^T \left(\mathrm{b}_\alpha^{1T} \beta_3^2 \mathrm{b}_\beta^1 \right) \bar{v}_{\parallel;\beta} \right\} \\
&\rho_0 \left\{ \dot{\bar{\psi}}_3^2 + 2h \dot{\bar{\psi}}_3 \left[\left\langle qD_1 \right\rangle \dot{\bar{\varepsilon}} + \left\langle qD_2 \right\rangle (h \dot{\bar{\kappa}}) + \left\langle q\mathrm{n}_\alpha \right\rangle \dot{\bar{\psi}}_{\parallel;\alpha} + \left\langle q\mathrm{r}_\alpha \right\rangle \dot{\bar{v}}_{\parallel;\alpha} \right] \right\} \\
&= \rho_0 \left\{ \dot{\bar{\psi}}_3 + h \left[\mathrm{a}^2 \dot{\bar{\varepsilon}} + \mathrm{b}^2 (h \dot{\bar{\kappa}}) + \mathrm{b}_\alpha^3 \dot{\bar{\psi}}_{\parallel;\alpha} + \mathrm{a}_\alpha^3 \dot{\bar{v}}_{\parallel;\alpha} \right] \right\} \\
&- \rho_0 h^2 \left\{ \dot{\bar{\psi}}_{\parallel;\alpha}^T \left(\mathrm{b}_\alpha^{3T} \mathrm{b}_\beta^3 \right) \dot{\bar{\psi}}_{\parallel;\beta} + \dot{\bar{v}}_{\parallel;\alpha}^T \left(\mathrm{a}_\alpha^{3T} \mathrm{a}_\beta^3 \right) \dot{\bar{v}}_{\parallel;\beta} \right\} \\
&= \rho_0 \left\{ \dot{\psi}_3^2 \right\} - \mu_0 \left\{ \bar{\psi}_{\parallel;\alpha}^T \left(\mathrm{b}_\alpha^{3T} \beta_1^2 \mathrm{b}_\beta^3 \right) \bar{\psi}_{\parallel;\beta} + \bar{v}_{\parallel;\alpha}^T \left(\mathrm{a}_\alpha^{3T} \beta_3^2 \mathrm{a}_\beta^3 \right) \bar{v}_{\parallel;\beta} \right\} \\
&\rho_0 \left\{ \dot{\bar{v}}_{\parallel}^T \dot{\bar{v}}_{\parallel} + 2h \dot{\bar{v}}_{\parallel}^T \left\langle \mathrm{p}^T \mathrm{s}_\alpha \right\rangle \dot{\bar{\psi}}_{3;\alpha} \right\} \\
&= \rho_0 \left\{ \left[\dot{\bar{v}}_{\parallel} + h \bar{\mathrm{a}}_\alpha^4 \dot{\bar{\psi}}_{3;\alpha} \right]^T \left[\dot{\bar{v}}_{\parallel} + h \bar{\mathrm{a}}_\beta^4 \dot{\bar{\psi}}_{3;\beta} \right] \right\} - \rho_0 h^2 \left(\bar{\mathrm{a}}_\alpha^{4T} \bar{\mathrm{a}}_\beta^4 \right) \dot{\bar{\psi}}_{3;\alpha} \dot{\bar{\psi}}_{3;\beta} \\
&= \rho_0 \left\{ \dot{v}_{\parallel}^T \dot{v}_{\parallel} \right\} - \mu_0 \left\{ \beta_2^2 \left(\bar{\mathrm{a}}_\alpha^{4T} \bar{\mathrm{a}}_\beta^4 \right) \right\} \bar{\psi}_{3;\alpha} \bar{\psi}_{3;\beta}
\end{aligned}
\tag{120}
$$

On the other hand, based on Eq. (118) one can make the changes of variable for $\kappa_{\alpha\beta}$

and ψ_α.

$$
\begin{aligned}
&\mu_0 \left\{ (h\bar{\kappa})^T \, \overline{\mathrm{C}} \, (h\bar{\kappa}) + 2 \, (h\bar{\kappa})^T \left[\langle \zeta D_c^* I_\alpha \mathrm{g} \rangle \, \bar{\psi}_{\|;\alpha} + \langle \zeta D_c^* I_\alpha \mathrm{p} \rangle \, \bar{v}_{\|;\alpha} \right] \right\} \\
&= \mu_0 \left\{ \left[h\bar{\kappa} + \left(\bar{\mathrm{d}}_\alpha^4 \bar{\psi}_{\|;\alpha} + \bar{\mathrm{e}}_\alpha^6 \bar{v}_{\|;\alpha} \right) \right]^T \overline{\mathrm{C}} \left[h\bar{\kappa} + \left(\bar{\mathrm{d}}_\beta^4 \bar{\psi}_{\|;\beta} + \bar{\mathrm{e}}_\alpha^6 \bar{v}_{\|;\beta} \right) \right] \right\} \\
&- \mu_0 \left\{ \bar{\psi}_{\|;\alpha}^T \left(\bar{\mathrm{d}}_\alpha^{4T} \overline{\mathrm{C}} \bar{\mathrm{d}}_\beta^4 \right) \bar{\psi}_{\|;\beta} + \bar{v}_{\|;\alpha}^T \left(\bar{\mathrm{e}}_\alpha^{6T} \overline{\mathrm{C}} \bar{\mathrm{e}}_\beta^6 \right) \bar{v}_{\|;\beta} \right\} \\
&= \mu_0 \left\{ (h\kappa)^T \, \overline{\mathrm{C}} \, (h\kappa) \right\} - \mu_0 \left\{ \bar{\psi}_{\|;\alpha}^T \left(\bar{\mathrm{d}}_\alpha^{4T} \overline{\mathrm{C}} \bar{\mathrm{d}}_\beta^4 \right) \bar{\psi}_{\|;\beta} + \bar{v}_{\|;\alpha}^T \left(\bar{\mathrm{e}}_\alpha^{6T} \overline{\mathrm{C}} \bar{\mathrm{e}}_\beta^6 \right) \bar{v}_{\|;\beta} \right\} \\
&\mu_0 \left\{ \left(\frac{1}{h} \right)^2 \bar{\psi}_\|^T \left(\beta_1^2 \left\langle \mathrm{g}^T \mathrm{g} \right\rangle \right) \bar{\psi}_\| + 2 \bar{\psi}_\|^T \left[\left(\frac{1}{h} \right) \left\langle \mathrm{g}_{|\zeta}^T D_s^* \mathrm{s}_{\alpha|\zeta} \right\rangle \bar{\psi}_{3;\alpha} + \left\langle \mathrm{g}_{|\zeta}^T D_s^* e_\alpha D_2 \right\rangle (h\bar{\kappa}_{;\alpha}) \right] \right\} \\
&= \mu_0 \left(\frac{1}{h} \right)^2 \left\{ \left[\bar{\psi}_\| + h \bar{\mathrm{b}}_\alpha^4 \bar{\psi}_{3;\alpha} + h^2 \bar{\mathrm{d}}_\alpha^5 \, (h\bar{\kappa}_{;\alpha}) \right]^T \beta_1^2 \mathrm{c}_1 \left[\bar{\psi}_\| + h \bar{\mathrm{b}}_\beta^4 \bar{\psi}_{3;\beta} + h^2 \bar{\mathrm{d}}_\beta^5 \, (h\bar{\kappa}_{;\beta}) \right] \right\} \\
&- \mu_0 \left(\bar{\mathrm{b}}_\alpha^{4T} \beta_1^2 \mathrm{c}_1 \bar{\mathrm{b}}_\beta^4 \right) \bar{\psi}_{3;\alpha} \bar{\psi}_{3;\beta} \\
&= \mu_0 \left(\frac{1}{h} \right)^2 \left\{ \left(h\psi_\| \right)^T \beta_1^2 \mathrm{c}_1 \left(h\psi_\| \right) \right\} - \mu_0 \left\{ \left(\bar{\mathrm{b}}_\alpha^{4T} \beta_1^2 \mathrm{c}_1 \bar{\mathrm{b}}_\beta^4 \right) \right\} \bar{\psi}_{3;\alpha} \bar{\psi}_{3;\beta}
\end{aligned}
\tag{121}
$$

where

$$
\begin{aligned}
&\mathrm{a}_\alpha^1 = \langle \mathrm{s}_\alpha \rangle \qquad \mathrm{a}_\alpha^5 = \langle \mathrm{n}_\alpha \rangle \qquad \mathrm{b}_\alpha^1 = \langle \mathrm{r}_\alpha \rangle \\
&\bar{\mathrm{a}}_{\alpha\beta}^1 = I_\beta \mathrm{a}_\alpha^1 \qquad \bar{\mathrm{d}}_\alpha^4 = \left(\overline{\mathrm{C}}^{-T} \right) \mathrm{d}_\alpha^4 \qquad \bar{\mathrm{e}}_\alpha^6 = \left(\overline{\mathrm{C}}^{-T} \right) \mathrm{e}_\alpha^6 \\
&\overline{\mathrm{C}} = \left\langle \zeta^2 D_c^* \right\rangle \qquad \mathrm{d}_\alpha^4 = \langle \zeta D_c^* I_\alpha \mathrm{g} \rangle \qquad \mathrm{e}_\alpha^6 = \langle \zeta D_c^* I_\alpha \mathrm{p} \rangle \\
&\mathrm{a}^2 = \langle q D_1 \rangle \qquad \mathrm{b}^2 = \langle q D_2 \rangle \qquad \mathrm{b}_\alpha^3 = \langle q \mathrm{n}_\alpha \rangle \\
&\mathrm{a}_\alpha^3 = \langle q \mathrm{r}_\alpha \rangle \qquad \bar{\mathrm{b}}_\alpha^4 = \left(\mathrm{c}_1^{-T} \right) \mathrm{b}_\alpha^4 \qquad \bar{\mathrm{d}}_\alpha^5 = \left(\beta_1 \mathrm{c}_1 \right)^{-T} \mathrm{d}_\alpha^5 \\
&\mathrm{c}_1 = \left\langle \mathrm{g}^T \mathrm{g} \right\rangle \qquad \mathrm{b}_\alpha^4 = \left\langle \mathrm{g}^T \mathrm{s}_\alpha \right\rangle \qquad \mathrm{d}_\alpha^5 = \left\langle \mathrm{g}_{|\zeta}^T D_s^* e_\alpha D_2 \right\rangle \\
&\bar{\mathrm{a}}_\alpha^4 = \left\langle \mathrm{p}^T \mathrm{s}_\alpha \right\rangle
\end{aligned}
\tag{122}
$$

Finally, the changes of variable are defined as:

$$
\begin{aligned}
V_\| &= \bar{V}_\| + h \mathrm{a}_\alpha^1 \dot{\bar{\psi}}_{3;\alpha} \\
V_3 &= \bar{V}_3 + h \left[\mathrm{a}_\alpha^5 \dot{\bar{\psi}}_{\|;\alpha} + \mathrm{b}_\alpha^1 \dot{\bar{v}}_{\|;\alpha} \right] \\
\varepsilon &= \bar{\varepsilon} + h \bar{a}_{\alpha\beta}^1 \overline{\psi}_{3;\alpha\beta} \\
h\kappa &= h\bar{\kappa} + \bar{d}_\alpha^4 \bar{\psi}_{\|;\alpha} + \bar{e}_\alpha^6 \bar{v}_{\|;\alpha} \\
\psi_3 &= \bar{\psi}_3 + h \left[\mathrm{a}^2 \bar{\varepsilon} + \mathrm{b}^2 \, (h\bar{\kappa}) + \mathrm{b}_\alpha^3 \bar{\psi}_{\|;\alpha} + \mathrm{a}_\alpha^3 \bar{v}_{\|;\alpha} \right] \\
\psi_\| &= \frac{1}{h} \left\{ \bar{\psi}_\| + h \big(\bar{b}_\alpha^4 \bar{\psi}_{3;\alpha} \big) + h^2 \left[\bar{d}_\alpha^5 \, (h\bar{\kappa}_{;\alpha}) \right] \right\} \\
v_\| &= \bar{v}_\| + h \bar{a}_\alpha^4 \bar{\psi}_{3;\alpha}
\end{aligned}
\tag{123}
$$

Retaining the leading terms in V_α , V_3, $\varepsilon_{\alpha\beta}$, $\kappa_{\alpha\beta}$, ψ_α, ψ_3 and v_α and extrapolating the total energy functional to the short-wavelength regime, we arrive finally at the 3-D refined energy functional with the kinetic and strain energies per unit area, valid for a wide range of frequencies for monoclinic composite laminated shells

$$\mathcal{J} = h \int_{t_1}^{t_2} \int_s (\mathcal{K} - \mathcal{P})\, dSdt \tag{124}$$

where

$$\mathcal{K} = \frac{1}{2}\rho_0 \left\{ V_\parallel^T V_\parallel + V_3^2 + \left(h\dot{\psi}_\parallel\right)^T \mathrm{c}_1 \left(h\dot{\psi}_\parallel\right) + \dot{\psi}_3^2 + \dot{v}_\parallel^T \dot{v}_\parallel \right\} \tag{125}$$

and

$$\begin{aligned}\mathcal{P} = \frac{1}{2}\mu_0 \Bigg\{ & \varepsilon^T \mathrm{A}\varepsilon + 2\varepsilon^T \mathrm{B}\,(h\kappa) + (h\kappa)^T \mathrm{C}\,(h\kappa) + \left(\frac{1}{h}\right)^2 \left[\left(h\psi_\parallel\right)^T \mathrm{I}^1 \left(h\psi_\parallel\right) + \mathrm{I}^2 \psi_3^2 + v_\parallel^T \mathrm{I}^3 v_\parallel \right] \\ & + 2\left(\frac{1}{h}\right) \left[\left(\varepsilon^T \mathrm{S}^{e2} + (h\kappa)^T \mathrm{S}^{c2} + \left(h\psi_{\parallel;\alpha}\right)^T \mathrm{S}_\alpha^{12} + v_{\parallel;\alpha}^T \mathrm{S}_\alpha^{32} \right) \psi_3 + \left(\left(h\psi_\parallel\right)^T \mathrm{S}_\alpha^{21} + v^T \mathrm{S}_\alpha^{23} \right) \psi_{3;\alpha} \right] \\ & + \left(h\psi_{\parallel;\alpha}\right)^T \mathrm{K}_{\alpha\beta}^1 \left(h\psi_{\parallel;\beta}\right) + \mathrm{K}_{\alpha\beta}^2 \psi_{3;\alpha}\psi_{3;\beta} + v_{\parallel;\alpha}^T \mathrm{K}_{\alpha\beta}^3 v_{\parallel;\beta} \Bigg\} - \mathrm{F}^{1T} \left(h\psi_\parallel\right) - \mathrm{F}^2 \psi_3 - \mathrm{F}^{3T} v_\parallel \end{aligned} \tag{126}$$

For simplicity of the derivation we use the following notation:

$$\begin{aligned} & \mathrm{d}^1 = \left\langle D_{et}^* q_{|\zeta} \right\rangle \quad \mathrm{e}^1 = \left\langle \zeta D_{et}^* q_{|\zeta} \right\rangle \quad \mathrm{e}_\alpha^2 = \left\langle q_{|\zeta} D_{et}^{*T} I_\alpha \mathrm{g} \right\rangle \\ & \mathrm{e}_\alpha^8 = \left\langle \mathrm{g}_{|\zeta}^T D_s^* e_\alpha q \right\rangle \quad \mathrm{d}_\alpha^2 = \left\langle q_{|\zeta} D_{et}^{*T} I_\alpha \mathrm{p} \right\rangle \quad \mathrm{d}_\alpha^3 = \left\langle \mathrm{p}_{|\zeta}^T D_s^* e_\alpha q \right\rangle \\ & \mathrm{e}_\alpha^7 = \left\langle \mathrm{p}_{|\zeta}^T D_s^* e_\alpha D_2 \right\rangle \end{aligned} \tag{127}$$

Using Eqs. (122) and (127), all the coefficients are defined as:

$$
\begin{aligned}
&\mathrm{A} = \overline{\mathrm{A}} - \beta_2^2 \left(\mathrm{a}^{2T}\mathrm{a}^2\right) - 2\left(\mathrm{d}^1\mathrm{a}^2\right) \\
&\mathrm{B} = \overline{\mathrm{B}} - \beta_2^2 \left(\mathrm{a}^{2T}\mathrm{b}^2\right) - \left(\mathrm{d}^1\mathrm{b}^2\right) - \left(\mathrm{a}^2\mathrm{e}^1\right) \\
&\mathrm{C} = \overline{\mathrm{C}} - \beta_2^2 \left(\mathrm{b}^{2T}\mathrm{b}^2\right) - 2\left(\mathrm{e}^1\mathrm{b}^2\right) \\
&\mathrm{I}^1 = \beta_1^2 \mathrm{c}_1 + (h)^2 \bar{\mathrm{I}}^1 \quad \mathrm{I}^2 = \beta_2^2 + (h)^2 \bar{\mathrm{I}}^2 \quad \mathrm{I}^3 = \beta_3^2 + (h)^2 \bar{\mathrm{I}}^3 \\
&\mathrm{S}^{e2} = \mathrm{d}^1 \quad \mathrm{S}^{c2} = \mathrm{e}^1 \quad \mathrm{S}_\alpha^{12} = \mathrm{e}_\alpha^{2T} - \left(\bar{\mathrm{d}}_\alpha^{4T}\mathrm{e}^1\right) \quad \mathrm{S}_\alpha^{32} = \mathrm{d}_\alpha^{2T} - \left(\bar{\mathrm{e}}_\alpha^{6T}\mathrm{e}^1\right) \\
&\mathrm{S}_\alpha^{12} = \mathrm{e}_\alpha^8 \quad \mathrm{S}_\alpha^{23} = \mathrm{d}_\alpha^3 \quad \mathrm{F}^1 = \overline{\mathrm{F}}^1 \quad \mathrm{F}^2 = \overline{\mathrm{F}}^2 \quad \mathrm{F}^3 = \overline{\mathrm{F}}^3 \\
&\mathrm{K}_{\alpha\beta}^1 = \overline{\mathrm{K}}_{\alpha\beta}^1 + \left(\mathrm{a}_\alpha^{5T}\beta_1^2\mathrm{a}_\beta^5\right) + \left(\mathrm{b}_\alpha^{3T}\beta_1^2\mathrm{b}_\beta^3\right) \\
&\qquad + 2\left[\beta_2^2\left(\mathrm{b}^2\bar{\mathrm{d}}_\alpha^4\right)^T\mathrm{b}_\beta^3 + \left(\bar{\mathrm{d}}_\alpha^{4T}\mathrm{e}^1\mathrm{b}_\beta^3\right) + \left(\mathrm{b}^2\bar{\mathrm{d}}_\alpha^4\right)^T\left(\mathrm{e}_\beta^2 - \mathrm{e}_\beta^{8T}\right)\right] \\
&\qquad - \left[\left(\bar{\mathrm{d}}_\alpha^{4T}\overline{\mathrm{C}}\bar{\mathrm{d}}_\beta^4\right) + \beta_2^2\left(\mathrm{b}_\alpha^{3T}\mathrm{b}_\beta^3\right) + \beta_2^2\left(\mathrm{b}^2\bar{\mathrm{d}}_\alpha^4\right)^T\mathrm{b}^2\bar{\mathrm{d}}_\alpha^4\right] - 2\left[\left(\bar{\mathrm{d}}_\alpha^{4T}\mathrm{e}^1\mathrm{b}^2\bar{\mathrm{d}}_\beta^4\right) + \mathrm{b}_\alpha^{3T}\left(\mathrm{e}_\beta^2 - \mathrm{e}_\beta^{8T}\right)\right] \\
&\mathrm{K}_{\alpha\beta}^2 = \overline{\mathrm{K}}_{\alpha\beta}^2 + \beta_2^2\left[\left(\mathrm{a}_\alpha^{1T}\mathrm{a}_\beta^1\right) + \left(\bar{\mathrm{b}}_\alpha^{4T}\bar{\mathrm{b}}_\alpha^4\right) + \left(\bar{\mathrm{a}}_\alpha^{4T}\bar{\mathrm{a}}_\alpha^4\right)\right] \\
&\qquad + 2\left[\left(\bar{\mathrm{a}}_{\alpha\beta}^{1T}\mathrm{d}^1\right) + \left(\mathrm{e}_\alpha^2 - \mathrm{e}_\alpha^{8T}\right)\overline{\mathrm{b}}_\beta^4 + \left(\mathrm{d}_\alpha^2 - \mathrm{d}_\alpha^{3T}\right)\bar{\mathrm{a}}_\beta^4\right] \\
&\qquad - \left[\left(\bar{\mathrm{b}}_\alpha^{4T}\beta_1^2\mathrm{c}_1\bar{\mathrm{b}}_\beta^4\right) + \left(\bar{\mathrm{a}}_\alpha^{4T}\beta_3^2\bar{\mathrm{a}}_\alpha^4\right)\right] - 2\left[\left(\bar{\mathrm{d}}_\alpha^4\bar{\mathrm{b}}_\beta^4\right)^T\mathrm{e}^1 + \left(\bar{\mathrm{e}}_\alpha^6\bar{\mathrm{a}}_\beta^4\right)^T\mathrm{e}^1\right] \\
&\mathrm{K}_{\alpha\beta}^3 = \overline{\mathrm{K}}_{\alpha\beta}^3 + \left(\mathrm{b}_\alpha^{1T}\beta_3^2\mathrm{b}_\beta^1\right) + \left(\mathrm{a}_\alpha^{3T}\beta_3^2\mathrm{a}_\beta^3\right) \\
&\qquad + 2\left[\beta_2^2\left(\mathrm{b}^2\bar{\mathrm{e}}_\alpha^6\right)^T\mathrm{a}_\beta^3 + \left(\bar{\mathrm{e}}_\alpha^{6T}\mathrm{e}^1\mathrm{a}_\beta^3\right) + \left(\mathrm{b}^2\bar{\mathrm{e}}_\alpha^6\right)^T\left(\mathrm{d}_\beta^2 - \mathrm{d}_\beta^{3T}\right) + \left(\mathrm{e}_\alpha^7\bar{\mathrm{e}}_\beta^6\right)\right] \\
&\qquad - \left[\left(\bar{\mathrm{e}}_\alpha^{6T}\overline{\mathrm{C}}\bar{\mathrm{e}}_\beta^6\right) + \beta_2^2\left(\mathrm{a}_\alpha^{3T}\mathrm{a}_\beta^3\right) + \beta_2^2\left(\mathrm{b}^2\bar{\mathrm{e}}_\alpha^6\right)^T\mathrm{b}^2\bar{\mathrm{e}}_\beta^6\right] \\
&\qquad - 2\left[\left(\bar{\mathrm{e}}_\alpha^{6T}\mathrm{e}^1\mathrm{b}^2\bar{\mathrm{e}}_\beta^6\right) + \mathrm{a}_\alpha^{3T}\left(\mathrm{d}_\beta^2 - \mathrm{d}_\beta^{3T}\right)\right]
\end{aligned}
\tag{128}
$$

While transforming Eqs. (117) and (118) to Eqs. (125) and (126) terms of the type, $\left(h\Omega_\parallel\right)^T \mathrm{C}_1 h(\dot{\psi}_\parallel)$ and $\left(\Omega_\parallel\right)^T \mathrm{C}_2\dot{\upsilon}_\parallel$, $\varepsilon^T\mathrm{C}_3(h\psi_{\parallel;\alpha})$, $\varepsilon^T\mathrm{C}_4\upsilon_{\parallel;\alpha}$, $(h\kappa)^T\,\mathrm{C}_5(h\psi_{\parallel;\alpha})$ and $(h\kappa)^T\,\mathrm{C}_6\upsilon_{\parallel;\alpha}$ in the Eqs. (125) and (126) are neglected as small compared with the remaining terms in the long-wavelength regime [9], where C_i with $i = 1, 2, \cdots, 6$ are the coefficients corresponding to those cross term functions.

Now we digress here to point out that the present theory is different from the Berdichevsky-Le theory mainly in the following two aspects. First, the Berdichevsky-Le theory is restricted to linear theory with a homogenous and isotropic material, while the present theory is

the intrinsic formulation for a monoclinic laminated composite material. Second, in the Berdichevsky-Le theory, all terms of the type containing $\left(h\psi_{\|;\alpha}\right)$ are neglected due to additional analysis, which shows that a hyperbolic short-wavelength extrapolation describing exactly the curvature of the dispersion curve near the cut-off frequency of the branch $F_{\|}(0)$ does not exist [9]. However, those terms are proved to be important in reconstructing the 3-D stresses on the basis of 2-D results [38]. Therefore, we retain this term in the present theory.

Despite the fact that the theory involves more unknown functions than in the classical theory of shells, it provides much more predictive capability: The theory is no longer a zeroth-order approximation theory, but is instead a refined theory. Indeed, it describes in an asymptotically exact manner the vibrations of a shell for both low- and high-frequencies in the long-wavelength regime, and it can represent qualitatively the 3-D stress states in the short-wavelength regime. Note that the coefficients of the present 2-D theory can be determined by solving the 1-D through-thickness problems, viz., Eqs. (78), (81), (96), (98), (106), (108) and (115). They are complicated and can generally be solved only with the help of the numerical methods. As mentioned before, this aspect is a key part of the research contribution of this thesis and is dealt with in Chapter 4.

2.6 Recovery Relation

While it is necessary to accurately calculate the 2-D displacement field of composite shells, this is not always sufficient in many engineering applications. Ultimately, the fidelity of a 2-D surface modeling such as this rely on how well it can predict the 3-D results in the original 3-D structure. Hence appropriate recovery relations are required to complete the 2-D surface modeling, and the results can then be compared with those of the original 3-D modeling. The term recovery relations refers to expressions for 3-D displacement, strain, and strain fields in terms of 2-D quantities and functions of ζ.

Using Eqs. (6), (18), (49), (77), (80) and (123), one can recover the 3-D displacement

field through the zeroth order as

$$\begin{aligned} U_1^{3d} &= u_1^{2d} + h\zeta C_{31} + hg_{1\alpha}(\zeta)\left(\psi_\alpha - C_{3\alpha}\right) + p_{1\alpha}(\zeta)\upsilon_\alpha \\ U_2^{3d} &= u_2^{2d} + h\zeta C_{32} + hg_{2\alpha}(\zeta)\left(\psi_\alpha - C_{3\alpha}\right) + p_{2\alpha}(\zeta)\upsilon_\alpha \\ U_3^{3d} &= u_3^{2d} + q(\zeta)\psi_3 \end{aligned} \tag{129}$$

where U_i^{3d} are the 3-D displacement components, u_i^{2d} are the average displacements of the shell. In addition, following to the explanation of Le [9], $(\psi_\alpha - C_{3\alpha})$ can be represented as the amplitudes of the sinusoidal shear of the transverse fibers and ψ_3 describes their sinusoidal extension, while υ_α measure the amplitudes of the complicated motion of the transverse fibers when particles that make up the upper and lower surfaces move in one direction and those of the reference surface in the opposite sense (see Figs. 6 and 7).

From Eqs. (23), one can recover the 3-D strain field through the zero order as

$$\begin{aligned} \Gamma_e &= \left[\varepsilon + \zeta\left(h\kappa\right)\right] + I_\alpha\left[\mathrm{g}\big(h\psi_{\|;\alpha}\big) + \mathrm{p}\upsilon_{\|;\alpha}\right] + C_R^e\left(q\psi_3\right) \\ 2\Gamma_s &= \frac{1}{h}\left[\mathrm{g}_{|\zeta}\left(h\psi_\|\right) + \mathrm{p}_{|\zeta}\,\upsilon_\|\right] + e_\alpha\left(q\psi_{3;\alpha}\right) + C_R^s\left[\mathrm{g}\big(h\psi_\|\big) + \mathrm{p}\upsilon_\|\right] \\ \Gamma_t &= \frac{1}{h}\left(q_{|\zeta}\,\psi_3\right) \end{aligned} \tag{130}$$

Then, one can use the 3-D constitutive law to obtain 3-D stresses σ_{ij}.

CHAPTER III

NUMERICAL PROCEDURE

Although all the derived formulas in the previous chapter are given in an explicit and elegant analytical form, the whole procedure is not straightforward, even for shells made of homogeneous and isotropic materials. Even with the help of the phenomenal power of present day computer facilities and the ready availability of very sophisticated mathematical and engineering software packages such as Mathematica^{TM} and Matlab^{TM}, it is still tedious and essentially intractable. The main objective of this chapter is to propose a new numerical procedure corresponding to the present theory derived in the previous chapter. First, the dynamic 3-D elasticity problem is formulated in a dynamic intrinsic form exactly describing the complex geometry of shell structures (Section 3.1). This step is very close to one introduced in Sections 2.1 and 2.2 of the previous chapter. Since the numerical procedure is a direct extension of the previous chapter, some sentences or equations may be skipped here for the purpose of avoiding duplication of reading, but the main and important ones may be repeated for clarity and smoothness of presentation. Then as before VAM is used to rigorously divide this 3-D problem into a linear 1-D through-the-thickness analysis and a nonlinear 2-D surface analysis in the asymptotic sense. Moreover, in the long-wavelength regime, VAM is able to correctly split both analysis into low- and high-frequency cases based on the characteristic time-scale (Section 3.1). This time, however, the 1-D through-the-thickness analysis is set up and solved using the finite element method by discretizing the undetermined fields associated with all unknown 3-D functions along the normal line. First, the same numerical procedure as the static case [57] is used to solve the warping field for the low-frequency vibration approximations (Section 3.2). Next, the standard procedure of solving eigenvalue problems is chosen to obtain eigenvalues and eigenvectors that are used throughout the rest of the numerical procedure. However, unlike the previous works [44, 45], we introduce a different numerical procedure to solve for the fields associated with all

undetermined 3-D functions and their refinements for high-frequency vibration, each branch (Section 3.3) up to the first approximation. As mentioned before, even though the resulting theory is asymptotically correct within the long-wavelength regime, it does not always lead a positive definite matrix of stiffness coefficients. Therefore, the same procedure as used in the previous chapter, the hyperbolic short-wavelength extrapolation, is used to fix this (Section 3.4). The resulting theory provides a constitutive law (mass and stiffness matrices) as an input for 2-D nonlinear shell analysis, as well as recovery relations to approximately express the 3-D displacement, strain and stress fields in terms of shell variables calculated in the surface analysis (Section 3.5). Finally, an additional procedure of reductions from the resulting theory to a similar Ressiner-Minlin's plate/shell theory and to the classical theory of low-frequency vibrations is introduced. As the first attempt to implement the above whole procedure, the computer program Dynamic Variational Asymptotic Plate and Shell Analysis (DVAPAS), has been developed. Fig. 10 shows the main functionality of DVAPAS.

DVAPAS is used to calculate mass and stiffness matrices with respect to a chosen plate/shell modeling - i) refined modeling with transverse shear effects ii) refined modeling with through-the-thickness extension effect (just to check the effects of short-wavelength extrapolation), and iii) refined modeling with high-frequency vibration effects. It can provide these as input for a 2-D dynamic surface solver. In addition, DVAPAS can also recover the 3-D results based on the 2-D strain measures, the 2-D internal degrees of freedom and their derivatives.

3.1 Shell Kinematics and 3-D Formulation

Let us consider the vibrations of a laminated composite shell with constant mass density through the thickness, each layer of which is made of a monoclinic material. For use in our computational procedure, one can express the 3-D strain and velocity fields in matrix form from Eqs. (50) and (51) as:

$$\begin{aligned}\Gamma = \frac{1}{h}\Gamma_h w + \Gamma_e \varepsilon + \Gamma_c \left(h\kappa\right) + \Gamma_{L\alpha} w_{;\alpha} + \Gamma_R w \\ + h\Gamma_{Re}\varepsilon + h\Gamma_{Rc}\left(h\kappa\right) + \Gamma_{RL\alpha} w_{;\alpha} + h\Gamma_{RR} w\end{aligned} \tag{131}$$

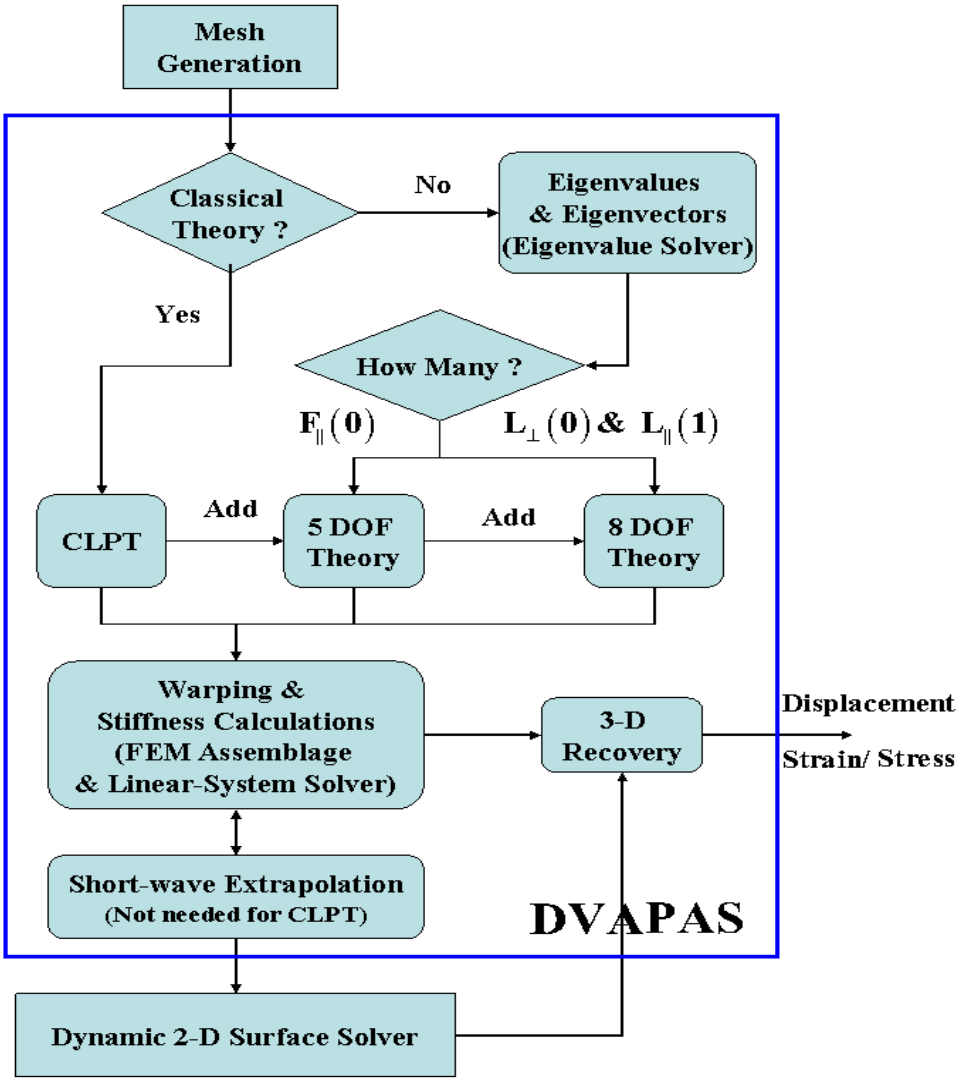

Figure 10: Main block of DVAPAS

and

$$\Lambda = V_S + V_T + \tilde{\xi}\left(h\Omega\right) + \dot{w} \tag{132}$$

where

$$\begin{aligned}
\Gamma &= \lfloor \Gamma_{11} \;\; 2\Gamma_{12} \;\; \Gamma_{22} \;\; 2\Gamma_{13} \;\; 2\Gamma_{23} \;\; \Gamma_{33} \rfloor^T \\
w &= \lfloor w_1 \;\; w_2 \;\; w_3 \rfloor^T \\
\varepsilon &= \lfloor \varepsilon_{11} \;\; 2\varepsilon_{12} \;\; \varepsilon_{22} \rfloor^T \\
\kappa &= \lfloor \kappa_{11} \;\; \kappa_{12} + \kappa_{21} \;\; \kappa_{22} \rfloor^T \\
V_S &= \lfloor V_1 \;\; V_2 \;\; 0 \rfloor^T \\
V_T &= \lfloor 0 \;\; 0 \;\; V_3 \rfloor^T \\
\Omega &= \lfloor \Omega_1 \;\; \Omega_2 \;\; \Omega_3 \rfloor^T
\end{aligned} \tag{133}$$

and

$$\tilde{\xi} = \zeta \begin{bmatrix} 0 & -1 & 0 \\ 1 & 0 & 0 \\ 0 & 0 & 0 \end{bmatrix} \tag{134}$$

with $(\bullet)_{;\alpha} = \partial(\bullet)/A_\alpha \partial x_\alpha$ and $(\dot{\bullet}) = \partial(\bullet)/\partial t$. Since A_α are slowly varying, they behave as if they are constants as far as differentiation concerned. Thus all the rules of differentiation apply to this new notation. Thus, all operators are defined as:

$$\Gamma_h = \begin{bmatrix} 0 & 0 & 0 \\ 0 & 0 & 0 \\ 0 & 0 & 0 \\ \dfrac{\partial}{\partial\zeta} & 0 & 0 \\ 0 & \dfrac{\partial}{\partial\zeta} & 0 \\ 0 & 0 & \dfrac{\partial}{\partial\zeta} \end{bmatrix} \tag{135}$$

$$\Gamma_e = \begin{bmatrix} 1 & 0 & 0 \\ 0 & 1 & 0 \\ 0 & 0 & 1 \\ 0 & 0 & 0 \\ 0 & 0 & 0 \\ 0 & 0 & 0 \end{bmatrix} \qquad \Gamma_c = \zeta \begin{bmatrix} 1 & 0 & 0 \\ 0 & 1 & 0 \\ 0 & 0 & 1 \\ 0 & 0 & 0 \\ 0 & 0 & 0 \\ 0 & 0 & 0 \end{bmatrix} \tag{136}$$

$$\Gamma_{Re} = -\zeta \begin{bmatrix} k_{11} & 0 & 0 \\ 0 & \dfrac{(k_{11}+k_{22})}{2} & 0 \\ 0 & 0 & k_{22} \\ 0 & 0 & 0 \\ 0 & 0 & 0 \\ 0 & 0 & 0 \end{bmatrix} \qquad \Gamma_{Rc} = -\zeta^2 \begin{bmatrix} k_{11} & 0 & 0 \\ 0 & \dfrac{(k_{11}+k_{22})}{2} & 0 \\ 0 & 0 & k_{22} \\ 0 & 0 & 0 \\ 0 & 0 & 0 \\ 0 & 0 & 0 \end{bmatrix} \tag{137}$$

$$\Gamma_{R} = \begin{bmatrix} 0 & 0 & k_{11} \\ 0 & 0 & 0 \\ 0 & 0 & k_{22} \\ -k_{11} & 0 & 0 \\ 0 & -k_{22} & 0 \\ 0 & 0 & 0 \end{bmatrix} \qquad \Gamma_{RR} = \zeta \begin{bmatrix} 0 & 0 & -k_{11}^2 \\ 0 & 0 & 0 \\ 0 & 0 & -k_{22}^2 \\ k_{11}^2 & 0 & 0 \\ 0 & k_{22}^2 & 0 \\ 0 & 0 & 0 \end{bmatrix} \tag{138}$$

$$\Gamma_{RL1} = -\zeta \begin{bmatrix} k_{11} & 0 & 0 \\ 0 & k_{11} & 0 \\ 0 & 0 & 0 \\ 0 & 0 & k_{11} \\ 0 & 0 & 0 \\ 0 & 0 & 0 \end{bmatrix} \qquad \Gamma_{RL2} = -\zeta \begin{bmatrix} 0 & 0 & 0 \\ k_{22} & 0 & 0 \\ 0 & k_{22} & 0 \\ 0 & 0 & 0 \\ 0 & 0 & k_{22} \\ 0 & 0 & 0 \end{bmatrix} \tag{139}$$

$$\Gamma_{L1} = \begin{bmatrix} 1 & 0 & 0 \\ 0 & 1 & 0 \\ 0 & 0 & 0 \\ 0 & 0 & 1 \\ 0 & 0 & 0 \\ 0 & 0 & 0 \end{bmatrix} \qquad \Gamma_{L2} = \begin{bmatrix} 0 & 0 & 0 \\ 1 & 0 & 0 \\ 0 & 1 & 0 \\ 0 & 0 & 0 \\ 0 & 0 & 1 \\ 0 & 0 & 0 \end{bmatrix} \tag{140}$$

To solve the resulting minimization problems, a finite element discretization is generally used. Moreover, for the laminated case, we have chosen the variable-order finite element method developed by Hodges [58, 59]. Unlike conventional finite element methods, degrees of freedom can be added without generation of a new element geometry. Similar with static

plate/shell modelings introduced by Yu *et al.* [57], a 5-noded isoparametric line element is recommended inherently to express numerically the correct orthogonality characteristics of the warping fields of each branch and frequency regime in polynomials up to the fourth order. In the laminated case, as the number of plies and ply groups increases, it is obvious that the size of the matrices expands very fast. However, Refs. [44] and [60] presented that for the problems they investigated (similar to the present but not identical), one can achieve better accuracy by using fewer elements with higher-order polynomials. Therefore, discretizing the transverse normal line into 1-D finite elements, one can express the undetermined functional as

$$w\left(x_1, x_2, \zeta, t\right) = S\left(\zeta\right) W\left(x_1, x_2, t\right) \tag{141}$$

where S is the $3 \times 3N$ matrix of shape functions, and W is the $3N \times 1$ column matrix of the N nodal values of the functional along the local normal line. Let us mention that in Eqs. (131) and (132), the procedure already includes results of the primary step for low-frequency vibration. In addition, unlike most published 2-D shell theories, the orders of unknown 3-D functions w are not assumed *a priori* to derive Eqs. (131) and (132), but rather they are obtained as results of the minimization in the first stage for low-frequency, long-wavelength vibration approximations and in the primary step for high-frequency ones. Using the above up to the zeroth-order approximations, the total energy functional per unit area for each frequency regime can be expressed in different discretized form as:

$$\overline{\mathcal{L}} = \overline{\mathcal{K}} - \overline{\mathcal{P}} \tag{142}$$

At first, for the low-frequency vibration case, w can be represented within the accuracy of our approximation as a general warping displacement, just as in the static case:

$$2\overline{\mathcal{K}} = \rho \left\{ V_S^T V_S + V_T^T V_T \right\} \tag{143}$$

and

$$\begin{aligned} 2\overline{\mathcal{P}} = {} & \left(\frac{1}{h}\right)^2 W^T \bar{E} W + 2\left(\frac{1}{h}\right) W^T \left[\bar{D}_{he}\varepsilon + \bar{D}_{hc}\left(h\kappa\right)\right] \\ & + \varepsilon^T \bar{D}_{ee}\varepsilon + 2\varepsilon^T \bar{D}_{ec}\left(h\kappa\right) + \left(h\kappa\right)^T \bar{D}_{cc}\left(h\kappa\right) \end{aligned} \tag{144}$$

On the other hand, for the case of the high-frequency vibration up to the zeroth-order approximation,

$$2\overline{\mathcal{K}} = \rho \left\{ \dot{W}^T M \dot{W} \right\} \tag{145}$$

and

$$\begin{aligned} 2\overline{\mathcal{P}} = & \left(\frac{1}{h}\right)^2 W^T E W + 2\left(\frac{1}{h}\right) W^T \left[D_{hL\alpha} W_{;\alpha} + D_{hR} W \right] \\ & + 2W^T \left[\overline{D}_{hRL\alpha} W_{;\alpha} + \bar{D}_{hRR} W + \bar{D}_{L\alpha R} W_{;\alpha} \right] \\ & + W_{;\alpha}^T \bar{D}_{L\alpha L\beta} W_{;\beta} + W^T \bar{D}_{RR} W + 2W^T L \end{aligned} \tag{146}$$

where L contains the load related terms such that

$$L = -S^{+T}\alpha - S^{-T}\beta - \left\langle S^T \phi \right\rangle \tag{147}$$

The new matrices carry the properties of both the geometry and material

$$\begin{aligned} E &= \left\langle [\Gamma_h S]^T D [\Gamma_h S] \eta \right\rangle & \bar{E} &= \left\langle [\Gamma_h S]^T D [\Gamma_h S] \right\rangle \\ D_{hR} &= \left\langle [\Gamma_h S]^T D [\Gamma_R S] \eta^* \right\rangle & D_{hL\alpha} &= \left\langle [\Gamma_h S]^T D [\Gamma_{L\alpha} S] \eta^* \right\rangle \\ \bar{D}_{hRR} &= \left\langle [\Gamma_h S]^T D [\Gamma_{RR} S] \right\rangle & \bar{D}_{hRL\alpha} &= \left\langle [\Gamma_h S]^T D [\Gamma_{RL\alpha} S] \right\rangle \\ \bar{D}_{L\alpha R} &= \left\langle [\Gamma_{L\alpha} S]^T D [\Gamma_R S] \right\rangle & \bar{D}_{L\alpha L\beta} &= \left\langle [\Gamma_{L\alpha} S]^T D [\Gamma_{L\beta} S] \right\rangle \\ \bar{D}_{he} &= \left\langle [\Gamma_h S]^T D [\Gamma_e] \right\rangle & \bar{D}_{RR} &= \left\langle [\Gamma_R S]^T D [\Gamma_R S] \right\rangle \\ \bar{D}_{ee} &= \left\langle [\Gamma_e]^T D [\Gamma_e] \right\rangle & \bar{D}_{hc} &= \left\langle [\Gamma_h S]^T D [\Gamma_c] \right\rangle \\ \bar{D}_{cc} &= \left\langle [\Gamma_c]^T D [\Gamma_c] \right\rangle & \bar{D}_{ec} &= \left\langle [\Gamma_e]^T D [\Gamma_c] \right\rangle \\ \bar{M} &= \left\langle [S]^T [S] \right\rangle & M &= \left\langle [S]^T [S] \eta \right\rangle \end{aligned} \tag{148}$$

where

$$\begin{aligned} \eta &= 1 + 2h\zeta H + (h\zeta)^2 K \\ \eta^* &= 1 + 2h\zeta H \end{aligned} \tag{149}$$

Here $H = (k_{11} + k_{22})/2$ and $K = k_{11}k_{22}$ are called the mean and the Gaussian curvatures of the surface, respectively. Now one is now ready to use the VAM to solve for the unknown 3-D functions asymptotically.

3.2 Low-frequency, Long-wavelength Vibration Approximations

The dimensional reduction from 3-D to 2-D cannot be done exactly. The best one can do is to accomplish it asymptotically by taking advantage of the smallness of h/l, h/R and $\hat{\varepsilon}$.

3.2.1 First approximation

As mentioned before, the results of the primary step under low-frequency vibration are already contained in Eqs. (143) and (144). According to the VAM procedure, in order to get the next approximation, one has to construct a series of functional according to different order. The first approximation of the energy functional can be constructed by discarding all the terms higher than $(h/R)^0$ and $(h/l)^0$, which leads to

$$\begin{aligned} 2\overline{\mathcal{L}} = \rho\left\{V_S^T V_S + V_T^T V_T\right\} - \Bigg\{ & \left(\frac{1}{h}\right)^2 W^T \bar{E} W + 2\left(\frac{1}{h}\right) W^T \left[\bar{D}_{he}\varepsilon + \bar{D}_{hc}\left(h\kappa\right)\right] \\ & + \varepsilon^T \bar{D}_{ee}\varepsilon + 2\varepsilon^T \bar{D}_{ec}\left(h\kappa\right) + \left(h\kappa\right)^T \bar{D}_{cc}\left(h\kappa\right)\Bigg\} \end{aligned} \tag{150}$$

Now, our problem has now been transformed into the numerical minimization of Eq. (150) subject to the constraints of Eqs. (43), which can be written in the following discretized form:

$$W^T \bar{M} \Psi_{cl} = 0 \tag{151}$$

where Ψ_{cl} is the $3N \times 3$ matrix where each of the three columns corresponds to one of the constraints of Eqs. (43). The set of columns Ψ_{cl} are determined by Eq. (40), which is the kernel (null-space) of matrix $\bar{E}$. This implies

$$\bar{E}\Psi_{cl} = 0 \tag{152}$$

For convenience and simplicity, let us suppose that the set of columns Ψ_{cl} is normalized in such a way that

$${\Psi_{cl}}^T \bar{M} \Psi_{cl} = \mathrm{I} \tag{153}$$

where I is the 3×3 identity matrix.

The Euler-Lagrange equation for this problem can be obtained by the usual procedure of calculus of variations with the aid of a Lagrange multiplier, yielding

$$\left(\frac{1}{h}\right)\bar{E}W + \bar{D}_{he}\varepsilon + \bar{D}_{hc}\left(h\kappa\right) = \bar{M}\Psi_{cl}\Delta \tag{154}$$

By pre-multiplying Eq. (154) by Ψ_{cl}^T and applying Eqs. (152) and (153) into Eq. (154), one can calculate the Lagrange multiplier Δ as

$$\Delta = \Psi_{cl}^T \left[\bar{D}_{he}\varepsilon + \bar{D}_{hc}\left(h\kappa\right) \right] \tag{155}$$

Substituting Eq. (155) back into Eq. (154), we obtain

$$\left(\frac{1}{h}\right) \bar{E}W = -\left[\mathrm{I} - \bar{M}\Psi_{cl}\Psi_{cl}^T \right] \left[\bar{D}_{he}\varepsilon + \bar{D}_{hc}\left(h\kappa\right) \right] \tag{156}$$

According to Refs. [44] and [60], there exists a unique solution for W, linearly independent of the null space of $\bar{E}$, because the right-hand-side of Eq. (156) is orthogonal to the null space. Since the solution is unique, we can choose any convenient constraints to make the problem determined. Hence the final solution minimizing the functional Eq. (150) subject to constraints of Eq. (151) is

$$W = -\left(\mathrm{H_l}\right)^+ \left[\bar{D}_{he}\varepsilon + \bar{D}_{hc}\left(h\kappa\right) \right] = hV_{0e}\varepsilon + hV_{0c}\left(h\kappa\right) \tag{157}$$

where

$$V_{0e} = -\left(\mathrm{H_l}\right)^+ \bar{D}_{he} \qquad V_{0c} = -\left(\mathrm{H_l}\right)^+ \bar{D}_{hc}$$

As expected, the above warping field is of the order $h\hat{\varepsilon}$. Here the matrix $\left(\mathrm{H_l}\right)^+$ can be satisfied with the following properties

$$\begin{aligned} \bar{E}\left(\mathrm{H_l}\right)^+ &= \mathrm{I} - \bar{M}\Psi_{cl}\Psi_{cl}^T \\ \left(\mathrm{H_l}\right)^+ \bar{E} &= \mathrm{I} - \Psi_{cl}\Psi_{cl}^T\bar{M} \\ \left(\mathrm{H_l}\right)^+ \bar{E}\left(\mathrm{H_l}\right)^+ &= \bar{E} \end{aligned} \tag{158}$$

See Ref. [44] for an explanation of how to calculate the matrix $\left(\mathrm{H_l}\right)^+$ in detail.

3.2.2 Total energy functional for low-frequency vibrations

Before closing this section it is convenient to derive the total energy functional for the low-frequency, long-wavelength regime. Substituting Eq. (157) back into Eq. (150), one can obtain the total energy functional, asymptotically correct through the order of $\mu\hat{\varepsilon}^2$ as

$$\overline{\mathcal{L}} = \frac{1}{2}\rho\left\{ V_S^T V_S + V_T^T V_T \right\} - \frac{1}{2}\left\{ \varepsilon^T \mathrm{A}\varepsilon + 2\varepsilon^T \mathrm{B}\left(h\kappa\right) + \left(h\kappa\right)^T \mathrm{C}\left(h\kappa\right) \right\} \tag{159}$$

where

$$\begin{aligned} \mathrm{A} &= \bar{D}_{ee} + V_{0e}^T \bar{D}_{he} \\ \mathrm{B} &= \bar{D}_{ec} + V_{0e}^T \bar{D}_{hc} \\ \mathrm{C} &= \bar{D}_{cc} + V_{0c}^T \bar{D}_{hc} \end{aligned} \tag{160}$$

Here μ represents the material elastic constants, all of which are assumed to be of the same order. The above average functional of this approximation coincides with Eq. (74), which is referred to as classical laminated plate theories. However, *ad hoc* kinematic assumptions such as the Kirchhoff hypothesis were not used to obtain this result.

3.3 High-frequency, Long-wavelength Vibration Approximations

In contrast to the case of low-frequency vibrations, the kinetic energy density must be retained in the primary step of the variational-asymptotic procedure since the frequencies are no longer small due to Eq. (27).

3.3.1 Primary approximation

According to the VAM, one should keep only the leading quadratic energy term with respect to the small parameter that contains the unknown function and the leading intersection term between the unknown function and the rest of the functional. Without *a priori* assumption of the order of undetermined functions W, we are left with the only following expression from Eq. (142)

$$2\overline{\mathcal{L}} = \rho \left\{ \dot{W}^T \bar{M} \dot{W} \right\} - \left\{ \left(\frac{1}{h} \right)^2 W^T \bar{E} W \right\} \tag{161}$$

By applying the usual procedure of the calculus of variations with the help of Eqs. (85), Eq. (167) can be minimized with respect to W and transformed into the form of a standard eigenvalue problem of the form

$$\left[\bar{E} - \lambda \bar{M} \right] W = 0 \tag{162}$$

Following the solution procedure of the eigenvalue problem [61], the non-trivial solutions λ_{ij} can be obtained from those for which satisfy

$$\det \left| \bar{E} - \lambda \bar{M} \right| = 0 \tag{163}$$

Substituting the resulting eigenvalue λ_{ij} back into Eq. (162), one can calculate a corresponding set of ϕ_k^{ij}, each one of which is the $3N \times 1$ eigenvector corresponding to eigenvalue λ_{ij}. Thus,

$$\left[\bar{E} - \lambda_{ij}\bar{M}\right] \phi_k^{ij} = 0 \qquad \mathrm{k} = 1, 2, \cdots, 3N \tag{164}$$

For convenience, let us introduce Λ as a $3N \times 3N$ diagonal matrix of eigenvalues:

$$\Lambda = \begin{bmatrix} \lambda_{11} & 0 & \cdots & 0 \\ 0 & \lambda_{21} & \cdots & 0 \\ \vdots & \vdots & \ddots & \vdots \\ 0 & 0 & 0 & \lambda_{3N3} \end{bmatrix} \tag{165}$$

with Φ a $3N \times 3N$ matrix of the eigenvectors composed of all ϕ_k^{ij} satisfied with Eq. (164) corresponding to each λ_{ij} and normalized such that

$$\Phi^T \bar{M} \Phi = I \tag{166}$$

Finally, one can obtain the following result at the primary approximation:

$$\bar{E}\Phi V = \bar{M}\Phi\Lambda V \tag{167}$$

Note that if the matrix of eigenvectors Φ is independent of in-plane coordinates x_α, each of the solutions given Eq. (167) represents an exact solution of 3-D dynamic equations of elasticity for an infinite plate, and corresponds to synchronous vibrations of the normal line elements over the plate surface with zero in-plane wave number. Except for the finite element-based formulation, Eq. (167) is the same as Eqs. (78) and (81).

Before proceeding to the first approximation, it is to convenient to redefine Eq. (167) mainly based on the following two characteristics: First, concerning the clamped boundary conditions at the shell edge, it turns out that the branches associated with the high-frequency vibrations possess an outstanding property: they retain the orthogonality property with respect to each other in the kinetic and strain energy densities up to the first approximation. This implies that, in the first approximation, vibrations of one type do not interact with vibrations of another type; thus, this remarkable characteristic can be used to investigate the vibrations of one branch independently of the vibrations of the rest

(excluding the classical branches describing low-frequency vibrations). Second, we can take advantage of the monoclinic symmetry of each layer in Eq. (167) to represent numerical-based forms such as analytical-based forms Eqs. (78) and (81). Taken advantage of orthogonal property and monoclinic symmetry one can rewrite Eq. (167) into the following forms corresponding to different high-frequency vibrations: First, for the branches associated with the thickness-extension vibrations (the series $L_\perp$ or $F_\perp$), Eqs. (141) can be expressed in the discretized form as

$$w\left(x_1, x_2, \zeta, t\right) = S\left(\zeta\right) W_0\left(x_1, x_2, t\right) = S\left(\zeta\right) \Phi^{3i} V\left(x_1, x_2, t\right) \tag{168}$$

Here Φ^{3i} satisfies the following equation

$$\bar{E}\Phi^{3i}V = \bar{M}\Phi^{3i}\Lambda_{3i}V \qquad \text{where} \quad i = 1, 2, \cdots, N \tag{169}$$

where Λ_{3i} and Φ^{3i} can be defined as 3×3 and $3N\times3$ matrices one in such a way, respectively:

$$\Lambda_{3i} = \begin{bmatrix} 0 & 0 & 0 \\ 0 & 0 & 0 \\ 0 & 0 & \lambda_{3i} \end{bmatrix} \tag{170}$$

and

$$\Phi^{3i} = \lfloor 0 \;\; 0 \;\; \phi_k^{3i} \rfloor \qquad \text{where} \quad k = 1, 2, \cdots, N \tag{171}$$

with

$$\Phi^{3i^T} \bar{M} \Phi^{3i} = \mathrm{I}^3 \tag{172}$$

Here I^3 is a 3×3 specific identity matrix for the thickness-extension vibration approximations,

$$\mathrm{I}^3 = \begin{bmatrix} 0 & 0 & 0 \\ 0 & 0 & 0 \\ 0 & 0 & 1 \end{bmatrix}$$

Analogously, for the branches associated with the thickness-shear vibrations (the series $L_\parallel$ or $F_\parallel$), Eqs. (141) can be expressed in a different discretized form, such that

$$w\left(x_1, x_2, \zeta, t\right) = S\left(\zeta\right) W_0\left(x_1, x_2, t\right) = S\left(\zeta\right) \Phi^{Si} V\left(x_1, x_2, t\right) \tag{173}$$

Here Φ^{Si} will satisfy the following equation

$$\bar{E}\Phi^{Si}V = \bar{M}\Phi^{Si}\Lambda_{Si}V \qquad \text{where} \quad i = 1, 2, \cdots, N \tag{174}$$

where

$$\Lambda_{Si} = \begin{bmatrix} \lambda_{1i} & 0 & 0 \\ 0 & \lambda_{2i} & 0 \\ 0 & 0 & 0 \end{bmatrix} \tag{175}$$

and

$$\Phi^{Si} = \lfloor \phi_k^{1i} \;\; \phi_k^{2i} \;\; 0 \rfloor \qquad \text{where} \quad k = 1, 2, \cdots, 3N \tag{176}$$

with

$$\Phi^{Si^T}\bar{M}\Phi^{Si} = \mathrm{I}^S \tag{177}$$

Here I^S is a 3×3 specific identity matrix for the thickness-shear vibration approximations,

$$\mathrm{I}^S = \begin{bmatrix} 1 & 0 & 0 \\ 0 & 1 & 0 \\ 0 & 0 & 0 \end{bmatrix}$$

Compared with the analytical results in the previous chapter, Eqs. (168) and (173) perfectly coincide with Eqs. (77) and (80).

3.3.2 First approximation (zeroth-order approximation)

Let us now consider the next refinement for the displacement fields in branches associated with thickness-extension vibrations. As expected, perturbing the primary result with a warping field hW^{3i} that is of order $(h/l + h/R)\, W_0$, one can express the warping as

$$W = W_0 + hW^{3i} \qquad \text{where} \quad i = 1, 2, \cdots, N \tag{178}$$

where W_0 denotes the the first term of Eq. (178)

$$W_0 = \Phi^{3i}V$$

Without loss of generality, the discretized form of Eq. (93) can be written as

$$W^{3i^T}\bar{M}W_0 = 0 \tag{179}$$

Substituting Eq. (178) back into Eq. (142), one can obtain the leading terms for the zeroth-order approximation as

$$\begin{aligned} 2\overline{\mathcal{L}} = \rho \Big\{ & h^2 \dot{W}^{3iT} \bar{M} \dot{W}^{3i} + 2\underline{h \dot{W}_0^T \bar{M} \dot{W}^{3i}} + 4h^2 H \dot{W}_0^T \hat{M} \dot{W}^{3i} \Big\} \\ - \Big\{ & W^{3iT} \bar{E} W^{3i} + 2\left(\frac{1}{h}\right) \underline{W_0^T \bar{E} W^{3i}} + 2 \left[W^{3iT} \bar{D}_{hL\alpha} W_{0;\alpha} \right. \\ & \left. \underline{\underline{-W^{3iT} \bar{D}_{hL\alpha} W_{0;\alpha}}} + W^{3iT} \bar{D}_{hR} W_0 + W_0^T \bar{D}_{hR} W^{3i} + 4H W_0^T \hat{E} W^{3i} \right] \Big\} \end{aligned} \tag{180}$$

where

$$\hat{E} = \left\langle [\Gamma_h S]^T D [\Gamma_h S] \zeta \right\rangle \qquad \hat{M} = \left\langle [S]^T [S] \zeta \right\rangle$$

Here with the help of Eqs. (85), the underlined terms are equal to zero because of Eq. (169) for W^{3i}. The double-underline term was obtained using integration by parts; terms evaluated at the boundary vanish due to the clamped edge condition. Similarly as the procedure of the first step in the low-frequency regime, one can solve the first-order warping field in the following way: First, the Euler-Lagrange equation for the functional of Eq. (180) can be obtained as

$$\left(\bar{E} - \lambda \bar{M}\right) W^{3i} + D_{L\alpha}^{3i} V_{;\alpha} + D_R^{3i} V = \bar{M} \Phi^{3i} \Delta \tag{181}$$

where Δ is the Lagrange multiplier which enforces the constraint in Eq. (179) and

$$\begin{aligned} D_{L\alpha}^{3i} &= \left(\bar{D}_{hL\alpha} - \bar{D}_{hL\alpha}^T\right) \Phi^{3i} \\ D_R^{3i} &= \left(\bar{D}_{hR} + \bar{D}_{hR}^T\right) \Phi^{3i} + 2H \left(\hat{E} \Phi^{3i} - \hat{H} \Phi^{3i} \Lambda_{3i}\right) \end{aligned} \tag{182}$$

By pre-multiplying Eq. (181) by Φ^{3i}, the first terms in Eq. (181) can be replaced by the asymptotically equivalent terms

$$\Phi^{3iT} \left(\bar{E} - \lambda \bar{M}\right) W^{3i} \approx \left[\Phi^{3iT} \bar{E} - \left(\Phi^{3i} \Lambda_{3i}\right)^T \bar{M} \right] W^{3i}$$

Then, by using Eqs. (169) and (172), one gets

$$\Delta = \Phi^{3iT} \left[D_{L\alpha}^{3i} V_{;\alpha} + D_R^{3i} V \right] \tag{183}$$

Substituting Eq. (183) back into Eq. (181) and applying the property of orthogonality with the high-frequency branches, one can rewrite the latter equation as

$$\mathrm{H_{3i}} W^{3i} = - \left[\mathrm{I} - \bar{M} \Phi^{3i} \Phi^{3iT} \right] \left[D_{L\alpha}^{3i} V_{;\alpha} + D_R^{3i} V \right] \tag{184}$$

where

$$\mathrm{H}_{3i} = \bar{E} - \lambda_{3i}\bar{M} \tag{185}$$

Since $\mathrm{H}_{3\mathrm{i}}$ has only one kernel for the thickness-extension vibrations, the inverse matrix of $\mathrm{H}_{3\mathrm{i}}$ does not exist. However, by modifying previously developed methodology (Refs. [44], [45] and [60]) using instead the constraint from Eq. (179), one can derive the pseudo-inverse $(\mathrm{H}_{3\mathrm{i}})^{+}$, which satisfies the following relations

$$\begin{aligned} \mathrm{H}_{3\mathrm{i}}\,(\mathrm{H}_{3\mathrm{i}})^{+} &= \mathrm{I} - \bar{M}\Psi^{3i}\Psi^{3iT} \\ (\mathrm{H}_{3\mathrm{i}})^{+}\,\mathrm{H}_{3\mathrm{i}} &= \mathrm{I} - \Psi^{3i}\Psi^{3iT}\bar{M} \\ (\mathrm{H}_{3\mathrm{i}})^{+}\,\mathrm{H}_{3\mathrm{i}}\,(\mathrm{H}_{3\mathrm{i}})^{+} &= \mathrm{H}_{3\mathrm{i}} \end{aligned} \tag{186}$$

Finally, the solution of Eq. (184) becomes

$$W^{3i} = -\,(\mathrm{H}_{3i})^{+}\left[D^{3i}_{L\alpha}V_{;\alpha} + D^{3i}_{R}V\right] = \Phi^{3i}_{L\alpha}V_{;\alpha} + \Phi^{3i}_{R}V \tag{187}$$

where

$$\Phi^{3i}_{L\alpha} = -\,(\mathrm{H}_{3i})^{+}\,D^{3i}_{L\alpha} \qquad \Phi^{3i}_{R} = -\,(\mathrm{H}_{3i})^{+}\,D^{3i}_{R}$$

Summarizing, we have the following distribution of the displacement fields over the thickness in the series of thickness-extension vibrations up to the first approximation:

$$\begin{aligned} w\,(x_1,x_2,\zeta,t) &= S\,(\zeta)\,W_0\,(x_1,x_2,t) + hS\,(\zeta)\,W^{3i}\,(x_1,x_2,t) \\ &= S\,(\zeta)\,\Phi^{3i}V\,(x_1,x_2,t) + hS\,(\zeta)\left[\Phi^{3i}_{L\alpha}V_{;\alpha}\,(x_1,x_2,t) + \Phi^{3i}_{R}V\,(x_1,x_2,t)\right] \end{aligned} \tag{188}$$

Analogously, we also can find the warping function for the displacement fields in the branches associated with the thickness-shear vibrations. Following the usual proceeding of the variational-asymptotic procedure, one has the correct expansion of W through the first-order

$$W = W_0 + hW^{Si} \qquad \text{where} \quad i = 1, 2, \cdots, N \tag{189}$$

where W_0 denotes the the first term of Eq. (189), given by

$$W_0 = \Phi^{Si}V$$

Unlike Eq. (190), for thickness-extension vibrations, another constraint can be imposed on the undetermined warping field W^{Si} in discretized form:

$$W^{Si^T}\bar{M}W_0 = 0 \tag{190}$$

Similarly to what was done before, substituting Eq. (189) back into Eq. (142) and discarding small terms of W^{Si} and small cross terms, one can obtain the leading term for the zeroth-order approximation as

$$\begin{aligned} 2\overline{\mathcal{L}} = \rho\Big\{ & h^2\dot{W}^{SiT}\bar{M}\dot{W}^{Si} + 2\underline{h\dot{W}_0^T\bar{M}\dot{W}^{Si}} + 4h^2H\dot{W}_0^T\hat{M}\dot{W}^{Si}\Big\} \\ - \Big\{ & W^{SiT}\bar{E}W^{Si} + 2\left(\frac{1}{h}\right)\underline{W_0^T\bar{E}W^{Si}} + 2\left[W^{SiT}\bar{D}_{hL\alpha}W_{0;\alpha}\right. \\ & \left.-\underline{\underline{W^{SiT}\bar{D}_{hL\alpha}W_{0;\alpha}}} + W^{SiT}\bar{D}_{hR}W_0 + W_0^T\bar{D}_{hR}W^{Si} + 4HW_0^T\hat{E}W^{Si}\right]\Big\} \end{aligned} \tag{191}$$

where, with the help of Eqs. (85), it can be determined that the underlined terms are equal to zero because of Eq. (174) for W^{Si}. In addition, the double-underlined term was obtained using integration by parts, and terms evaluated at the boundary vanish due to the clamped edge. Similarly as the above procedure, one can solve the first-order warping field. From Eq. (191), one obtains the Euler-Lagrange equation for the thickness-shear vibrations, as at first, with the Euler-Lagrange equation as

$$\left(\bar{E} - \lambda\bar{M}\right)W^{Si} + D_{L\alpha}^{Si}V_{;\alpha} + D_R^{Si}V = \bar{M}\Phi^{Si}\Delta \tag{192}$$

where Δ is the Lagrange multiplier that enforces the constraint in Eq. (190) and

$$\begin{aligned} D_{L\alpha}^{Si} &= \left(\bar{D}_{hL\alpha} - \bar{D}_{hL\alpha}^T\right)\Phi^{Si} \\ D_R^{Si} &= \left(\bar{D}_{hR} + \bar{D}_{hR}^T\right)\Phi^{Si} + 2H\left(\hat{E}\Phi^{Si} - \hat{H}\Phi^{Si}\Lambda_{Si}\right) \end{aligned} \tag{193}$$

Similarly, Eq. (192) is pre-multiplied by Φ^{Si} to calculate Δ for the thickness-shear vibrations.

$$\Phi^{SiT}\left(\bar{E} - \lambda\bar{M}\right)W^{Si} \approx \left[\Phi^{SiT}\bar{E} - \left(\Phi^{Si}\Lambda_{Si}\right)^T\bar{M}\right]W^{Si}$$

Then by following the same procedure as above and using the primary results found in Eqs. (174) and (177), one obtains

$$\Delta = \Phi^{SiT}\left[D_{L\alpha}^{Si}V_{;\alpha} + D_R^{Si}V\right] \tag{194}$$

and substituting Eq. (194) back into Eq. (192), one obtains

$$\left(\bar{E}-\lambda\bar{M}\right)W^{Si}=-\left[\mathrm{I}-\bar{M}\Phi^{Si}\Phi^{SiT}\right]\left[D_{L\alpha}^{Si}V_{;\alpha}+D_{R}^{Si}V\right] \tag{195}$$

Unlike the branches associated with the thickness-extension vibrations, there are two different eigenvalues $\lambda=\lambda_{\alpha i}$ for thickness-shear vibration cases for each $i=1,2,\cdots,N$, where $\alpha=1,2$. Therefore, it is clear that we have to establish two different kernels to solve for W^{Si}. First, for the $\lambda=\lambda_{1i}$ case, the solution of Eq. (192) becomes

$$W^{1i}=-\left(\mathrm{H}_{1i}\right)^{+}\left[D_{L\alpha}^{Si}V_{;\alpha}+D_{R}^{Si}V\right]=\Phi_{L\alpha}^{1i}V_{;\alpha}+\Phi_{R}^{1i}V \tag{196}$$

where

$$\Phi_{L\alpha}^{1i}=-\left(\mathrm{H}_{1i}\right)^{+}D_{L\alpha}^{Si}\qquad\Phi_{R}^{1i}=-\left(\mathrm{H}_{1i}\right)^{+}D_{R}^{Si}$$

and similarly one can also calculate the solution of Eq. (192) for the $\lambda=\lambda_{2i}$ case, such that

$$W^{2i}=-\left(\mathrm{H}_{2i}\right)^{+}\left[D_{L\alpha}^{Si}V_{;\alpha}+D_{R}^{Si}V\right]=\Phi_{L\alpha}^{2i}V_{;\alpha}+\Phi_{R}^{2i}V \tag{197}$$

where

$$\Phi_{L\alpha}^{2i}=-\left(\mathrm{H}_{2i}\right)^{+}D_{L\alpha}^{Si}\qquad\Phi_{R}^{2i}=-\left(\mathrm{H}_{2i}\right)^{+}D_{R}^{Si}$$

Here the matrices $\left(\mathrm{H}_{1\mathrm{i}}\right)^{+}$ and $\left(\mathrm{H}_{2\mathrm{i}}\right)^{+}$ are defined in the same way as Eqs. (186), except that usage of another constraint, such as Eq. (190), so that

$$\mathrm{H}_{1i}\left(\mathrm{H}_{1i}\right)^{+}=\mathrm{H}_{2i}\left(\mathrm{H}_{2i}\right)^{+}=\mathrm{I}-\bar{M}\Phi^{Si}\Phi^{SiT} \tag{198}$$

with

$$\mathrm{H}_{1i}=\bar{E}-\lambda_{1i}\bar{M}\qquad\mathrm{H}_{2i}=\bar{E}-\lambda_{2i}\bar{M} \tag{199}$$

Thus, for the series of thickness-shear vibrations (within the first approximation) we have

$$\begin{aligned}w\left(x_1,x_2,\zeta,t\right)&=S\left(\zeta\right)W_0\left(x_1,x_2,t\right)+hS\left(\zeta\right)W^{Si}\left(x_1,x_2,t\right)\\&=S\left(\zeta\right)\Phi^{Si}V\left(x_1,x_2,t\right)+hS\left(\zeta\right)\left[\Phi_{L\alpha}^{Si}V_{;\alpha}\left(x_1,x_2,t\right)+\Phi_{R}^{Si}V\left(x_1,x_2,t\right)\right]\end{aligned} \tag{200}$$

where, for convenience, $\Phi_{L\alpha}^{Si}$ and Φ_{R}^{Si} are introduced in such a way as

$$\Phi_{L\alpha}^{Si}=\frac{1}{2}\left(\Phi_{L\alpha}^{1i}+\Phi_{L\alpha}^{2i}\right)$$

$$\Phi_{R}^{Si}=\frac{1}{2}\left(\Phi_{R}^{1i}+\Phi_{R}^{2i}\right)$$

As expected, the order of the determined warping field W^{Si} is of the order $(1/l + 1/R)\, W_0$.

Before closing this subsection by deriving each average energy functional for high-frequency vibrations, let us consider the lowest thickness-shear vibrations ($i = 1$) to simplify the subsequent changes of unknown functions introduced by the procedure of hyperbolic short-wavelength extrapolation. One can express Eq. (116) as

$$\langle \zeta S \rangle \, \Phi^{S1} = \left\langle \zeta^2 \right\rangle \mathrm{I}^S \tag{201}$$

Based on the above normalization condition, the Lagrange multiplier Δ is a little changed unlike Eq. (194)

$$\Delta = \left[\Phi^{S1} \left(\alpha_{\mathrm{S1}} \right)^{+} \right]^T \left[D_{L\alpha}^{S1} V_{;\alpha} + D_R^{S1} V \right] \tag{202}$$

where the 3×3 matrix $\left(\alpha_{\mathrm{S1}} \right)^{+}$ will satisfy the following equation

$$\left(\alpha_{\mathrm{S1}} \right)^{+} \alpha_{\mathrm{S1}} = \mathrm{I}^S \tag{203}$$

with

$$\Phi^{S1 T} \bar{M} \Phi^{S1} = \alpha_{S1} \tag{204}$$

After this, the kernel matrices $\left(\mathrm{H}_{11} \right)^{+}$ and $\left(\mathrm{H}_{21} \right)^{+}$ are determined in a way similar to previous use of Eqs. (198) with Eq. (190), such that

$$\mathrm{H}_{11} \left(\mathrm{H}_{11} \right)^{+} = \mathrm{H}_{21} \left(\mathrm{H}_{21} \right)^{+} = \mathrm{I} - \bar{M} \Phi^{S1} \left[\Phi^{S1} \left(\alpha_{\mathrm{S1}} \right)^{+} \right]^T \tag{205}$$

with

$$\mathrm{H}_{11} = \bar{E} - \lambda_{11} \bar{M} \qquad \mathrm{H}_{21} = \bar{E} - \lambda_{21} \bar{M} \tag{206}$$

Thus, for the first lowest of the thickness-shear vibrations (within the first approximation) one obtains

$$\begin{aligned} w \left(x_1, x_2, \zeta, t \right) &= S \left(\zeta \right) W_0 \left(x_1, x_2, t \right) + h S \left(\zeta \right) W^{S1} \left(x_1, x_2, t \right) \\ &= S \left(\zeta \right) \Phi^{S1} V \left(x_1, x_2, t \right) + h S \left(\zeta \right) \left[\Phi_{L\alpha}^{S1} V_{;\alpha} \left(x_1, x_2, t \right) + \Phi_R^{S1} V \left(x_1, x_2, t \right) \right] \end{aligned} \tag{207}$$

where

$$\Phi_{L\alpha}^{S1} = \frac{1}{2} \left(\Phi_{L\alpha}^{11} + \Phi_{L\alpha}^{21} \right)$$

$$\Phi_R^{S1} = \frac{1}{2} \left(\Phi_R^{11} + \Phi_R^{21} \right)$$

By continuing the iteration process and following the same procedure, subsequent corrections to W for each of the branches can be found. However, since they do not contribute to the total energy functional of the zeroth-order approximation, one does not need to go any further.

3.3.3 Total energy functional for high-frequency vibrations

Note that here and throughout the rest of the shell development, we assume that $\hat{q}$ is the order of the displacement field of the high-frequency vibrations. Let us first consider the total energy functional for the thickness-extension vibrations $V_\perp$ that is asymptotically correct up to the order of $\mu\left(1/l\right)^2\hat{q}^2$ and $\mu\left(1/R\right)^2\hat{q}^2$ under the variational-asymptotic procedures. Substituting Eq. (188) into Eqs. (145), (146) and (147), retaining the leading quadratic terms and the leading cross term with respect to the small parameter under consideration, a total energy functional that is asymptotically correct through the zeroth-order can be expressed as

$$\begin{aligned}
2\overline{\mathcal{L}}_{3i} = \rho\Bigg\{ & \left(\Phi^{3i}\dot{V}_\perp\right)^T \bar{M}\left(\Phi^{3i}\dot{V}_\perp\right) + \underline{2hH\left(\Phi^{3i}\dot{V}_\perp\right)^T \hat{M}\left(\Phi^{3i}\dot{V}_\perp\right)} \\
& + h^2 K\left(\Phi^{3i}\dot{V}_\perp\right)^T \tilde{M}\left(\Phi^{3i}\dot{V}_\perp\right)\Bigg\} - \Bigg\{\left(\frac{1}{h}\right)^2 \left(\Phi^{3i}V_\perp\right)^T \bar{E}\left(\Phi^{3i}V_\perp\right) \\
& + 2\left(\frac{1}{h}\right)\underline{\left(\Phi^{3i}V_\perp\right)^T\left[H\hat{M}\left(\Phi^{3i}V_\perp\right) + \bar{D}_{hL\alpha}\left(\Phi^{3i}V_{\perp;\alpha}\right) + \bar{D}_{hR}\left(\Phi^{3i}V_\perp\right)\right]} \\
& + K\left(\Phi^{3i}V_\perp\right)^T \tilde{M}\left(\Phi^{3i}V_\perp\right) + 4H\left(\Phi^{3i}V_\perp\right)^T \hat{D}_{hR}\left(\Phi^{3i}V_\perp\right) \\
& + 2\left(\Phi^{3i}V_\perp\right)^T \bar{D}_{hRR}\left(\Phi^{3i}V_\perp\right) + \left(\Phi^{3i}V_{\perp;\alpha}\right)^T \bar{D}_{L\alpha L\beta}\left(\Phi^{3i}V_{\perp;\beta}\right) \\
& + \left(\Phi^{3i}V_\perp\right)^T \bar{D}_{RR}\left(\Phi^{3i}V_\perp\right) + \left[\Phi^{3i}_{L\alpha}V_{\perp;\alpha} + \Phi^{3i}_R V_\perp\right]^T \left[D^{3i}_{L\beta}V_{\perp;\alpha} + D^{3i}_R V_\perp\right]\Bigg\} \\
& - 2\left(\Phi^{3i}V_\perp\right)^T L
\end{aligned} \tag{208}$$

where

$$\tilde{E} = \left\langle \left[\Gamma_h S\right]^T D\left[\Gamma_h S\right]\zeta^2 \right\rangle \qquad \tilde{M} = \left\langle \left[S\right]^T\left[S\right]\zeta^2 \right\rangle$$

Here we have already taken advantage of monoclinic symmetry to obtain the asymptotically correct energy in Eq. (208). After eliminating the underlined terms in Eq. (208) as the primary and first approximation results for the thickness-extension vibrations ($i = 1, 2, \cdots, N$),

we obtain the total energy functional $\overline{\mathcal{L}}_{3i}$ given by

$$\begin{aligned}\overline{\mathcal{L}}_{3i} = \frac{1}{2}\rho\left\{\left(\dot{V}_\perp\right)^T \mathrm{I}^3\left(\dot{V}_\perp\right)\right\} - \frac{1}{2}\left\{(V_\perp)^T\left[\left(\frac{1}{h}\right)^2\Lambda_{3i} + \Psi^{3i}\right](V_\perp)\right. \\ \left. + (V_{\perp;\alpha})^T\,\mathrm{T}^{3i}_{\alpha\beta}\,(V_{\perp;\beta})\right\} - (V_\perp)^T\,\mathrm{F}^{3i}\end{aligned} \tag{209}$$

where I^3 and Λ_{3i} are defined as Eqs. (170) and (172) and

$$\begin{aligned}\Psi^{3i} &= \left(\Phi^{3i}\right)^T\left[\bar{D}_{RR} + 4H\hat{D}_{hR} + 2\bar{D}_{hRR}\right]\left(\Phi^{3i}\right) \\ &\quad + K\left[\left(\Phi^{3i}\right)^T\tilde{E} - \left(\Phi^{3i}\Lambda_{3i}\right)^T\tilde{M}\right]\left(\Phi^{3i}\right) + \left(\Phi^{3i}_R\right)^T D^{3i}_R \\ \mathrm{T}^{3i}_{\alpha\beta} &= \left(\Phi^{3i}\right)^T\bar{D}_{L\alpha L\beta}\left(\Phi^{3i}\right) + \left(\Phi^{3i}_{L\alpha}\right)^T D^{3i}_{L\beta} \\ \mathrm{F}^{3i} &= \left(\Phi^{3i}\right)^T L\end{aligned} \tag{210}$$

Analogously, we then turn to a branch in the series of thickness-shear vibrations, $V_\parallel$, the displacement fields of which are given by the asymptotic formula, Eq. (200). Taking advantage of monoclinic symmetry, substituting Eq. (200) back into Eq. (142), discarding the small quadratic terms and the small cross terms of the order $h/l, h/R$ compared to unity, and using Eqs. (174) and (192), one can obtain the total energy functional $\overline{\mathcal{L}}_{Si}$ defined as in Eq. (142), for the thickness-shear vibrations ($i = 2, 3, \cdots, N$):

$$\begin{aligned}\overline{\mathcal{L}}_{Si} = \frac{1}{2}\rho\left\{\left(\dot{V}_\parallel\right)^T \mathrm{I}^S\left(\dot{V}_\parallel\right)\right\} - \frac{1}{2}\left\{\left(V_\parallel\right)^T\left[\left(\frac{1}{h}\right)^2\Lambda_{Si} + \Psi^{Si}\right]\left(V_\parallel\right)\right. \\ \left. + \left(V_{\parallel;\alpha}\right)^T\mathrm{T}^{Si}_{\alpha\beta}\left(V_{\parallel;\beta}\right)\right\} - \left(V_\parallel\right)^T\mathrm{F}^{Si}\end{aligned} \tag{211}$$

where I^3 and Λ_{Si} are defined as Eqs. (175) and (177) and

$$\begin{aligned}\Psi^{Si} &= \left(\Phi^{Si}\right)^T\left[\bar{D}_{RR} + 4H\hat{D}_{hR} + 2\bar{D}_{hRR}\right]\left(\Phi^{Si}\right) \\ &\quad + K\left[\left(\Phi^{Si}\right)^T\tilde{E} - \left(\Phi^{Si}\Lambda_{Si}\right)^T\tilde{M}\right]\left(\Phi^{Si}\right) + \left(\Phi^{Si}_R\right)^T D^{Si}_R \\ \mathrm{T}^{Si}_{\alpha\beta} &= \left(\Phi^{Si}\right)^T\bar{D}_{L\alpha L\beta}\left(\Phi^{Si}\right) + \left(\Phi^{Si}_{L\alpha}\right)^T D^{Si}_{L\beta} \\ \mathrm{F}^{Si} &= \left(\Phi^{Si}\right)^T L\end{aligned} \tag{212}$$

Now let us consider the total energy functional of the first thickness-shear vibrations $W_\parallel$ with $i = 1$. Following the same procedure as before, one obtains $\overline{\mathcal{L}}_{S1}$ up to the first approximation:

$$\begin{aligned}\overline{\mathcal{L}}_{S1} = \frac{1}{2}\rho\left\{\left(\dot{W}_\parallel\right)^T\alpha_{S1}\left(\dot{W}_\parallel\right)\right\} - \frac{1}{2}\left\{\left(W_\parallel\right)^T\left[\left(\frac{1}{h}\right)^2\alpha_{S1}\Lambda_{S1} + \Psi^{S1}\right]\left(W_\parallel\right)\right. \\ \left. + \left(W_{\parallel;\alpha}\right)^T\mathrm{T}^{S1}_{\alpha\beta}\left(W_{\parallel;\beta}\right)\right\} - \left(W_\parallel\right)^T\mathrm{F}^{S1}\end{aligned} \tag{213}$$

where α_{S1} is defined as Eq. (204) and Λ_{S1} is given by

$$\Lambda_{S1} = \begin{bmatrix} \lambda_{11} & 0 & 0 \\ 0 & \lambda_{21} & 0 \\ 0 & 0 & 0 \end{bmatrix} \tag{214}$$

and

$$\begin{aligned} \Psi^{S1} &= \left(\Phi^{S1}\right)^T \left[\bar{D}_{RR} + 4H\hat{D}_{hR} + 2\bar{D}_{hRR}\right] \left(\Phi^{S1}\right) \\ &\quad + K\left[\left(\Phi^{S1}\right)^T \tilde{E} - \left(\Phi^{S1}\Lambda_{S1}\right)^T \tilde{M}\right] \left(\Phi^{S1}\right) + \left(\Phi_R^{S1}\right)^T D_R^{S1} \\ \mathrm{T}_{\alpha\beta}^{S1} &= \left(\Phi^{S1}\right)^T \bar{D}_{L\alpha L\beta} \left(\Phi^{S1}\right) + \left(\Phi_{L\alpha}^{S1}\right)^T D_{L\beta}^{S1} \\ \mathrm{F}^{S1} &= \left(\Phi^{S1}\right)^T L \end{aligned} \tag{215}$$

with

$$L = -\left\langle S^T \phi \right\rangle \tag{216}$$

Unlike published plate and shell theories the present theory describes correctly the low-frequency and high-frequency branches of vibrations of composite shells in the long-wavelength regime up to the first approximation.

3.4 Hyperbolic Short-wavelength Extrapolation

According to Refs. [32] and [9] it can be shown that each branch is orthogonal to other branches with different values of ω in the long-wavelength regimes with the asymptotic sense. However, in the short-wavelength regime the interaction between each branch is of crucial importance. In addition, as mentioned before, even though Eqs. (209), (211) and (213) are the asymptotically correct energy functionals, it does not always lead to positive definite energy density – loss of hyperbolic type. Therefore, we need an additional independent and logical process – hyperbolic short-wavelength extrapolation. The hypothesis assumed here is that it needs to be done by using changes of variable that are motivated by the necessity to match the dispersion curves associated with 2- and 3-D theories.

Now let us consider generalized refined shell modeling with clamped or free boundary conditions at the edge. Following the same way as in the previous chapter, we assume that the vibrations we are going to describe can be regarded with sufficient accuracy as the

superposition of the branches $F_{\perp}(0)$, $F_{\parallel}(0)$, $L_{\parallel}(0)$, $L_{\perp}(0)$ and $L_{\parallel}(1)$, where the branches $F_{\perp}(0)$ and $L_{\parallel}(0)$ correspond to low-frequency vibrations, but the other ones to thickness (high-frequency) vibrations with the first lowest branches. Such a choice is based on the following reasoning. First, these branches possess the lowest cut-off frequencies so that most of the vibrational energy is concentrated in them. Second, it is clear that $F_{\parallel}(0)$ is strongly coupled with the branch $F_{\perp}(0)$ and also the necessity of including $L_{\parallel}(1)$ into the present theory is dictated by its strong interaction with the branch $L_{\perp}(0)$ [27, 26]. Having made the above assumptions, one can write the warping fields for the full-range frequency vibrations under consideration as:

$$\begin{aligned} W = {} & h\left[V_{1e}^{0}\bar{\varepsilon} + V_{1c}^{0}\left(h\bar{\kappa}\right)\right] + \Phi^{S1}\bar{W}_{\parallel} + \Phi^{31}\bar{V}_{\perp} + \Phi^{S2}\bar{V}_{\parallel} \\ & + h\left[\Phi_{L\alpha}^{S1}\bar{W}_{\parallel;\alpha} + \Phi_{R}^{S1}\bar{W}_{\parallel} + \Phi_{L\alpha}^{31}\bar{V}_{\perp;\alpha} + \Phi_{R}^{31}\bar{V}_{\perp} + \Phi_{L\alpha}^{S2}\bar{V}_{\parallel;\alpha} + \Phi_{R}^{S2}\bar{V}_{\parallel}\right] \end{aligned} \tag{217}$$

where the first and second terms come from the first step of the low-frequency vibrations, terms from the third to fifth from the primary steps, and the remaining ones from the first steps of the high-frequency vibration approximations. Similar to the development in the previous chapter, the symbols without a bar are reserved for the functions in the final equations. By substituting Eq. (217) into the the total energy functional Eq. (142), discarding small terms in the asymptotic sense and using the all results of the previous sections, one can obtain

$$\overline{\mathcal{L}} = \overline{\mathcal{K}} - \overline{\mathcal{P}} \tag{218}$$

in terms of

$$\begin{aligned} 2\overline{\mathcal{K}} = \rho\Big\{ & \left(\bar{V}_S\right)^T\left(\bar{V}_S\right) + \left(\bar{V}_T\right)^T\left(\bar{V}_T\right) + \left(\dot{\bar{V}}_{\perp}\right)^T \mathrm{I}^3\left(\dot{\bar{V}}_{\perp}\right) + \left(\dot{\bar{W}}_{\parallel}\right)^T \alpha_{S1}\left(\dot{\bar{W}}_{\parallel}\right) \\ & + \left(\dot{\bar{V}}_{\parallel}\right)^T \mathrm{I}^S\left(\dot{\bar{V}}_{\parallel}\right) + 2\left(h\bar{\Omega}\right)^T \hat{N}\left[\Phi^{S1}\dot{\bar{W}}_{\parallel} + \Phi^{S2}\dot{\bar{V}}_{\parallel}\right] + 2h\left[\left(\bar{V}_S\right)^T \bar{N}\left(\Phi_{L\alpha}^{31}\dot{\bar{V}}_{\perp;\alpha}\right)\right. \\ & + \left(\bar{V}_T\right)^T \bar{N}\left(\Phi_{L\alpha}^{S1}\dot{\bar{W}}_{\parallel;\alpha}\right) + \left(\bar{V}_T\right)^T \bar{N}\left(\Phi_{L\alpha}^{S2}\dot{\bar{V}}_{\parallel;\alpha}\right) + \left(V_{0e}\dot{\bar{\varepsilon}}\right)^T \bar{M}\left(\Phi^{31}\dot{\bar{V}}_{\perp}\right) \\ & + \left(V_{0c}h\dot{\bar{\kappa}}\right)^T \bar{M}\left(\Phi^{31}\dot{\bar{V}}_{\perp}\right) + \left(\Phi^{31}\dot{\bar{V}}_{\perp}\right)^T \bar{M}\left(\Phi_{L\alpha}^{S1}\dot{\bar{W}}_{\parallel;\alpha}\right) + \left(\Phi^{31}\dot{\bar{V}}_{\perp}\right)^T \bar{M}\left(\Phi_{L\alpha}^{S2}\dot{\bar{V}}_{\parallel;\alpha}\right) \\ & \left. + \left(\Phi^{S1}\dot{\bar{W}}_{\parallel}\right)^T \bar{M}\left(\Phi_{L\alpha}^{31}\dot{\bar{V}}_{\perp;\alpha}\right) + \left(\Phi^{S2}\dot{\bar{V}}_{\parallel}\right)^T \bar{M}\left(\Phi_{L\alpha}^{31}\dot{\bar{V}}_{\perp;\alpha}\right)\right]\Big\} \end{aligned} \tag{219}$$

and

$$
\begin{aligned}
2\overline{\mathcal{P}} = & \Big\{ (\bar{\varepsilon})^T \, \bar{\mathrm{A}}_{2d} \, (\bar{\varepsilon}) + 2 \, (\bar{\varepsilon})^T \, \bar{\mathrm{B}}_{2d} \, (h\bar{\kappa}) + (h\bar{\kappa})^T \, \bar{\mathrm{C}}_{2d} \, (h\bar{\kappa}) \\
& + \left(\frac{1}{h} \right)^2 \Big[\left(\bar{W}_{\parallel} \right)^T \left(\alpha_{S1} \Lambda_{S1} + h^2 \bar{\Psi}^{S1} \right) \left(\bar{W}_{\parallel} \right) + \left(\bar{V}_{\parallel} \right)^T \left(\Lambda_{S2} + h^2 \bar{\Psi}^{S2} \right) \left(\bar{V}_{\parallel} \right) \\
& + \left(\bar{V}_{\perp} \right)^T \left(\Lambda_{31} + h^2 \bar{\Psi}^{31} \right) \left(\bar{V}_{\perp} \right) \Big] + \left(\bar{W}_{\parallel;\alpha} \right)^T \bar{\mathrm{T}}^{S1}_{\alpha\beta} \left(\bar{W}_{\parallel;\beta} \right) + \left(\bar{V}_{\parallel;\alpha} \right)^T \bar{\mathrm{T}}^{S2}_{\alpha\beta} \left(\bar{V}_{\parallel;\beta} \right) \\
& + \left(\bar{V}_{\perp;\alpha} \right)^T \bar{\mathrm{T}}^{31}_{\alpha\beta} \left(\bar{V}_{\perp;\beta} \right) + 2 \left(\frac{1}{h} \right) \Big[(V_{0e} \bar{\varepsilon})^T \, \bar{E} \left(\Phi^{31} \bar{V}_{\perp} \right) + (V_{0c} h\bar{\kappa})^T \, \bar{E} \left(\Phi^{31} \bar{V}_{\perp} \right) \\
& + \left(\Phi^{31} \bar{V}_{\perp} \right)^T \bar{E} \left(\Phi^{S1}_{L\alpha} \bar{W}_{\parallel;\alpha} \right) + \left(\Phi^{31} \bar{V}_{\perp} \right)^T \bar{E} \left(\Phi^{S2}_{L\alpha} \bar{V}_{\parallel;\alpha} \right) + \left(\Phi^{S1} \bar{W}_{\parallel} \right)^T \bar{E} \left(\Phi^{31}_{L\alpha} \bar{V}_{\perp;\alpha} \right) \\
& + \left(\Phi^{S2} \bar{V}_{\parallel} \right)^T \bar{E} \left(\Phi^{31}_{L\alpha} \bar{V}_{\perp;\alpha} \right) + \left(\Phi^{31} \bar{V}_{\perp} \right)^T \bar{D}_{he} \, (\bar{\varepsilon}) + \left(\Phi^{31} \bar{V}_{\perp} \right)^T \bar{D}_{hc} \, (h\bar{\kappa}) \\
& + \left(\Phi^{31} \bar{V}_{\perp} \right)^T \bar{D}_{hL\alpha} \left(\Phi^{S1} \bar{W}_{\parallel;\alpha} \right) + \left(\Phi^{31} \bar{V}_{\perp} \right)^T \bar{D}_{hL\alpha} \left(\Phi^{S2} \bar{V}_{\parallel;\alpha} \right) + \left(\Phi^{S1} \bar{W}_{\parallel} \right)^T \bar{D}_{hL\alpha} \left(\Phi^{31} \bar{V}_{\perp;\alpha} \right) \\
& + \left(\Phi^{S2} \bar{V}_{\parallel} \right)^T \bar{D}_{hL\alpha} \left(\Phi^{31} \bar{V}_{\perp;\alpha} \right) \Big] + 2 \Big[(V_{0e} \bar{\varepsilon})^T \, \bar{E} \left(\Phi^{S1}_{L\alpha} \bar{W}_{\parallel;\alpha} \right) + (V_{0e} \bar{\varepsilon})^T \, \bar{E} \left(\Phi^{S2}_{L\alpha} \bar{V}_{\parallel;\alpha} \right) \\
& + (V_{0c} h\bar{\kappa})^T \, \bar{E} \left(\Phi^{S1}_{L\alpha} \bar{W}_{\parallel;\alpha} \right) + (V_{0c} h\bar{\kappa})^T \, \bar{E} \left(\Phi^{S2}_{L\alpha} \bar{V}_{\parallel;\alpha} \right) + \left(\Phi^{S1}_{L\alpha} \bar{W}_{\parallel;\alpha} \right)^T \bar{D}_{he} \, (\bar{\varepsilon}) \\
& + \left(\Phi^{S2}_{L\alpha} \bar{V}_{\parallel;\alpha} \right)^T \bar{D}_{he} \, (\bar{\varepsilon}) + \left(\Phi^{S1}_{L\alpha} \bar{W}_{\parallel;\alpha} \right)^T \bar{D}_{hc} \, (h\bar{\kappa}) + \left(\Phi^{S2}_{L\alpha} \bar{V}_{\parallel;\alpha} \right)^T \bar{D}_{hc} \, (h\bar{\kappa}) \\
& + (V_{0e} \bar{\varepsilon})^T \, \bar{D}_{hL\alpha} \left(\Phi^{S1} \bar{W}_{\parallel;\alpha} \right) + (V_{0e} \bar{\varepsilon})^T \, \bar{D}_{hL\alpha} \left(\Phi^{S2} \bar{V}_{\parallel;\alpha} \right) + (V_{0c} h\bar{\kappa})^T \, \bar{D}_{hL\alpha} \left(\Phi^{S1} \bar{W}_{\parallel;\alpha} \right) \\
& + (V_{0c} h\bar{\kappa})^T \, \bar{D}_{hL\alpha} \left(\Phi^{S2} \bar{V}_{\parallel;\alpha} \right) + \left(\Phi^{S1} \bar{W}_{\parallel} \right)^T \bar{D}_{hL\alpha} \left(V_{0e} \bar{\varepsilon}_{;\alpha} \right) + \left(\Phi^{S1} \bar{W}_{\parallel} \right)^T \bar{D}_{hL\alpha} \left(V_{0c} h\bar{\kappa}_{;\alpha} \right) \\
& + \left(\Phi^{S2} \bar{V}_{\parallel} \right)^T \bar{D}_{hL\alpha} \left(V_{0e} \bar{\varepsilon}_{;\alpha} \right) + \left(\Phi^{S2} \bar{V}_{\parallel} \right)^T \bar{D}_{hL\alpha} \left(V_{0c} h\bar{\kappa}_{;\alpha} \right) + (\bar{\varepsilon})^T \, \bar{D}_{\varepsilon L\alpha} \left(\Phi^{S1} \bar{W}_{\parallel;\alpha} \right) \\
& + (\bar{\varepsilon})^T \, \bar{D}_{eL\alpha} \left(\Phi^{S2} \bar{V}_{\parallel;\alpha} \right) + (h\bar{\kappa})^T \, \bar{D}_{cL\alpha} \left(\Phi^{S1} \bar{W}_{\parallel;\alpha} \right) + (h\bar{\kappa})^T \, \bar{D}_{cL\alpha} \left(\Phi^{S2}_{L\alpha} \bar{V}_{\parallel;\alpha} \right) \Big] \\
& + \left(\bar{W}_{\parallel} \right)^T \bar{\mathrm{F}}^{S1} + \left(\bar{V}_{\parallel} \right)^T \bar{\mathrm{F}}^{S2} + \left(\bar{V}_{\perp} \right)^T \bar{\mathrm{F}}^{31} \Big\}
\end{aligned}
\tag{220}
$$

where

$$
\begin{aligned}
\bar{N} &= \langle [S] \rangle \qquad \hat{N} = \langle \zeta \, [S] \rangle \\
\bar{\mathrm{F}}^{31} &= \left(\Phi^{31} \right)^T L^{31} \quad \text{with} \quad L^{31} = - \left\langle S^T \phi \right\rangle \\
\bar{\mathrm{F}}^{S2} &= \left(\Phi^{S2} \right)^T L^{S2} \quad \text{with} \quad L^{S2} = -S^{+T} \alpha - S^{-T} \beta
\end{aligned}
\tag{221}
$$

In Eqs. (219) and (220), results of previous sections are used to define the eigenvalue matrices Λ_{S1}, Λ_{31} and Λ_{S2} and the coefficients associated with $\bar{\Psi}^{S1}$, $\bar{\Psi}^{31}$ and $\bar{\Psi}^{S2}$, $\bar{\mathrm{T}}^{S1}$, $\bar{\mathrm{T}}^{31}$, and $\bar{\mathrm{T}}^{S2}$, I^S, I^3 and α_{S1} and $\bar{\mathrm{F}}^{S1}$. Here we have already taken advantage of monoclinic symmetry and the orthogonality property to obtain asymptotically correct kinetic and potential energies in Eqs. (219) and (220).

Applying a procedure similar to that of the previous chapter regarding Eqs. (219) and (220), one can derive the general changes of variables in the following discretized form:

$$
\begin{aligned}
V_S &= \bar{V}_S + h\bar{N}\left(\Phi^{31}_{L\alpha}\dot{\bar{V}}_{\perp;\alpha}\right) \\
V_T &= \bar{V}_T + h\bar{N}\left(\Phi^{S1}_{L\alpha}\dot{\bar{W}}_{\|;\alpha} + \Phi^{S2}_{L\alpha}\dot{\bar{V}}_{\|;\alpha}\right) \\
\varepsilon &= \bar{\varepsilon} + h\left[\bar{I}_\beta \bar{N}\left(\Phi^{31}_{L\alpha}\bar{V}_{\perp;\alpha\beta}\right)\right] \\
h\kappa &= h\bar{\kappa} + \left(\bar{\mathrm{C}}^{+}_{2d}\right)^T\left[\bar{D}_{cL\alpha} + \left(V_{0c}\right)^T\bar{D}_{hL\alpha}\right]\left(\Phi^{S1}\bar{W}_{\|;\alpha} + \Phi^{S2}\bar{V}_{\|;\alpha}\right) \\
V_\perp &= \bar{V}_\perp + h\left(\Phi^{31}\right)^T\bar{M}\left[V_{0e}\left(\bar{\varepsilon}\right) + V_{0c}\left(h\bar{\kappa}\right) + \Phi^{S1}_{L\alpha}\bar{W}_{\|;\alpha} + \Phi^{S2}_{L\alpha}\bar{V}_{\|;\alpha}\right] \\
hW_\| &= \bar{W}_\| + h\left(\Phi^{S1}\alpha^{+}_{S1}\right)^T\bar{M}\left(\Phi^{31}_{L\alpha}\bar{V}_{\perp;\alpha}\right) + h^2\left[\Phi^{S1}\left(\alpha_{S1}\Lambda_{S1}\right)^{+}\right]^T\bar{D}_{hL\alpha}\left[V_{0c}\left(h\bar{\kappa}_{;\alpha}\right)\right] \\
V_\| &= \bar{V}_\| + h\left(\Phi^{S2}\right)^T\bar{M}\left(\Phi^{31}_{L\alpha}\bar{V}_{\perp;\alpha}\right)
\end{aligned}
\tag{222}
$$

where ${\alpha_{S1}\Lambda_{S1}}^{+}$ and $\bar{\mathrm{C}}^{+}_{2d}$ are defined on the similar way as ${\alpha_{S1}}^{+}$

$$
\left(\alpha_{\mathrm{S1}}\Lambda_{\mathrm{S1}}\right)^{+}\alpha_{\mathrm{S1}}\Lambda_{\mathrm{S1}} = \mathrm{I}^S \qquad \bar{\mathrm{C}}^{+}_{2d}\bar{\mathrm{C}}_{2d} = \mathrm{I}
$$

and

$$
\bar{I}_1 = \begin{bmatrix} 1 & 0 & 0 \\ 0 & 1 & 0 \\ 0 & 0 & 0 \end{bmatrix} \qquad \bar{I}_2 = \begin{bmatrix} 0 & 0 & 0 \\ 0 & 1 & 0 \\ 0 & 0 & 1 \end{bmatrix}
\tag{223}
$$

Retaining the leading terms in V_S, V_T, ε, κ, $W_\|$, $V_\perp$ and $V_\|$ and extrapolating the total energy functional to the short wavelength regime, after lengthy but otherwise straightforward calculations, one finally obtains the 2-D refined energy functional with kinetic and potential energies per unit area, valid over a wide range of frequencies for layered shells for which each layer is made of a monoclinic material:

$$
\mathcal{J} = h\int_{t_1}^{t_2}\int_s \left(\mathcal{K} - \mathcal{P}\right) dSdt
\tag{224}
$$

where

$$
\begin{aligned}
\mathcal{K} = \frac{1}{2}\rho\Big\{&\left(V_S\right)^T\left(V_S\right) + \left(V_T\right)^T\left(V_T\right) \\
&+ \left(h\dot{W}_\|\right)^T\alpha_{S1}\left(h\dot{W}_\|\right) + \left(\dot{V}_\|\right)^T\mathrm{I}^S\left(\dot{V}_\|\right) + \left(\dot{V}_\perp\right)^T\mathrm{I}^3\left(\dot{V}_\perp\right)\Big\}
\end{aligned}
\tag{225}
$$

and

$$
\begin{aligned}
\mathcal{P} = \frac{1}{2}\Big\{ & (\varepsilon)^T \, \mathrm{A}_{2d} \, (\varepsilon) + 2 \, (\varepsilon)^T \, \mathrm{B}_{2d} \, (h\kappa) + (h\kappa)^T \, \mathrm{C}_{2d} \, (h\kappa) \\
& + \left(\frac{1}{h}\right)^2 \Big[\left(hW_{\|}\right)^T \Psi^{S1} \left(hW_{\|}\right) + \left(V_{\|}\right)^T \Psi^{S2} \left(V_{\|}\right) + \left(V_{\perp}\right)^T \Psi^{31} \left(V_{\perp}\right) \Big] \\
& + \left(hW_{\|;\alpha}\right)^T \mathrm{T}^{S1}_{\alpha\beta} \left(hW_{\|;\beta}\right) + \left(V_{\|;\alpha}\right)^T \mathrm{T}^{S2}_{\alpha\beta} \left(V_{\|;\beta}\right) + \left(V_{\perp;\alpha}\right)^T \mathrm{T}^{31}_{\alpha\beta} \left(V_{\perp;\beta}\right) \\
& + 2\left(\frac{1}{h}\right) \Big[\left(V_{\perp}\right)^T \left[\mathrm{S}^{31e} \left(\varepsilon\right) + \mathrm{S}^{31c} \left(h\kappa\right) \right] + \left(V_{\perp}\right)^T \left[\mathrm{S}^{31S1}_{\alpha} \left(hW_{\|;\alpha}\right) + \mathrm{S}^{31S2}_{\alpha} \left(V_{\|;\alpha}\right) \right] \\
& + \Big[\left(hW_{\|}\right)^T \mathrm{S}^{S131}_{\alpha} + \left(V_{\|}\right)^T \mathrm{S}^{S231}_{\alpha} \Big] \left(V_{\perp;\alpha}\right) \Big] \\
& + 2\left(hW_{\|}\right)^T \mathrm{F}^{S1} + 2\left(V_{\|}\right)^T \mathrm{F}^{S2} + 2\left(V_{\perp}\right)^T \mathrm{F}^{31} \Big\}
\end{aligned}
\tag{226}
$$

All the coefficients are defined in the discretized forms as:

$$
\begin{aligned}
\mathrm{A}_{2d} &= \bar{\mathrm{A}}_{2d} - \left\{ \left[\left(\Phi^{31}\right)^T \bar{M} \left(V_{0e}\right) \right]^T \Lambda_{31} \left[\left(\Phi^{31}\right)^T \bar{M} \left(V_{0e}\right) \right] \right\} \\
&\quad - 2 \left\{ \left[\left(\Phi^{31}\right)^T \bar{M} \left(V_{0e}\right) \right]^T \left[\left(\Phi^{31}\right)^T \bar{D}_{he} \right] \right\} \\
\mathrm{B}_{2d} &= \bar{\mathrm{B}}_{2d} - \left\{ \left[\left(\Phi^{31}\right)^T \bar{M} \left(V_{0e}\right) \right]^T \Lambda_{31} \left[\left(\Phi^{31}\right)^T \bar{M} \left(V_{0c}\right) \right] \right\} \\
&\quad - \left\{ \left[\left(\Phi^{31}\right)^T \bar{D}_{he} \right]^T \left[\left(\Phi^{31}\right)^T \bar{M} \left(V_{0c}\right) \right] \right\} - \left\{ \left[\left(\Phi^{31}\right)^T \bar{M} \left(V_{0e}\right) \right]^T \left[\left(\Phi^{31}\right)^T \bar{D}_{hc} \right] \right\} \\
\mathrm{C}_{2d} &= \bar{\mathrm{C}}_{2d} - \left\{ \left[\left(\Phi^{31}\right)^T \bar{M} \left(V_{0c}\right) \right]^T \Lambda_{31} \left[\left(\Phi^{31}\right)^T \bar{M} \left(V_{0c}\right) \right] \right\} \\
&\quad - 2 \left\{ \left[\left(\Phi^{31}\right)^T \bar{M} \left(V_{0c}\right) \right]^T \left[\left(\Phi^{31}\right)^T \bar{D}_{hc} \right] \right\} \\
\Psi^{S1} &= \alpha_{S1}\Lambda_{S1} + h^2 \bar{\Psi}^{S1} \qquad \Psi^{31} = \Lambda_{31} + h^2 \bar{\Psi}^{31} \qquad \Psi^{S2} = \Lambda_{S2} + h^2 \bar{\Psi}^{S2} \\
\mathrm{F}^{S1} &= \bar{\mathrm{F}}^{S1} \qquad\qquad \mathrm{F}^{31} = \bar{\mathrm{F}}^{31} \qquad\qquad \mathrm{F}^{S2} = \bar{\mathrm{F}}^{S2} \\
\mathrm{S}^{31e} &= \left(\Phi^{31}\right)^T \bar{D}_{he} \qquad\qquad \mathrm{S}^{31c} = \left(\Phi^{31}\right)^T \bar{D}_{hc} \\
\mathrm{S}^{31S1}_{\alpha} &= \left(\Phi^{31}\right)^T \bar{D}_{hL\alpha} \left(\Phi^{S1}\right) - \left\{ \left[\left(\Phi^{31}\right)^T \bar{D}_{hc} \right] \left(\bar{\mathrm{C}}^{+}_{2d}\right)^T \left[\bar{D}_{cL\alpha} + \left(V_{0c}\right)^T D_{hL\alpha} \right] \left(\Phi^{S1}\right) \right\} \\
\mathrm{S}^{S131}_{\alpha} &= \left(\Phi^{S1}\right)^T \bar{D}_{hL\alpha} \left(\Phi^{31}\right) \\
\mathrm{S}^{31S2}_{\alpha} &= \left(\Phi^{31}\right)^T \bar{D}_{hL\alpha} \left(\Phi^{S2}\right) - \left\{ \left[\left(\Phi^{31}\right)^T \bar{D}_{hc} \right] \left(\bar{\mathrm{C}}^{+}_{2d}\right)^T \left[\bar{D}_{cL\alpha} + \left(V_{0c}\right)^T D_{hL\alpha} \right] \left(\Phi^{S2}\right) \right\} \\
\mathrm{S}^{S231}_{\alpha} &= \left(\Phi^{S2}\right)^T \bar{D}_{hL\alpha} \left(\Phi^{31}\right)
\end{aligned}
\tag{227}
$$

After performing hyperbolic short-wavelength extrapolation, the two branches of the first lowest thickness-shear vibration $\bar{\mathrm{T}}^{S1}_{\alpha\beta}$ and $\bar{\mathrm{T}}^{S2}_{\alpha\beta}$ become more complicated in the discretized

form

$$
\begin{aligned}
&\mathrm{T}^{S1}_{\alpha\beta} = \bar{\mathrm{T}}^{S1}_{\alpha\beta} + \left\{ \left[\bar{N} \left(\Phi^{S1}_{L\alpha} \Lambda_{S1} \right) \right]^T \left[\bar{N} \left(\Phi^{S1}_{L\beta} \right) \right] \right\} + \left\{ \left[\left(\Phi^{31} \right)^T \bar{M} \left(\Phi^{S1}_{L\alpha} \Lambda_{S1} \right) \right]^T \left[\left(\Phi^{31} \right)^T \bar{M} \left(\Phi^{S1}_{L\beta} \right) \right] \right\} \\
&+ 2 \left\{ \left[\left(\Phi^{31} \right)^T \bar{M} \left(V_{0c} \right) \left(\bar{\mathrm{C}}^{+}_{2d} \right)^T \left[\bar{D}_{cL\alpha} + \left(V_{0c} \right)^T D_{hL\alpha} \right] \left(\Phi^{S1} \right) \right]^T \Lambda_{31} \left[\left(\Phi^{31} \right)^T \bar{M} \left(\Phi^{S1}_{L\beta} \right) \right] \right\} \\
&+ 2 \left\{ \left[\left(\Phi^{31} \right)^T \bar{M} \left(V_{0c} \right) \left(\bar{\mathrm{C}}^{+}_{2d} \right)^T \left[\bar{D}_{cL\alpha} + \left(V_{0c} \right)^T D_{hL\alpha} \right] \left(\Phi^{S1} \right) \right]^T \left[\left(\Phi^{31} \right)^T D^{S1}_{L\beta} \right] \right\} \\
&+ 2 \left[\left(\Phi^{31} \right)^T \bar{M} \left(\Phi^{S1}_{L\alpha} \right) \right]^T \left\{ \left[\left(\Phi^{31} \right)^T \bar{D}_{hc} \right] \left(\bar{\mathrm{C}}^{+}_{2d} \right)^T \left[\bar{D}_{cL\beta} + \left(V_{0c} \right)^T \bar{D}_{hL\beta} \right] \left(\Phi^{S1} \right) \right\} \\
&- \left\{ \left[\left(\Phi^{31} \right)^T \bar{M} \left(V_{0c} \right) \left(\bar{\mathrm{C}}^{+}_{2d} \right)^T \left[\bar{D}_{cL\alpha} + \left(V_{0c} \right)^T D_{hL\alpha} \right] \left(\Phi^{S1} \right) \right]^T \Lambda_{31} \right. \\
&\left. \left[\left(\Phi^{31} \right)^T \bar{M} \left(V_{0c} \right) \left(\bar{\mathrm{C}}^{+}_{2d} \right)^T \left[\bar{D}_{cL\beta} + \left(V_{0c} \right)^T D_{hL\beta} \right] \left(\Phi^{S1} \right) \right] \right\} \\
&- \left\{ \left[\left(\bar{\mathrm{C}}^{+}_{2d} \right)^T \left[\bar{D}_{cL\alpha} + \left(V_{0c} \right)^T D_{hL\alpha} \right] \left(\Phi^{S1} \right) \right]^T \bar{\mathrm{C}}_{2d} \left[\left(\bar{\mathrm{C}}^{+}_{2d} \right)^T \left[\bar{D}_{cL\beta} + \left(V_{0c} \right)^T D_{hL\beta} \right] \left(\Phi^{S1} \right) \right] \right\} \\
&- \left\{ \left[\left(\Phi^{31} \right)^T \bar{M} \left(\Phi^{S1}_{L\alpha} \right) \right]^T \Lambda_{31} \left[\left(\Phi^{31} \right)^T \bar{M} \left(\Phi^{S1}_{L\beta} \right) \right] \right\} - 2 \left\{ \left[\left(\Phi^{31} \right)^T \bar{M} \left(\Phi^{S1}_{L\alpha} \right) \right]^T \left[\left(\Phi^{31} \right)^T D^{S1}_{L\beta} \right] \right\} \\
&- 2 \left\{ \left[\left(\Phi^{31} \right)^T \bar{M} \left(V_{0c} \right) \right] \left(\bar{\mathrm{C}}^{+}_{2d} \right)^T \left[\bar{D}_{cL\alpha} + \left(V_{0c} \right)^T \bar{D}_{hL\alpha} \right] \left(\Phi^{S1} \right) \right\}^T \\
&\left\{ \left[\left(\Phi^{31} \right)^T \bar{D}_{hc} \right] \left(\bar{\mathrm{C}}^{+}_{2d} \right)^T \left[\bar{D}_{cL\beta} + \left(V_{0c} \right)^T \bar{D}_{hL\beta} \right] \left(\Phi^{S1} \right) \right\} \\
&\mathrm{T}^{S2}_{\alpha\beta} = \bar{\mathrm{T}}^{S2}_{\alpha\beta} + \left\{ \left[\bar{N} \left(\Phi^{S2}_{L\alpha} \Lambda_{S2} \right) \right]^T \left[\bar{N} \left(\Phi^{S2}_{L\beta} \right) \right] \right\} + \left\{ \left[\left(\Phi^{31} \right)^T \bar{M} \left(\Phi^{S2}_{L\alpha} \Lambda_{S2} \right) \right]^T \left[\left(\Phi^{31} \right)^T \bar{M} \left(\Phi^{S2}_{L\beta} \right) \right] \right\} \\
&+ 2 \left\{ \left[\left(\Phi^{31} \right)^T \bar{M} \left(V_{0c} \right) \left(\bar{\mathrm{C}}^{+}_{2d} \right)^T \left[\bar{D}_{cL\alpha} + \left(V_{0c} \right)^T D_{hL\alpha} \right] \left(\Phi^{S2} \right) \right]^T \Lambda_{31} \left[\left(\Phi^{31} \right)^T \bar{M} \left(\Phi^{S2}_{L\beta} \right) \right] \right\} \\
&+ 2 \left[\left(\Phi^{31} \right)^T \bar{M} \left(\Phi^{S2}_{L\alpha} \right) \right]^T \left\{ \left[\left(\Phi^{31} \right)^T \bar{D}_{hc} \right] \left(\bar{\mathrm{C}}^{+}_{2d} \right)^T \left[\bar{D}_{cL\beta} + \left(V_{0c} \right)^T \bar{D}_{hL\beta} \right] \Phi^{S2} \right\} \\
&+ 2 \left\{ \left[\left(\Phi^{31} \right)^T \bar{M} \left(V_{0c} \right) \left(\bar{\mathrm{C}}^{+}_{2d} \right)^T \left[\bar{D}_{cL\alpha} + \left(V_{0c} \right)^T D_{hL\alpha} \right] \left(\Phi^{S2} \right) \right]^T \left[\left(\Phi^{31} \right)^T D^{S2}_{L\beta} \right] \right\} \\
&+ 2 \left\{ \left[\left(\Phi^{S2} \right)^T \bar{D}_{hL\alpha} \left(V_{0c} \right) \right] \left[\left(\bar{\mathrm{C}}^{+}_{2d} \right)^T \left[\bar{D}_{cL\beta} + \left(V_{0c} \right)^T D_{hL\beta} \right] \left(\Phi^{S2} \right) \right] \right\} \\
&- \left\{ \left[\left(\Phi^{31} \right)^T \bar{M} \left(V_{0c} \right) \left(\bar{\mathrm{C}}^{+}_{2d} \right)^T \left[\bar{D}_{cL\alpha} + \left(V_{0c} \right)^T D_{hL\alpha} \right] \left(\Phi^{S2} \right) \right]^T \Lambda_{31} \right. \\
&\left. \left[\left(\Phi^{31} \right)^T \bar{M} \left(V_{0c} \right) \left(\bar{\mathrm{C}}^{+}_{2d} \right)^T \left[\bar{D}_{cL\beta} + \left(V_{0c} \right)^T D_{hL\beta} \right] \left(\Phi^{S2} \right) \right] \right\} \\
&- \left\{ \left[\left(\Phi^{31} \right)^T \bar{M} \left(\Phi^{S2}_{L\alpha} \right) \right]^T \Lambda_{31} \left[\left(\Phi^{31} \right)^T \bar{M} \left(\Phi^{S2}_{L\beta} \right) \right] \right\} \\
&- \left\{ \left[\left(\bar{\mathrm{C}}^{+}_{2d} \right)^T \left[\bar{D}_{cL\alpha} + \left(V_{0c} \right)^T D_{hL\alpha} \right] \left(\Phi^{S2} \right) \right]^T \bar{\mathrm{C}}_{2d} \left[\left(\bar{\mathrm{C}}^{+}_{2d} \right)^T \left[\bar{D}_{cL\beta} + \left(V_{0c} \right)^T D_{hL\beta} \right] \left(\Phi^{S2} \right) \right] \right\} \\
&- 2 \left\{ \left[\left(\Phi^{31} \right)^T \bar{M} \left(V_{0c} \right) \right] \left(\bar{\mathrm{C}}^{+}_{2d} \right)^T \left[\bar{D}_{cL\alpha} + \left(V_{0c} \right)^T \bar{D}_{hL\alpha} \right] \left(\Phi^{S2} \right) \right\}^T \\
&\left\{ \left[\left(\Phi^{31} \right)^T \bar{D}_{hc} \right] \left(\bar{\mathrm{C}}^{+}_{2d} \right)^T \left[\bar{D}_{cL\beta} + \left(V_{0c} \right)^T \bar{D}_{hL\beta} \right] \left(\Phi^{S2} \right) \right\} - 2 \left\{ \left[\left(\Phi^{31} \right)^T \bar{M} \left(\Phi^{S2}_{L\alpha} \right) \right]^T \left[\left(\Phi^{31} \right)^T D^{S2}_{L\beta} \right] \right\}
\end{aligned}
\tag{228}
$$

and for the first lowest branch of the thickness-extension vibration $\bar{\mathrm{T}}^{31}_{\alpha\beta}$,

$$
\begin{aligned}
\mathrm{T}^{31}_{\alpha\beta} &= \bar{\mathrm{T}}^{31}_{\alpha\beta} + \left\{ \left[\bar{N} \left(\Phi^{31}_{L\alpha} \Lambda_{31} \right) \right]^T \left[\bar{N} \left(\Phi^{31}_{L\beta} \right) \right] \right\} \\
&+ \left\{ \left[\left(\Phi^{S1} \alpha^+_{S1} \right)^T \bar{M} \left(\Phi^{31}_{L\alpha} \Lambda_{31} \right) \right]^T \alpha_{S1} \left[\left(\Phi^{S1} \alpha^+_{S1} \right)^T \bar{M} \left(\Phi^{31}_{L\beta} \right) \right] \right\} \\
&+ \left\{ \left[\left(\Phi^{S2} \right)^T \bar{M} \left(\Phi^{31}_{L\alpha} \Lambda_{31} \right) \right]^T \left[\left(\Phi^{S2} \right)^T \bar{M} \left(\Phi^{31}_{L\beta} \right) \right] \right\} + 2 \left\{ \left[\left(\Phi^{31} \right)^T \bar{D}_{h\varepsilon} \right] \left[\bar{I}_\alpha \bar{N} \left(\Phi^{31}_{L\beta} \right) \right] \right\} \\
&+ 2 \left\{ \left[\left(\Phi^{31} \right)^T D^{S1}_{L\alpha} \right] \left[\left(\Phi^{S1} \alpha^+_{S1} \right)^T \bar{M} \left(\Phi^{31}_{L\beta} \right) \right] \right\} + 2 \left\{ \left[\left(\Phi^{31} \right)^T D^{S2}_{L\alpha} \right] \left[\left(\Phi^{S2} \right)^T \bar{M} \left(\Phi^{31}_{L\beta} \right) \right] \right\} \\
&- \left\{ \left[\left(\Phi^{S1} \alpha^+_{S1} \right)^T \bar{M} \left(\Phi^{31}_{L\alpha} \right) \right]^T \left(\alpha_{S1} \Lambda_{S1} \right) \left[\left(\Phi^{S1} \alpha^+_{S1} \right)^T \bar{M} \left(\Phi^{31}_{L\beta} \right) \right] \right\} \\
&- \left\{ \left[\left(\Phi^{S2} \right)^T \bar{M} \left(\Phi^{31}_{L\alpha} \right) \right]^T \left(\Lambda_{S2} \right) \left[\left(\Phi^{S2} \right)^T \bar{M} \left(\Phi^{31}_{L\beta} \right) \right] \right\} \\
&- 2 \left\{ \left[\left(\Phi^{31} \right)^T \bar{D}_{hc} \right] \left(\bar{\mathrm{C}}^+_{2d} \right)^T \left[\bar{D}_{cL\alpha} + \left(V_{0c} \right)^T \bar{D}_{hL\alpha} \right] \left(\Phi^{S1} \right) \left[\left(\Phi^{S1} \alpha^+_{S1} \right)^T \bar{M} \left(\Phi^{31}_{L\beta} \right) \right] \right\} \\
&- 2 \left\{ \left[\left(\Phi^{31} \right)^T \bar{D}_{hc} \right] \left(\bar{\mathrm{C}}^+_{2d} \right)^T \left[\bar{D}_{cL\alpha} + \left(V_{0c} \right)^T \bar{D}_{hL\alpha} \right] \left(\Phi^{S2} \right) \left[\left(\Phi^{S2} \right)^T \bar{M} \left(\Phi^{31}_{L\beta} \right) \right] \right\}
\end{aligned}
\tag{229}
$$

Finally, we derive the asymptotically correct, 2-D dynamic equations for a full range of frequencies, up to the first approximation. All numerical procedures have been completely implemented in the computer program DVAPAS. For more convenience and simplicity, the 2-D total energy functional per unit area can be rewritten in the dynamic intrinsic formulation:

$$
\mathcal{L} = \frac{1}{2} \mathcal{V}^T \mathrm{M}_{2d} \mathcal{V} - \frac{1}{2} \mathcal{E}^T \mathrm{K}_{2d} \mathcal{E} - \mathcal{E}^T \mathrm{F}_{2d} \tag{230}
$$

with

$$
\begin{aligned}
\mathcal{V} &= \lfloor v_\alpha \;\; v_3 \;\; h\dot{\psi}_\alpha \;\; \dot{\psi}_3 \;\; \dot{v}_\alpha \rfloor \\
\mathcal{E} &= \lfloor \varepsilon_{\alpha\beta} \;\; h\kappa_{\alpha\beta} \;\; \psi_\alpha \;\; \frac{1}{h}\psi_3 \;\; \frac{1}{h} v_\alpha \;\; h\psi_{\alpha;\beta} \;\; \psi_{3;\alpha} \;\; v_{\alpha;\beta} \rfloor
\end{aligned}
\tag{231}
$$

Here M_{2d} is an 8×8 mass matrix, K_{2d} is a 21×21 stiffness one, and F_{2d} denotes a 5×1 generalized force vector. DVAPAS provides the 2-D generalized constitutive law to be input into a corresponding 2-D surface solver to carry a 2-D analysis. Afterwards DVAPAS can take the output from that to recover the 3-D displacement, strain and stress fields. The development of the surface analysis is beyond the scope of this thesis.

Before closing in section for constructing recovery relations, it is interesting to note that one can specialize the above theory to the form of a generalized Ressiner-Mindlin plate

theory from Eq. (224). In addition, one can reduce from Eq. (224) to the classical theory previously obtained by VAM., Eq. (159), for low-frequency vibrations.

Originally Ressiner-Mindlin plate theory was based on five 2-D (surface) variables to be found: three displacements and two rotations. According to Ref. [26] the lowest first branch of the thickness-shear vibrations could be approximated as in-plane rotations, associated with transverse shear effects. Therefore, having made the above assumptions, one can rewrite the warping fields under consideration as:

$$W = h\left[V_{1e}^{0}\bar{\varepsilon} + V_{1c}^{0}\left(h\bar{\kappa}\right)\right] + \Phi^{S1}\bar{W}_{\|} + h\left[\Phi_{L\alpha}^{S1}\bar{W}_{\|;\alpha} + \Phi_{R}^{S1}\bar{W}_{\|}\right] \tag{232}$$

Following the same procedure of the above, one obtain the changes of variables:

$$\begin{aligned}
V_S &= \bar{V}_S \\
V_T &= \bar{V}_T + h\bar{N}\left(\Phi_{L\alpha}^{S1}\dot{\bar{W}}_{\|;\alpha}\right) \\
\varepsilon &= \bar{\varepsilon} \\
h\kappa &= h\bar{\kappa} + \left(\bar{\mathrm{C}}_{2d}^{+}\right)^{T}\left[\bar{D}_{cL\alpha} + \left(V_{0c}\right)^{T}\bar{D}_{hL\alpha}\right]\left(\Phi^{S1}\bar{W}_{\|;\alpha}\right) \\
hW_{\|} &= \bar{W}_{\|} + h^{2}\left[\Phi^{S1}\left(\alpha_{S1}\Lambda_{S1}\right)^{+}\right]^{T}\bar{D}_{hL\alpha}\left[V_{0c}\left(h\bar{\kappa}_{;\alpha}\right)\right]
\end{aligned} \tag{233}$$

Retaining the leading terms in V_S, V_T, ε, κ and $W_{\|}$ and extrapolating the total energy functional to the short-wavelength regime, i.e. Eqs. (233), one arrive finally at the 2-D refined energy functional Eq. (224) with the kinetic and strain energies per unit area for composite laminated plates/shells in which each layer is monoclinic:

$$\mathcal{K} = \frac{1}{2}\rho\left\{\left(V_S\right)^{T}\left(V_S\right) + \left(V_T\right)^{T}\left(V_T\right) + \left(h\dot{W}_{\|}\right)^{T}\alpha_{S1}\left(h\dot{W}_{\|}\right)\right\} \tag{234}$$

and

$$\begin{aligned}
\mathcal{P} = \frac{1}{2}\Big\{&\left(\varepsilon\right)^{T}\mathrm{A}_{2d}\left(\varepsilon\right) + 2\left(\varepsilon\right)^{T}\mathrm{B}_{2d}\left(h\kappa\right) + \left(h\kappa\right)^{T}\mathrm{C}_{2d}\left(h\kappa\right) \\
&+ \left(\frac{1}{h}\right)^{2}\left[\left(hW_{\|}\right)^{T}\Psi_{S1}\left(hW_{\|}\right)\right] + \left(hW_{\|;\alpha}\right)^{T}\mathrm{T}_{\alpha\beta}^{S1}\left(hW_{\|;\beta}\right) + 2\left(hW_{\|}\right)^{T}\mathrm{F}^{S1}\Big\}
\end{aligned} \tag{235}$$

where

$$\mathrm{A}_{2d} = \bar{\mathrm{A}}_{2d} \qquad \mathrm{B}_{2d} = \bar{\mathrm{B}}_{2d} \qquad \mathrm{C}_{2d} = \bar{\mathrm{C}}_{2d}$$

$$\Psi^{S1} = \alpha_{S1}\Lambda_{S1} + h^2\bar{\Psi}^{S1}$$

$$\begin{aligned}\mathrm{T}^{S1}_{\alpha\beta} = {} & \bar{\mathrm{T}}^{S1}_{\alpha\beta} + \left\{ \left[\bar{N}\left(\Phi^{S1}_{L\alpha}\Lambda_{S1}\right)\right]^T \left[\bar{N}\left(\Phi^{S1}_{L\beta}\right)\right] \right\} \\ & - \left\{ \left[\left(\bar{\mathrm{C}}^{+}_{2d}\right)^T \left[\bar{D}_{cL\alpha} + \left(V_{0c}\right)^T D_{hL\alpha}\right]\left(\Phi^{S1}\right)\right]^T \bar{\mathrm{C}}_{2d} \left[\left(\bar{\mathrm{C}}^{+}_{2d}\right)^T \left[\bar{D}_{cL\beta} + \left(V_{0c}\right)^T D_{hL\beta}\right]\left(\Phi^{S1}\right)\right] \right\}\end{aligned} \tag{236}$$

The above modeling also has been implemented into the computer code DVAPAS.

On the other hand, let us consider the reduction procedure from Eq. (224) to Eq. (159). Following the methodology introduced by Le [9], in the low-frequency regime, Eq. (26), it can be proved by the VAM that the present theory for full-range frequency vibrations, Eq. (224), is asymptotically equivalent to classical theory for low-frequency vibrations. Indeed, since the functional contains the small parameter h, one can investigate its asymptotic behavior as $h \to 0$ and $\omega h/c_0 \to 0$. In the first step of the variational asymptotic procedure when $\omega h/c_0$ approaches zero, the entire kinetic energy per unit area can be neglected; but the leading terms in the strain energy density be kept, which are given by

$$\begin{aligned}\mathcal{P} = {} & \left(\frac{1}{h}\right)^2 \left[\left(hW_{\|}\right)^T \Psi^{S1}\left(hW_{\|}\right) + \left(V_{\|}\right)^T \Psi^{S2}\left(V_{\|}\right) + \left(V_{\perp}\right)^T \Psi^{31}\left(V_{\perp}\right)\right] \\ & + 2\left(\frac{1}{h}\right)\left[\left(V_{\perp}\right)^T \left[\mathrm{S}^{31e}\left(\varepsilon\right) + \mathrm{S}^{31c}\left(h\kappa\right)\right] + \left(V_{\perp}\right)^T \left[\mathrm{S}^{31S1}_{\alpha}\left(hW_{\|;\alpha}\right) + \mathrm{S}^{31S2}_{\alpha}\left(V_{\|;\alpha}\right)\right]\right. \\ & \left. + \left[\left(hW_{\|}\right)^T \mathrm{S}^{S131}_{\alpha} + \left(V_{\|}\right)^T \mathrm{S}^{S231}_{\alpha}\right]\left(V_{\perp;\alpha}\right)\right\}\end{aligned} \tag{237}$$

It is clear that one can determine the following asymptotic formulae as $h \to 0$ from Eq. (237):

$$\begin{aligned} V_{\perp} &= -h\left(\Lambda_{31}\right)^{+}\left[\mathrm{S}^{31e}(\varepsilon) + \mathrm{S}^{31c}(h\kappa)\right] \\ hW_{\|} &= -h\left[\left(\alpha_{S1}\Lambda_{S1}\right)^{+}\mathrm{S}^{S131}_{\alpha}\right]\left(V_{\perp;\alpha}\right) \\ &= h^2\left[\left(\alpha_{S1}\Lambda_{S1}\right)^{+}\mathrm{S}^{S131}_{\alpha}\left(\Lambda_{31}\right)^{+}\right]\left[\mathrm{S}^{31e}(\varepsilon_{;\alpha}) + \mathrm{S}^{31c}(h\kappa_{;\alpha})\right] \\ V_{\|} &= -h\left[\left(\Lambda_{S2}\right)^{+}\mathrm{S}^{S231}_{\alpha}\right]\left(V_{\perp;\alpha}\right) \\ &= h^2\left[\left(\Lambda_{S2}\right)^{+}\mathrm{S}^{S231}_{\alpha}\left(\Lambda_{31}\right)^{+}\right]\left[\mathrm{S}^{31e}(\varepsilon_{;\alpha}) + \mathrm{S}^{31c}(h\kappa_{;\alpha})\right] \end{aligned} \tag{238}$$

with

$$\left(\Lambda_{31}\right)^{+}\Lambda_{31} = \mathrm{I}^3$$

Thus, in the low-frequency application limit, the internal degrees of freedom can be determined by the external ones. Based on the relations Eqs. (238) one can also determine the arbitrary orders of the internal degrees of freedom $W_{\|}$, $V_{\perp}$ and $V_{\|}$ as follows:

$$\begin{aligned} V_{\perp} &\sim O\left(h\hat{\varepsilon}\right) \\ hW_{\|} \sim V_{\|} &\sim O\left(\frac{h^2}{l}\hat{\varepsilon}\right) \end{aligned} \tag{239}$$

Substituting Eqs. (238) into Eq. (224) and discarding all small terms based on Eqs (239), we obtain the classical 2-D total energy functional per unit area, Eq. (159), viz.,

$$\begin{aligned} \mathcal{L} &= \frac{1}{2}\rho\left\{V_S^T V_S + V_T^T V_T\right\} - \frac{1}{2}\left\{\varepsilon^T \mathrm{A}'\varepsilon + 2\varepsilon^T \mathrm{B}'\left(h\kappa\right) + \left(h\kappa\right)^T \mathrm{C}'\left(h\kappa\right)\right\} \\ &= \frac{1}{2}\rho\left\{V_S^T V_S + V_T^T V_T\right\} - \frac{1}{2}\left\{\varepsilon^T \mathrm{A}\varepsilon + 2\varepsilon^T \mathrm{B}\left(h\kappa\right) + \left(h\kappa\right)^T \mathrm{C}\left(h\kappa\right)\right\} \end{aligned} \tag{240}$$

where

$$\begin{aligned} \mathrm{A}' &= \mathrm{A}_{2d} - 2\left[\left(\Lambda_{31}\right)^{+}\mathrm{S}^{31e}\right]^T \mathrm{S}^{31e} + \left[\left(\Lambda_{31}\right)^{+}\mathrm{S}^{31e}\right]^T \left(\Lambda_{31}\right)\left[\left(\Lambda_{31}\right)^{+}\mathrm{S}^{31e}\right] \\ \mathrm{B}' &= \mathrm{B}_{2d} - \left[\left(\Lambda_{31}\right)^{+}\mathrm{S}^{31e}\right]^T \mathrm{S}^{31c} - \left[\left(\Lambda_{31}\right)^{+}\mathrm{S}^{31c}\right]^T \mathrm{S}^{31e} \\ &\quad + \left[\left(\Lambda_{31}\right)^{+}\mathrm{S}^{31c}\right]^T \left(\Lambda_{31}\right)\left[\left(\Lambda_{31}\right)^{+}\mathrm{S}^{31c}\right] \\ \mathrm{C}' &= \mathrm{C}_{2d} - 2\left[\left(\Lambda_{31}\right)^{+}\mathrm{S}^{31c}\right]^T \mathrm{S}^{31c} + \left[\left(\Lambda_{31}\right)^{+}\mathrm{S}^{31c}\right]^T \left(\Lambda_{31}\right)\left[\left(\Lambda_{31}\right)^{+}\mathrm{S}^{31c}\right] \end{aligned}$$

Let us note that there is also a strong similarity between the above reduction and the reduction from Timoshenko beam theory to Euler-Bernoulli beam theory.

3.5 Recovery Relations

Now one can use the mass and stiffness matrices as input for the 2-D dynamic shell theory to accurately calculate the 2-D displacement field, 2-D generalized strains and stress resultants of laminated composite shells. However, in many applications this is not sufficient. The fidelity of a 2-D model such as this depends on how well it can predict the 3-D results in the original 3-D dynamic structure. Hence recovery relations should be provided to complete the 2-D model and then the results compared with those of the original 3-D model. By recovery relations, then, we mean expressions for 3-D displacement, strain, and stress fields in terms of 2-D quantities and ζ.

Since the total energy functional that is asymptotically correct through the zeroth-order is based on a first-order correction of the warping field, we can recover the 3-D displacement,

strain and stress fields only through the zeroth order. Following the same procedure as the previous chapter with Eqs. (7), (18), (49) and (217), one can recover the 3-D displacement field through the zeroth-order as

$$U_{3d} = u_{2d} + h\zeta \begin{bmatrix} C_{31} \\ C_{32} \\ C_{33} - 1 \end{bmatrix} + C_{ij} \left[SW_0 \right] \tag{241}$$

where U_{3d} is the column matrix of 3-D displacements, u_{2d} is the average shell displacements, C_{ij} are the components of global rotation tensor from Eq. (18) and W_0 is the primary results of high-frequency vibration approximations, such as

$$W_0 = \Phi^{S1} W_{\|} + \Phi^{31} V_{\perp} + \Phi^{S2} V_{\|} \tag{242}$$

From Eqs. (131), one can recover the 3-D strain field through the zeroth order as

$$\Gamma = \frac{1}{h} \Gamma_h S W_0 + \Gamma_e \varepsilon + \Gamma_c \left(h\kappa \right) + \Gamma_{L\alpha} S W_{0;\alpha} + \Gamma_R S W_0 \tag{243}$$

Then, one can use the 3-D constitutive law to obtain 3-D stresses σ_{ij}.

CHAPTER IV

NUMERICAL RESULTS

The objective of this chapter is to validate the present theory and the associated computer program, DVAPAS, and to present sample results from the program. As mentioned before, based on the VAM, this thesis represents the first attempt to obtain an asymptotically correct dynamic plate/shell theory made of composite laminated materials. Both analytical and numerical forms have been presented in prior chapters and are valid over a wide range of frequencies. Some independent work will be needed to verify the process and to compare results with the previous works. By validation procedure, we provide two ways: (a) Indirect way, which is a self-inspection way based on mutual relations between our analytical and numerical procedures (Section 4.1) and (b) Direct way, which makes a comparison between our results and available published works (Section 4.2).

To consider the behavior of the mass and stiffness matrices as calculated from DVAPAS, we provide some numerical results for plates with varying ply angles (a) where ply angles are symmetric about the mid-plane and (b) where ply angles are antisymmetric about the mid-plane (Section 4.3). For this purpose, the standard procedure of the eigenvalue problem has been carried out first to obtain eigenvalues for the eight-layer case with varying angles, and then the corresponding eigenvectors for each case are demonstrated in plots. We provide main diagonal and cross terms of the inertia and stiffness coefficients before and after performing short-wave extrapolation. Analogously, for fixed ply angles, we also present some mass stiffness and inertia coefficients varying number of layers in three different shell cases: (a) a symmetric angle ply case, (b) an antisymmetric angle ply case and (c) an cross angle ply case (Section 4.4).

Here and throughout the rest of the chapter, the results presented labeled as "analytic" are generated from Le's equations. In addition, we align our coordinate axes with x_1 along the length ("longitudinal in-plane") and x_2 along the width ("lateral in-plane"). These

Table 1: Relations between analytical and discretized coefficients

Analytical Form	Discretized Form
β_1^2	Λ_{S1}
β_2^2	Λ_{31}
β_3^2	Λ_{S2}
a_α^1	$\bar{N}\left(\Phi_{L\alpha}^{31}\right)$
a^2	$\left(\Phi^{31}\right)^T \bar{M}\left(V_{0e}\right)$
a_α^3	$\left(\Phi^{31}\right)^T \bar{M}\left(\Phi_{L\alpha}^{S2}\right)$
$\bar{\mathrm{a}}_\alpha^4$	$\left(\Phi^{S2}\right)^T \bar{M}\left(\Phi_{L\alpha}^{31}\right)$
a_α^5	$\bar{N}\left(\Phi_{L\alpha}^{S1}\right)$
$\bar{\mathrm{a}}_{\alpha\beta}^1$	$\bar{I}_\beta \bar{N}\left(\Phi_{L\alpha}^{31}\right)$
b_α^1	$\bar{N}\left(\Phi_{L\alpha}^{S2}\right)$
b^2	$\left(\Phi^{31}\right)^T \bar{M}\left(V_{0c}\right)$
b_α^3	$\left(\Phi^{31}\right)^T \bar{M}\left(\Phi_{L\alpha}^{S1}\right)$
$\bar{\mathrm{b}}_\alpha^4$	$\left(\Phi^{S1}\alpha_{S1}^+\right)^T \bar{M}\left(\Phi_{L\alpha}^{31}\right)$
c_1	α_{S1}
$\mathrm{d}^{1\mathrm{T}}$	$\left(\Phi^{31}\right)^T \bar{D}_{he}$
d_α^2	$\left(\Phi^{31}\right)^T \bar{D}_{hL\alpha}\left(\Phi^{S2}\right)$
d_α^3	$\left(\Phi^{S2}\right)^T \bar{D}_{hL\alpha}\left(\Phi^{31}\right)$
$\bar{\mathrm{d}}_\alpha^4$	$\left(\bar{\mathrm{C}}_{2d}^+\right)^T \left[\bar{D}_{cL\alpha} + \left(V_{0c}\right)^T \bar{D}_{hL\alpha}\right]\left(\Phi^{S1}\right)$
$\bar{\mathrm{d}}_\alpha^5$	$\left[\Phi^{S1}\left(\alpha_{S1}\Lambda_{S1}\right)^+\right]^T \bar{D}_{hL\alpha}\left(V_{0c}\right)$
$\mathrm{e}^{1\mathrm{T}}$	$\left(\Phi^{31}\right)^T \bar{D}_{hc}$
e_α^2	$\left(\Phi^{31}\right)^T \bar{D}_{hL\alpha}\left(\Phi^{S1}\right)$
$\bar{\mathrm{e}}_\alpha^6$	$\left(\bar{\mathrm{C}}_{2d}^+\right)^T \left[\bar{D}_{cL\alpha} + \left(V_{0c}\right)^T \bar{D}_{hL\alpha}\right]\left(\Phi^{S2}\right)$
e_α^7	$\left(\Phi^{S2}\right)^T \bar{D}_{hL\alpha}\left(V_{0c}\right)$
e_α^8	$\left(\Phi^{S1}\right)^T \bar{D}_{hL\alpha}\left(\Phi^{31}\right)$

are not necessarily aligned with any material axes, but for convenience and simplicity we assume that our coordinates are the lines of curvatures.

4.1 Indirect Validation

The primary type of validation procedure is to compare the present numerical and analytical procedures with each other. To do so, relations among the various coefficients can be established based on calculations from the analytical and numerical procedures. Results obtained from this study are given in Table 1. As expected, Eq. (124) in terms of Eqs. (125) and (126) perfectly match with that with Eqs. (225) and (226).

4.2 Direct Validation

The intent of this section is directly compare results from the available analytic solutions with those from our computer code, DVAPAS. As mentioned before, a difficulty is met when one tries to validate our results calculated from DVAPAS, because most of those published are limited to homogeneous and isotropic cases and do not directly provide their results in terms of the mass and stiffness matrices. Fortunately, mass and stiffness matrices for any kinds of homogeneous and isotropic plates/shells are directly provided by Refs. [16] and [9], which show very good agreement with 3-D numerical results of Gazis [22, 23]. Also, all results calculated from Le's procedure are summarized very well in the literature. For these reasons, we choose his analytical solutions for the key part of the validation process, to check our analytical and numerical procedures in detail. We have already showed that our analytical formulation can directly reproduce his results for homogeneous and isotropic materials. Therefore, we now only consider the comparison between his analytical results and our numerical ones in this section.

For our examples, let us consider free vibration of an elastic shell made of a homogenous, isotropic material with the following properties:

$$E = 26 \times 10^6 \text{ psi} \qquad G = 10 \times 10^6 \text{ psi} \qquad \nu = 0.3$$

and the following geometric properties

$$k_{11} = 0.5 \text{ in} \qquad k_{22} = 0.5 \text{ in} \qquad h = 1.0 \text{ in}$$

4.2.1 Primary approximation

All plates/shells have three zero eigenvalues, which correspond to the external degrees of freedom of the normal line element, viz. the average displacement components of that line element ($L_{\|}(0)$ and $F_{\perp}(0)$). In Table 2, the lowest five nonzero eigenvalues are shown for the homogeneous, isotropic shell, both from the analytic solution ([16]) and from our finite element approximation, DVAPAS, by changing N, the number of elements.

As expected, it is clear that all eigenvalues calculated by the finite element method are very close to the analytical results. Also, the corresponding eigenvectors associated

Table 2: Eigenvalues for a homogeneous and isotropic material

	Analytic	Numerical Results			
		ISO_1	ISO_2	ISO_3	ISO_4
λ_{11}	98.69604	98.75097	98.69617	98.69617	98.69604
λ_{21}	98.69604	98.75097	98.69617	98.69617	98.69604
λ_{12}	394.7841	397.6486	395.0039	394.7873	394.7847
λ_{22}	394.7841	397.6486	395.0039	394.7873	394.7847
λ_{31}	345.4361	345.6284	345.4366	345.4366	345.4361

with those five nonzero eigenvalues of this example are presented in Fig. 11 for the anti-symmetric thickness shear vibrations, Fig. 12 for the symmetric ones and Fig. 13 for the symmetric thickness-extension vibrations. Here the finite element results were obtained using N elements with four-order shape functions; and each analytical eigenvector, shown as solid lines, is indistinguishable from the finite element results in the plots.

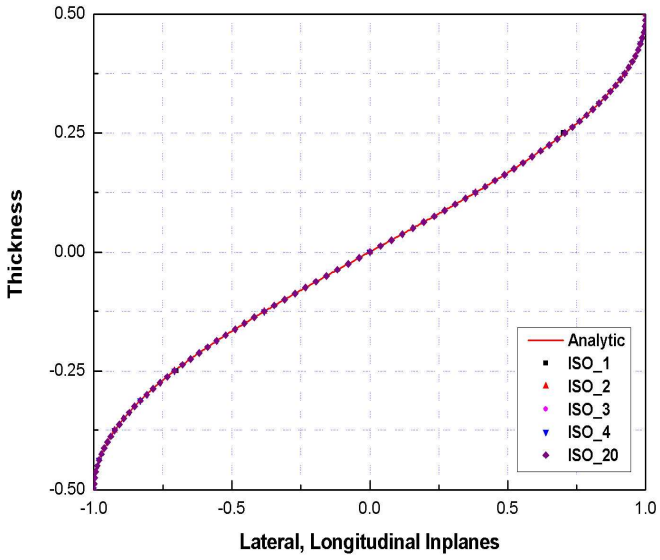

Figure 11: Eigenvectors for $F_{\|}(0)$

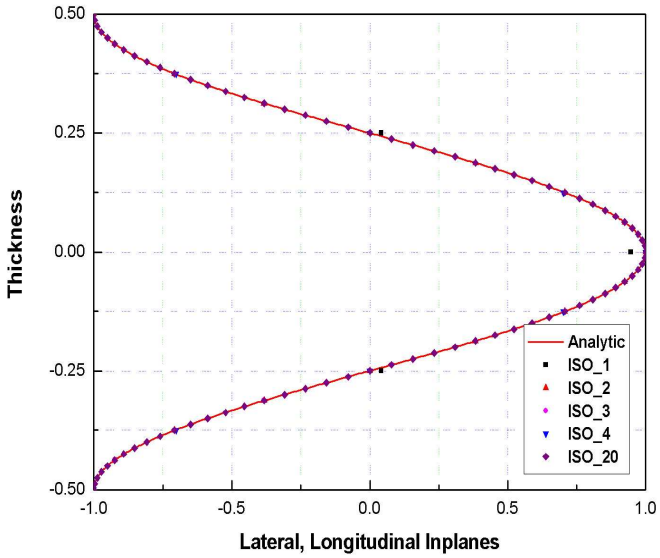

Figure 12: Eigenvectors for $L_{\|}\,(1)$

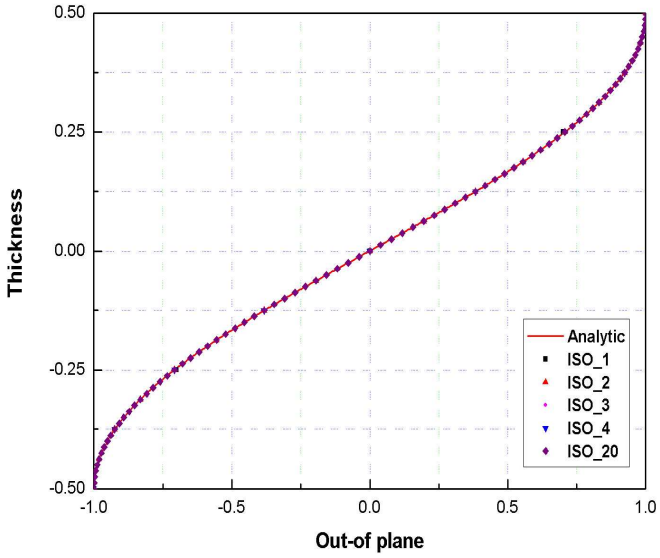

Figure 13: Eigenvectors for $L_{\perp}\,(0)$

4.2.2 Before performing short-wavelength extrapolation

With the eigenvalues and eigenvectors obtained, one can determine the warping fields for low- and high-frequency vibrations, and then calculate the mass and stiffness matrices. Table 3 summarizes each result for the mass and stiffness matrices before performing hyperbolic, short-wavelength extrapolation. From Table 3, it is shown that our numerical results exhibit excellent agreement with those obtained from the analytical solution. It is interesting to note that in Table 3, the relative error for all the terms even in ISO1 is smaller than 1%, where the relative error is defined as

$$\text{Relative Error} = \left| \frac{K_{analytic} - K_{DVAPAS}}{K_{analytic}} \right| \tag{244}$$

Table 3: Mass and stiffness matrices before performing short-wavelength extrapolation

	Analytic	Numerical Results			
		ISO_1	ISO_2	ISO_3	ISO_4
M_{11}	1.0	1.0	1.0	1.0	1.0
M_{44}	0.084556	0.084453	0.084556	0.084556	0.084556
M_{66}	1.0	1.0	1.0	1.0	1.0
M_{88}	1.0	1.0	1.0	1.0	1.0
K_{11}	28.57142	28.57142	28.57142	28.57142	28.57142
K_{44}	2.380952	2.380952	2.380952	2.380952	2.380952
K_{77}	8.345392	8.339833	8.345384	8.345376	8.345392
K_{99}	345.4361	345.6284	345.4366	345.4366	345.4361
K_{1010}	394.7841	397.6486	395.0039	394.7873	394.7847
K_{1616}	-97.32210	-92.54766	-96.99843	-97.31424	-97.32123
K_{1818}	135.0105	132.0426	134.7303	135.0099	135.0098

From Table 3, although we can verify that our procedure is correct in the asymptotic sense, the coefficient K_{1616} becomes negative, which is not a physically reasonable value. This shows clearly that hyperbolic short-wavelength extrapolation is necessary in some cases.

4.2.3 After performing short-wavelength extrapolation

After performing short-wavelength extrapolation, DVAPAS can recalculate the altered mass and stiffness matrices. Let us fist consider the plate model. Table 4 shows these results,

which as expected exhibit excellent agreement with the analytical solution. Now we consider the free vibration of homogeneous and isotropic shells including initial curvature. Unlike the plate case, it is noteworthy that for the shell case, there is a need to use more elements in order to obtain good agreement with analytical results. Note that as presented in prior chapters, the shell results are the same as the those for the plate except for K_{ij} with $i, j = 7, \cdots, 11$. Even so, Table 5 shows excellent agreement between analytical and numerical results. Indeed, it has thus been shown that the new numerical procedure provides excellent agreement with Le's analytical solutions for the entire process.

Table 4: Mass and stiffness matrices after performing short-wavelength extrapolation

	Analytic	Numerical Results			
		ISO_1	ISO_2	ISO_3	ISO_4
M_{11}	1.0	1.0	1.0	1.0	1.0
M_{44}	0.084556	0.084453	0.084556	0.084556	0.084556
M_{66}	1.0	1.0	1.0	1.0	1.0
M_{88}	1.0	1.0	1.0	1.0	1.0
K_{11}	33.78223	33.79151	33.78225	33.78225	33.78223
K_{44}	2.380952	2.380952	2.380952	2.380952	2.380952
K_{77}	8.345392	8.339833	8.345384	8.345376	8.345392
K_{99}	345.4361	345.6284	345.4366	345.4366	345.4361
K_{1010}	394.7841	397.6486	395.0039	394.7873	394.7847
K_{1616}	6.443656	6.741581	6.470505	6.443636	6.443702
K_{1818}	26.03399	27.53328	26.05056	26.04125	26.03406
K_{91}	42.42640	42.47598	42.42651	42.42653	42.42640
K_{189}	19.99999	19.82078	20.00944	19.99906	20.00001
K_{1610}	-53.33333	-53.91254	-53.38646	-53.33363	-53.33344

Table 5: Mass and stiffness matrices before performing short-wavelength extrapolation for the shell

	Analytic	Numerical Results				
		ISO_1	ISO_3	ISO_5	ISO_7	ISO_9
K_{77}	9.613739	9.605928	9.613717	9.613739	9.613739	9.613740
K_{99}	365.4361	365.4540	365.4361	365.4361	365.4361	365.4361
K_{1010}	409.7841	413.6703	409.7934	409.7842	409.7842	409.7842

4.3 Effects of Varying Angles

For our examples here and throughout the rest of this chapter, we first choose a fiber reinforced composite material which has the following material properties

$$E_L = 25 \times 10^6 \text{ psi} \qquad E_T = 10^6 \text{ psi}$$

$$G_{LT} = 0.5 \times 10^6 \text{ psi} \qquad G_{TT} = 0.3 \times 10^6 \text{ psi}$$

$$\nu_{LT} = \nu_{TT} = 0.25$$

where L denotes the direction parallel to the fibers and T the transverse direction. In this section, some numerical results obtained from DVAPAS are presented for two different cases, which are investigated for a eight-layer plate with varying the size of a angle ply:

- case 1: symmetric angle ply, $[\theta/-\theta]$ with $\theta = 0°$, $15°$ and $30°$.
- case 2: antisymmetric angle ply, $[\theta/-\theta]$ with $\theta = 0°$, $15°$ and $30°$.

4.3.1 Symmetric angle ply case

First, we investigate the free vibration of a laminated composite plate with lay-up $[\theta/-\theta]_{sym}$. Because we consider plates with layers having monoclinic symmetry and this is a symmetric ply angle case, there is thus no coupling between in-plane and out-plane displacement components before extrapolating this problem to the short-wavelength regime; certain modes will be entirely out-of plane and others entirely in-plane.

In Table 6 the lowest five nonzero eigenvalues are shown for the eight-layer plate with varying angles. As one can see, the eigenvalues associated with thickness-shear vibrations become changed in terms of increasing angle while that related to thickness-extension vibrations is fixed regarding thickness being kept constant.

Eigenvectors for a symmetric ply angle case with various angles are presented in Figs. 14 - 16, along with the corresponding eigenvalues. The finite element results were obtained using eight layers with a 5-noded isoparametric line element. Fig. 14 shows the eigenvfunctions for an antisymmetric thickness-shear vibration mode dominated by longitudinal displacement, while Fig. 15 shows the lateral displacement for a higher symmetric thickness-shear vibration

Table 6: Eigenvalues for various symmetric angle ply cases

	$\theta = 0°$	$\theta = 15°$	$\theta = 30°$
λ_{11}	49.34802	47.35515	42.83283
λ_{21}	29.60881	30.35325	32.50776
λ_{12}	197.3921	188.5959	168.4608
λ_{22}	118.4353	121.6126	131.2736
λ_{31}	105.7173	105.7173	105.7173

mode. As expected, the fifth nonzero eigenvalue in Table 6 has an eigenvector with only out-of plane displacement, as shown in Fig. 16.

While the longitudinal displacement in Fig. 14 appears to be continuous, it is the lateral displacement that is continuous in Fig. 15. The corresponding lateral displacement in Fig. 16 exhibits discontinuities, which reflect the layered structure of the material. As the ply angles increase, the discontinuities noticeably increase.

With the eigenvalues and corresponding eigenvectors obtained above, the diagonal terms in the resulting inertia and stiffness coefficients are given by Table 7. As one can see, like the homogeneous and isotropic example, some of these terms may not be positive until short-wavelength extrapolation is performed. Note that in Table 7 results for a low-frequency, long-wave vibration approximation agree perfectly with those from VAPAS developed by Yu *et al.* [57].

Table 8 shows main diagonal and cross terms after performing short-wave extrapolation. In contrast of K_{1616} and K_{1717} coefficients in Table 8, both ones become positive in Table 8.

4.3.2 Antisymmetric angle ply case

Analogously, as the size of an angle ply is increased, the eigenvalues for an antisymmetric ply angle case can be calculated from the solution procedure of the eigenvalue problem. The lowest five eigenvalues are summarized in Table 9.

By comparison with the eigenvalues for the symmetric case, those for the antisymmetric case have almost the same values for symmetric thickness-shear and thickness-extension

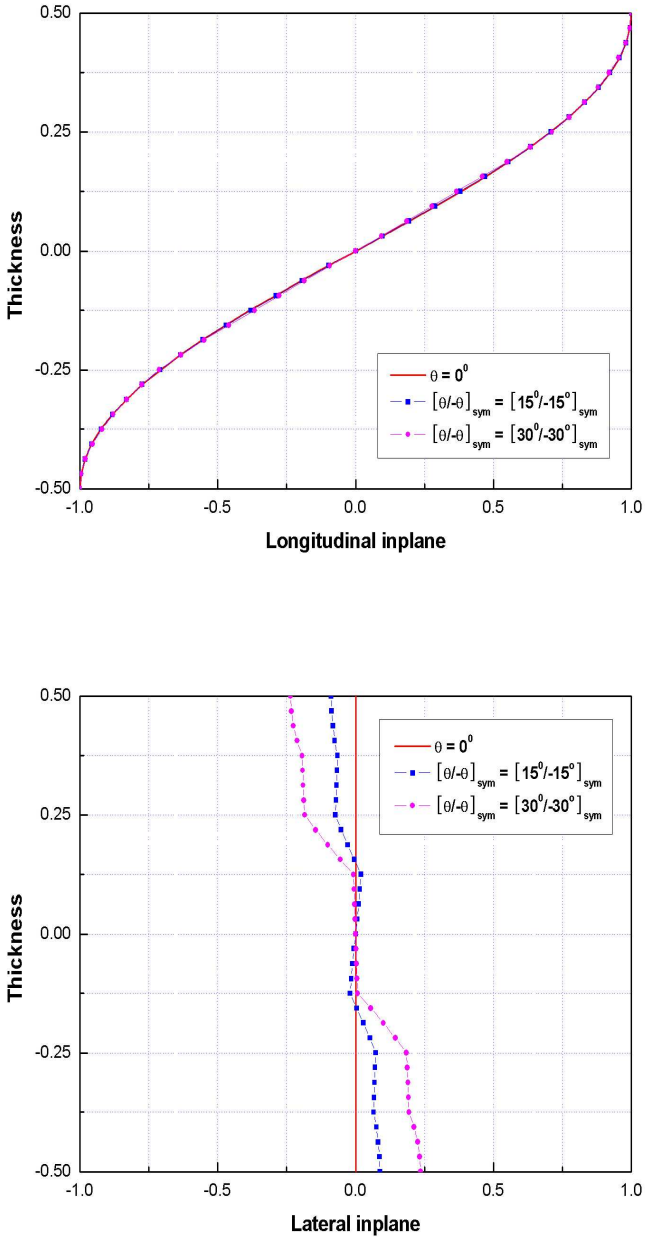

Figure 14: Eigenvectors for λ_{11} with various symmetric angle 8 layer plates

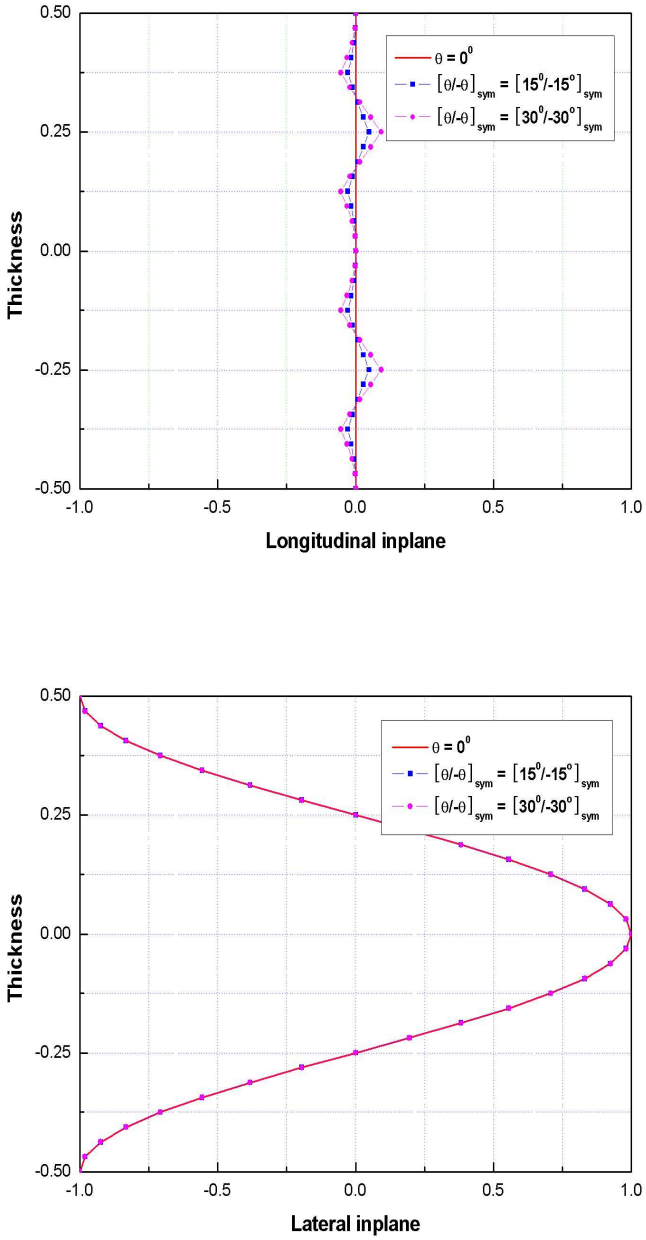

Figure 15: Eigenvectors for λ_{22} with various symmetric angle 8 layer plates

Table 7: Various symmetric angle ply cases before performing short-wave extrapolation

	$\theta = 0°$	$\theta = 15°$	$\theta = 30°$
M_{11}	1.0	1.0	1.0
M_{44}	0.084556	0.085094	0.088652
M_{55}	0.084556	0.085077	0.088715
M_{66}	1.0	1.0	1.0
M_{77}	1.0	1.0	1.0
M_{88}	1.0	1.0	1.0
K_{11}	250.6265	219.7818	146.2938
K_{33}	10.02506	11.41486	25.99310
K_{44}	20.88554	18.31515	12.19115
K_{66}	0.835421	0.951238	2.166092
K_{77}	4.172696	4.029653	3.797237
K_{88}	2.503617	2.582391	2.883956
K_{99}	105.7173	105.7173	105.7173
K_{1010}	197.3921	188.5960	168.4608
K_{1111}	118.4353	121.6126	131.2736
K_{1212}	21.57698	18.74445	12.07283
K_{1515}	0.977317	1.126999	2.810603
K_{1616}	-6.308167	-6.688499	-7.950582
K_{1717}	-27.72322	-22.80353	-15.33437
K_{1818}	292.7253	253.1878	167.8457
K_{2121}	26.66288	26.00317	38.75916

Table 8: Various symmetric angle ply cases after performing short-wave extrapolation

	$\theta = 0°$	$\theta = 15°$	$\theta = 30°$
K_{11}	251.4787	220.6122	147.0661
K_{33}	10.58139	11.98904	26.61750
K_{1212}	1.300674	1.111338	0.813880
K_{1515}	0.273490	0.293962	0.381956
K_{1616}	3.417939	3.240295	2.855284
K_{1717}	3.086237	3.189641	3.466871
K_{1818}	384.0770	290.1928	162.3965
K_{2121}	2.020112	4.746369	22.20085
K_{91}	9.491367	9.369293	9.035781
K_{189}	4.474272	4.414333	4.255121
K_{1610}	-26.66667	-25.44645	-22.69703

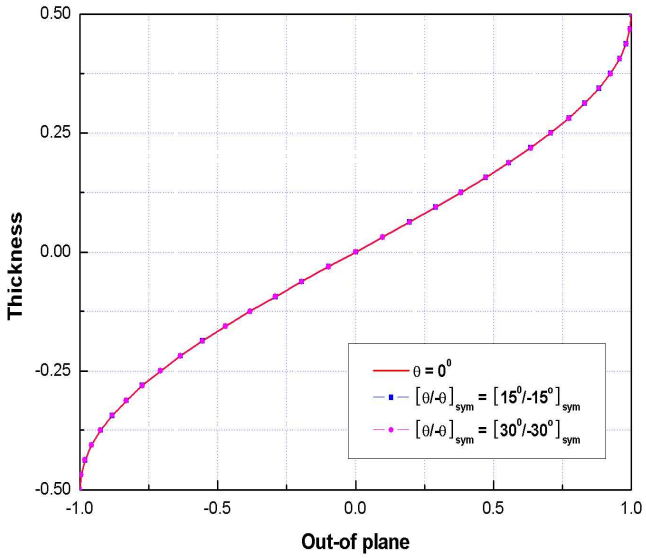

Figure 16: Eigenvectors for λ_{31} with various symmetric angle 8 layer plates

Table 9: Eigenvalues for various antisymmetric angle ply cases

	$\theta = 0°$	$\theta = 15°$	$\theta = 30°$
λ_{11}	49.34802	47.22180	42.26269
λ_{21}	29.60881	30.41965	32.88208
λ_{12}	197.3921	188.5938	168.4604
λ_{22}	118.4353	121.6127	131.2737
λ_{31}	105.7173	105.7173	105.7173

vibrations. Corresponding eigenvectors associated with the lowest five eigenvalues are presented in Figs. 17 – 19 in the same way as the previous case. As one can see, Figs. 17 and 18 show the eigenvectors for thickness-shear vibration cases, the former having more longitudinal in-plane displacement with an antisymmetric curve, while the latter has more lateral in-plane displacement with a symmetric curve. The fifth nonzero eigenvalue again has a smooth eigenvector with only out-of plane displacement, shown in Fig. 19, as expected. Again, in sharp contrast to results for homogenous plates, the displacement has discontinuous slopes in Figs. 17 and 18. In contrast to the symmetric case shown in Figs. 14 and 15, Figs. 17 and 18 are for the antisymmetric case and show the opposite tendencies.

Without performing a non-trivial extrapolation procedure, we now turn to the inertia and stiffness coefficients estimated in terms of determined eigenvalues and eigenvectors. In Table 10 most of the inertia and stiffness coefficients vary as ply angle increases while those related to symmetric thickness-extension vibrations do not, as expected.

From Table 10, although our procedure is asymptotically correct, the coefficients K_{1616} and K_{1717} have negative values, which are not physically reasonable values. Therefore, this shows clearly that we need to apply short-wavelength extrapolation to fix them.

After performing short-wavelength extrapolation, DVAPAS can recalculate the mass and stiffness matrices for an antisymmetric angle ply case. Table 11 includes each result as the ply angles increase.

As expected, the coefficients K_{1616} and K_{1717}, both become positive in Table 8. Unlike the symmetric angle ply case, some coefficients associated with the branch $F_{\perp}(0)$ and $F_{\parallel}(0)$ appear in the above stiffness matrices (K_{95}, K_{139} and K_{177}).

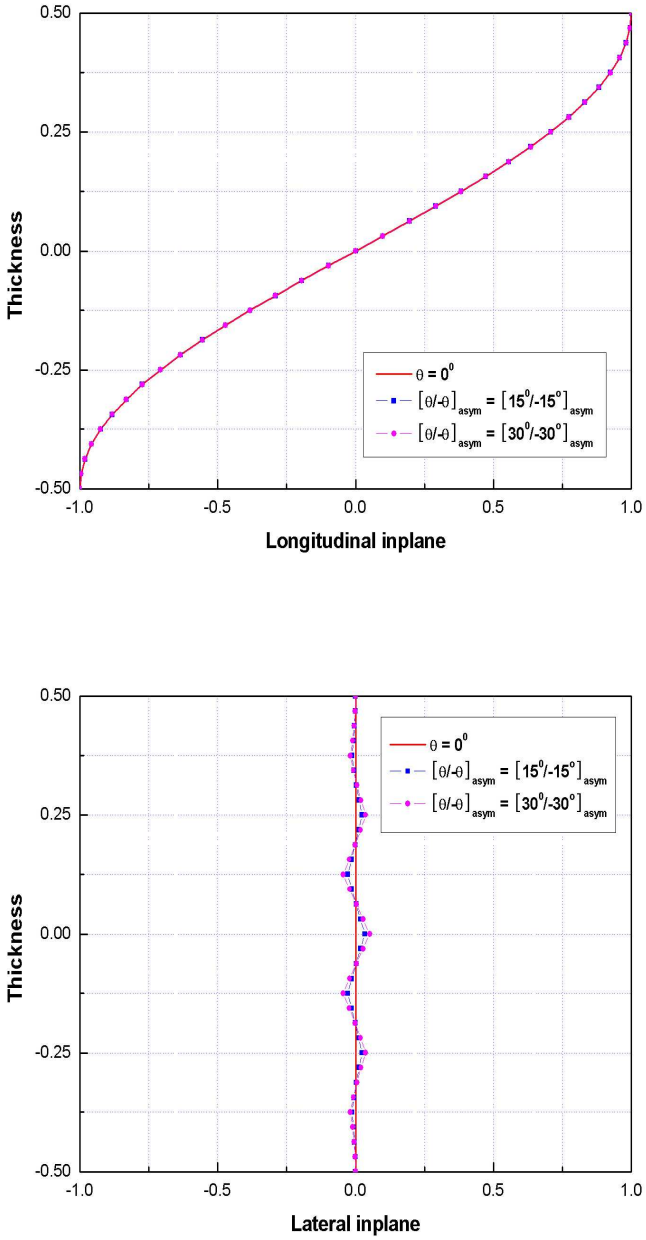

Figure 17: Eigenvectors for λ_{11} with various antisymmetric angle 8 layer plates

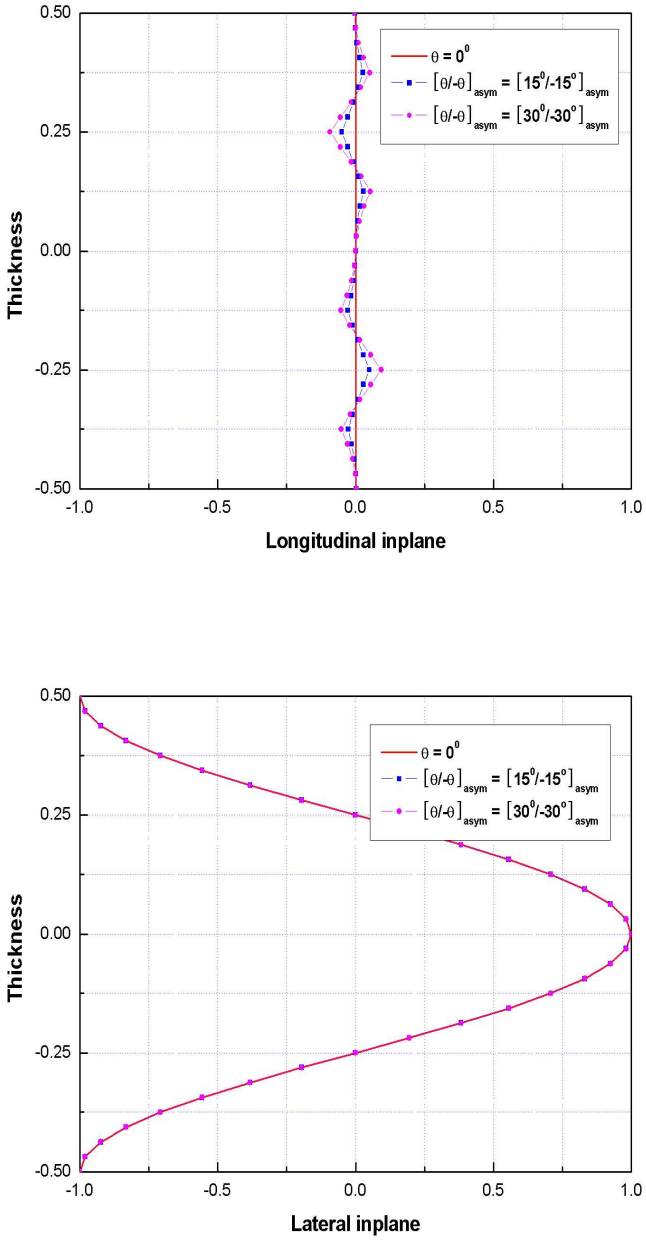

Figure 18: Eigenvectors for λ_{22} with various antisymmetric angle 8 layer plates

Table 10: Various antisymmetric angle ply cases before performing short-wave extrapolation

	$\theta = 0°$	$\theta = 15°$	$\theta = 30°$
M_{11}	1.0	1.0	1.0
M_{44}	0.084556	0.084587	0.084629
M_{55}	0.084556	0.084568	0.084599
M_{66}	1.0	1.0	1.0
M_{77}	1.0	1.0	1.0
M_{88}	1.0	1.0	1.0
K_{11}	250.6265	219.7818	146.2938
K_{33}	10.02506	11.41486	25.99310
K_{44}	20.88554	18.31515	12.19115
K_{66}	0.835421	0.951238	2.166092
K_{77}	4.172696	3.994364	3.576677
K_{88}	2.503617	2.572554	2.781821
K_{99}	105.7173	105.7173	105.7173
K_{1010}	197.3921	188.5938	168.4604
K_{1111}	118.4353	121.6127	131.2737
K_{1212}	21.57698	18.95752	12.69726
K_{1515}	0.977317	1.103924	2.374047
K_{1616}	-6.308167	-6.687874	-7.949568
K_{1717}	-27.72322	-22.80346	-15.33434
K_{1818}	292.7253	253.2192	167.8546
K_{2121}	26.66288	26.00250	38.75770

Table 11: Various antisymmetric angle ply cases after performing short-wave extrapolation

	$\theta = 0°$	$\theta = 15°$	$\theta = 30°$
K_{11}	251.4787	220.6122	147.0661
K_{33}	10.58139	11.98904	26.61750
K_{1212}	1.300674	1.154584	0.843994
K_{1515}	0.273490	0.294442	0.377202
K_{1616}	3.417939	3.240892	2.857048
K_{1717}	3.086237	3.176720	3.443967
K_{1818}	384.0770	273.8780	149.6667
K_{2121}	2.020112	4.639062	20.72581
K_{91}	9.491367	9.369293	9.035781
K_{95}	0.0	-0.000754	-0.001307
K_{139}	0.0	0.002279	0.004156
K_{177}	0.0	-0.001415	-0.002964
K_{189}	4.474272	4.415867	4.256630
K_{1610}	-26.66667	-25.44513	-22.69696

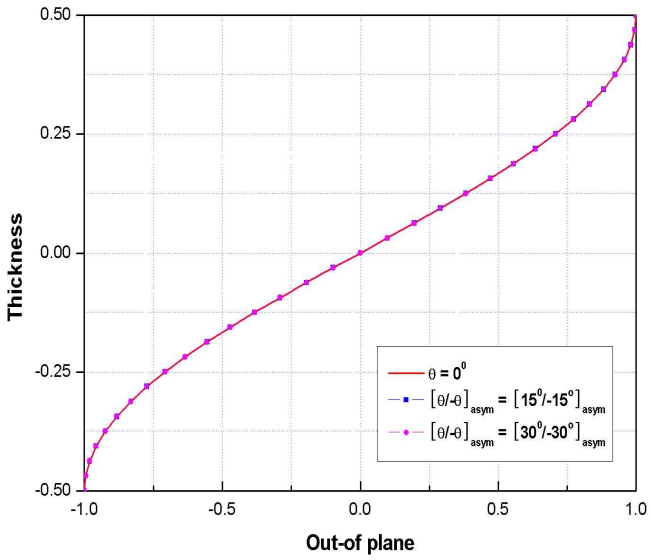

Figure 19: Eigenvectors for λ_{31} with various antisymmetric angle 8 layer plates

4.4 Effects of Varying Number of Layers

In this section, several numerical results obtained from DVAPAS are presented for three different cases, which are investigated for a shell with varying the number of layers:

- case 1: symmetric angle ply, $[30°/-30°]$ with $N = 4$, 8 and 12.
- case 2: antisymmetric angle ply, $[15°/-15°]$ with $N = 4$, 8 and 12.
- case 3: antisymmetric nearly cross ply, $[89.5°/-0.5°]$ with $N = 4$, 8, 12 and 16.

Our test problem is the free vibration of a shell made of the same material properties as that in the previous section (Section 4.3) and including the following geometric properties

$$k_{11} = 0.5 \text{ in} \qquad k_{22} = 0.5 \text{ in} \qquad h = 1.0 \text{ in}$$

4.4.1 Symmetric angle ply case

Let us first consider the free vibration of a laminated composite shell with increasing number of layers and fixed angle ply $[30°/-30°]_{sym}$. Following the solution procedure of the eigenvalue problem, eigenvalues for a symmetric ply angle case can be determined in general. The lowest five eigenvalues are presented in Table 12.

Table 12: Eigenvalues for the symmetric case with varying number of layers

	$N = 4$	$N = 8$	$N = 12$
λ_{11}	45.29122	42.83283	42.52380
λ_{21}	31.15058	32.50776	32.72905
λ_{12}	166.4511	168.4608	168.9248
λ_{22}	130.4789	131.2736	131.4709
λ_{31}	105.7173	105.7173	105.7173

As can be seen, the eigenvalues associated with thickness-shear vibrations change as the number of layers increases, while that related to thickness-extension vibrations remain constant. As before, inertia and stiffness coefficients for a shell are the same as those for a plate except K_{ij} with $i, j = 7, \cdots, 11$, regardless of our having performed short-wavelength extrapolation. Table 13 shows the main diagonal terms of mass and stiffness matrices obtained from DVAPAS.

Table 13: Symmetric angle ply cases with varying number of layers

	$N = 4$	$N = 8$	$N = 12$
M_{44}	0.100953	0.088652	0.086357
M_{55}	0.101790	0.088715	0.086387
K_{77}	5.569859	4.538850	4.380332
K_{88}	3.5478709	3.244149	3.181460
K_{99}	173.7736	173.7950	173.7962
K_{1010}	176.8739	179.0860	179.6376
K_{1111}	133.7609	134.4697	134.6740

4.4.2 Antisymmetric angle ply case

Analogously, as the number of layers increases, the eigenvalues for an antisymmetric ply angle case can be calculated from the solution procedure of the eigenvalue problem. The lowest five eigenvalues are summarized in Table 14.

Table 14: Eigenvalues for the antisymmetric case with varying number of layers

	$N = 4$	$N = 8$	$N = 12$
λ_{11}	47.14898	47.22180	47.23135
λ_{21}	30.40315	30.41965	30.42214
λ_{12}	186.6646	188.5938	188.8273
λ_{22}	121.5491	121.6127	121.6636
λ_{31}	105.7173	105.7173	105.7173

As one can see, the eigenvalues associated with thickness-shear vibrations change as the number of layers increases, while those related to thickness-extension vibrations remain constant. Also in Table 15 shows the main diagonal terms of mass and stiffness matrices obtained from DVAPAS.

4.4.3 Cross-ply case

Let us now consider the free vibration of a laminated composite shell with N layers $[89.5°/-0.5°]_{cp}$. In Table 16 the lowest five nonzero eigenvalues are shown for the cross-ply shell with varying number of layers. As one can see, the eigenvalues associated with thickness-shear vibrations change as the number of layers, while those related to thickness-extension

Table 15: Antisymmetric angle ply cases with varying number of layers

	$N = 4$	$N = 8$	$N = 12$
M_{44}	0.084770	0.084587	0.084569
M_{55}	0.084621	0.084568	0.084561
K_{77}	4.934705	4.934379	4.934634
K_{88}	2.860137	2.859894	2.859896
K_{99}	173.7079	173.7950	173.7962
K_{1010}	211.6696	214.9919	215.3703
K_{1111}	117.7872	100.1938	99.80420

vibrations become constant. Unlike symmetric and antisymmetric cases, there are only three different eigenvalues such as a homogeneous and isotropic shell.

Table 16: Eigenvalues for the cross-ply case with varying number of layers

	$N = 4$	$N = 8$	$N = 12$
λ_{11}	36.8544	36.97939	36.99744
λ_{21}	36.8544	36.97939	36.99744
λ_{12}	145.8102	147.4176	147.8072
λ_{22}	145.8102	147.4176	147.8072
λ_{31}	105.7173	105.7173	105.7173

The eigenvectors for an eight-layer shell are presented in Figs. 20 – 22, along with corresponding eigenvalues. Figs. 20 and 21 show the eigenvectors for thickness-shear vibration modes, the symmetric mode of which has more longitudinal in-plane displacement and the antisymmetric mode of which has more lateral in-plane displacement. The symmetric out-of plane mode is shown in Fig. 22, having a smooth eigenvector as before.

In contrast to results for the homogeneous shell, the displacement has discontinuous slope in the most cases for the thickness-shear vibrations. With the eigenvalues and corresponding eigenvectors calculated from DVAPAS, the main diagonal terms on the resulting inertia and stiffness coefficients are given by Table 17. As has been seen in other cases, before performing short-wavelength extrapolation some terms are not positive.

As one can see, there are no changes in the low-frequency long-wave vibration results.

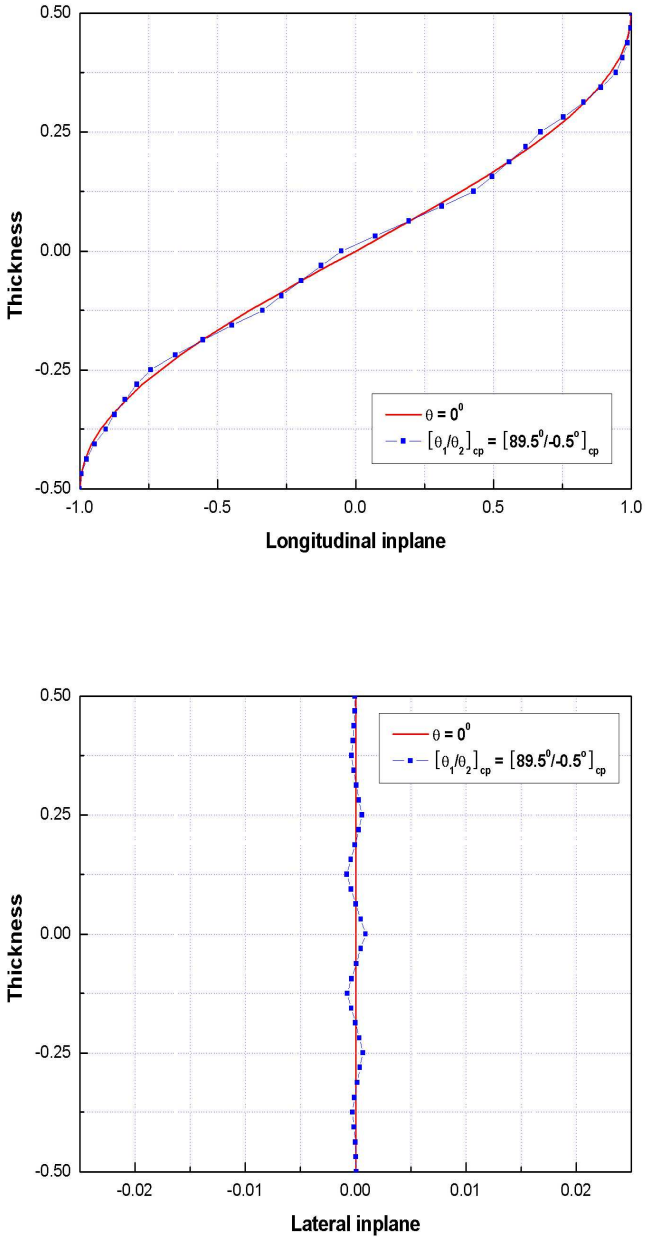

Figure 20: Eigenvector for λ_{11} with cross-ply 8 layer shell

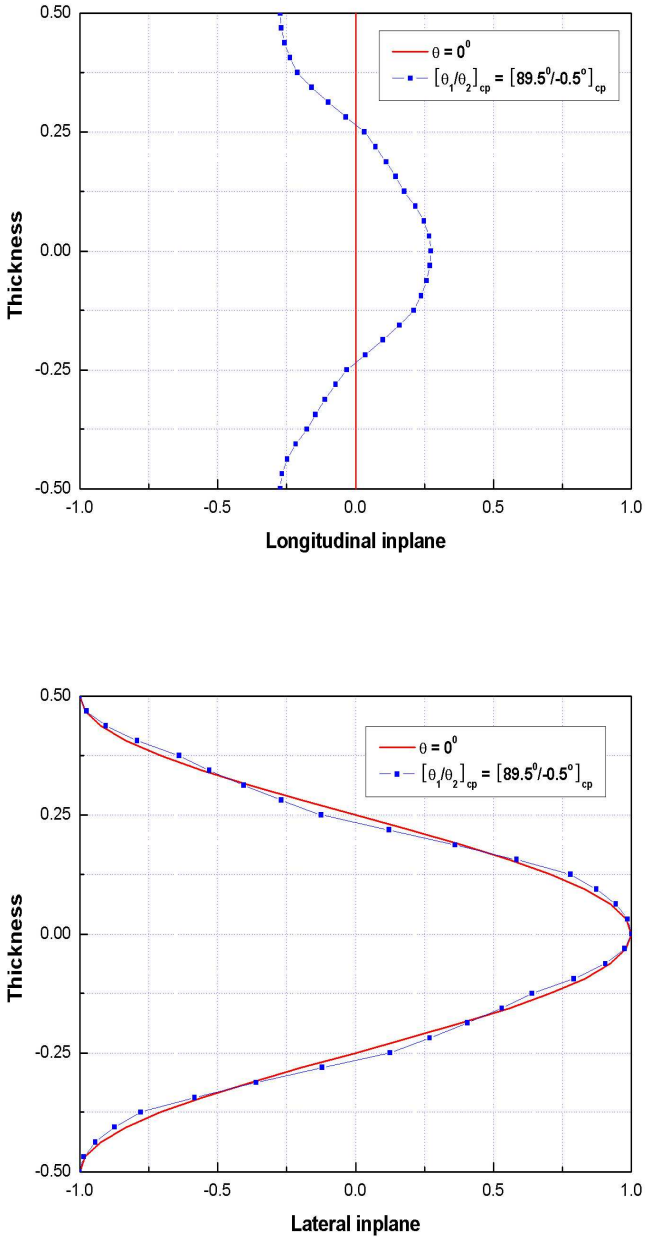

Figure 21: Eigenvector for λ_{22} with cross-ply 8 layer shell

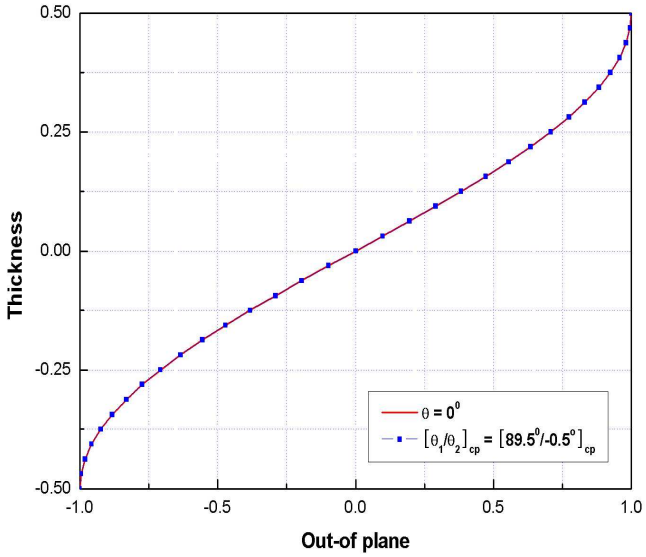

Figure 22: Eigenvector for λ_{31} with cross-ply 8 layer shell

Table 17: Cross-ply cases with varying number of layers before performing short-wave extrapolation

	$N = 4$	$N = 8$	$N = 12$	$N = 16$
M_{11}	1.0	1.0	1.0	1.0
M_{44}	0.084982	0.084630	0.084587	0.084573
M_{66}	1.0	1.0	1.0	1.0
M_{88}	1.0	1.0	1.0	1.0
K_{11}	130.3078	130.3078	130.3078	130.3078
K_{44}	10.85898	10.85898	10.85898	10.85898
K_{77}	3.605994	3.604810	3.604988	3.605058
K_{99}	173.7079	173.8031	173.7993	173.7977
K_{1010}	151.2687	152.9952	153.4143	153.5329
K_{1212}	11.62706	11.30644	11.26128	11.24624
K_{1616}	-10.73140	-10.53450	-10.48116	-10.46541
K_{1818}	128.7938	147.2594	144.7117	143.9777

Unlike symmetric and antisymmetric cases, the stiffness coefficient associated with a symmetric thickness-extension vibration mode changes with a varying number of layers.

Table 18: Cross-ply cases with varying number of layers after performing short-wave extrapolation

	$N = 4$	$N = 8$	$N = 12$	$N = 16$
K_{1212}	0.703569	0.636229	0.629894	0.627900
K_{1616}	2.362262	2.477373	2.502515	2.508733
K_{1818}	59.93709	122.0453	126.2114	127.6380
K_{91}	8.580195	8.580195	8.580195	8.580195
K_{94}	0.013299	0.015096	0.004301	0.001843
K_{129}	0.050555	0.005238	0.001469	0.000628
K_{139}	-0.007800	-0.000054	-0.000052	0.000001
K_{177}	-0.045533	-0.004598	-0.001283	-0.000548
K_{178}	0.007025	0.000048	0.000045	0.000001
K_{189}	4.085625	4.043171	4.044361	4.044530
K_{199}	-0.467840	-1.080521	-1.083141	-0.070764
K_{1610}	-19.42903	-19.86579	-19.95131	-19.97420
K_{1611}	2.224797	5.309054	5.343263	0.349472

As expected, the coefficient K_{1616} associated with a symmetric thickness-extension vibration mode, is positive in Table 18. In contrast with most ply angle cases, some additional coefficients associated with the branch $F_{\perp}(0)$ and $F_{\parallel}(0)$ appear in the stiffness matrices, e.g. K_{94}, K_{139} and K_{177}.

CHAPTER V

CONCLUSIONS AND RECOMMENDATIONS

The present development represents a new contribution, as there is no published work on variational-asymptotic modeling of composite laminated shells for a wide range frequencies and expressed in both analytic and finite element-based forms. This chapter summarizes the conclusions of the work and suggests possible areas of additional research.

5.1 Conclusions

Unlike most published work on shell modeling, the present research proposes new analytic and numerical procedures to rigorously construct an accurate model for composite laminated shells for a wide range frequencies. In these procedures, the concept of decomposition of the rotation tensor introduced by Danielson and Hodges [53] is first used to establish the original 3-D elasticity problem in intrinsic form, which helps to avoid unnecessary complexities of the mathematical description. Then, as the most essential and important procedure, the Variational Asymptotic Method [3, 9] introduced by Berdichevsky is used to perform a rigorous dimensional reduction. This takes advantage of small geometric parameters inherent in the structure. Unlike the static case, however, there is one more important physical parameter in the dynamics case. It is called the characteristic timescale for the change of the deformation with respect to time; it is also used in the long-wavelength range. Finally, another logically independent procedure is used, the extrapolation of the foregoing procedures to the short-wavelength regime; this procedure was introduced by Berdichevsky [3, 9].

In chapters II and III, the two different forms of dynamic shell theories valid over a wide range frequencies are proposed. However, both analytic and numerical procedures are very close because they share the same foundation. The first one (chapter II) is derived based on an analytical formulation, and is the first attempt to obtain an asymptotically correct dynamic shell theory made of composite laminated materials and valid over a wide range

of frequencies. It describes in an asymptotically correct manner not only the low-frequency but also some of the first high-frequency branches of vibrations in the long-wave range. Moreover, it allows recovery of the three-dimensional stress state in the short-wave range.

On the other hand, although the results of the first one (chapter II) is given in an explicit and elegant analytical form, the whole solution process is not easily implemented, even for the case of a homogeneous and isotropic material. Thus, this result is not suitable in practical analysis of shells. In chapter III, a corresponding finite element-based shell model is developed, based on the same procedure as the analytic shell model. As a direct outgrowth of the numerical procedure, the computer code DVAPAS is developed to inexpensively calculate the mass and stiffness matrices for composite laminated shells.

Finally, in chapter IV, two ways are suggested to validate the analytical and numerical procedures. The first is to perform mutual checks between the two different forms. The second is to compare in detail results from our numerical procedure with those of Ref. [16]. All validation has shown that the proposed theories have excellent agreement with results from Ref. [16].

The main contributions of the present work toward developing dynamic composite shell models valid over a wide range frequencies with sufficient accuracy are the following:

1. To provide insight and guidance for developing the finite element-based shell model and an analytic procedure for 1-D through-the-thickness analysis for laminated composite materials has been presented in the thesis.

2. The combination of (a) the compact and elegant representation of the dynamic intrinsic formulation [48], (b) the rigorous dimensional reduction procedure of the Variational Asymptotic Method, and (c) the hyperbolic short-wave procedure of the nontrivial extrapolation is itself a contribution.

3. An asymptotically correct shell model has been constructed that enables one to analyze shell dynamic response for vibrations in the low-frequency, long-wavelength area, including the high-frequency regime, and to achieve simple, accurate and positive definite strain and kinetic energy functionals for all wavelengths.

4. Companion analytical and numerical procedures of the 1-D through-the-thickness analysis have been developed.

5. To implement the numerical procedure as a 1-D finite element code, a computer program, DVAPAS, has been developed.

5.2 Recommendations

Although much has been investigated and achieved based on the approach utilized for this work, there are still some additional points that need to be studied as well as things to be improved. The present work can be considered as the very beginning step of a general and consistent construction of full range frequency models for composite shells by the Variational Asymptotic Method and the hyperbolic short-wave extrapolation. Moreover, because the theories are still under development, it is obvious that some independent work is needed to validate and compare results with other approaches. To complete the present research, a number of future tasks should be performed:

1. To validate our DVAPAS results with available 3-D finite element results and experimental data, the most urgent work is to develop the corresponding 2-D surface analysis associated with the present theories.

2. Under the Variational Asymptotic Method, there are other numerical codes. One is VAPAS (a computer program for 1-D through-thickness analysis of plates and shells) developed by Yu *et al.* [57], which is a generalized Reissner-like model to analyze the structural static responses. Some works is needed to establish the relationship between the two codes as far as range of applicability and accuracy.

3. In reality, many composite shells are coupled with actuated elements and serve in severe environments. Hence, it will be very important to take actuation, acoustics, and hygro-thermal effects into account to extend the versatility of the present research.

4. There are various engineering applications to use multi-layer plates and shells for which the materials vary through the thickness, such as sandwich plates and shells. However, the prediction and analysis modeling of the performance of such structures

is known to be unsatisfactory in some cases. Therefore, it is recommended to extend the present theory to model sandwich plates and shells by taking advantages of the Variational Asymptotic Method on the dynamic intrinsic formulation.

5. It should be noted that because the shell theory of chapter II is successfully implemented into a numerical form in the theory of chapter III, this will facilitate the extension of this work to include dynamic beam modeling valid over full range frequency with sufficient accuracy.

REFERENCES

[1] Langley, R. S. and Bardell, N. S., "A review of current analysis capabilities applicable to the applicable to the high frequency vibration prediction of aerospace structures," *The Aeronautical Journal*, Vol. 102, 1998, pp. 287–297.

[2] I. V. Andrianov, J. A. and Barantsev, R. G., "Asymptotic approaches in mechanics: New parameters and procedures," *Applied Mechanics Reviews*, Vol. 56, No. 1, 2003, pp. 87–110.

[3] Berdichevsky, V. L., *Variational Principles of Continuum Mechanics*, Nauka, Moscow, 1983.

[4] J. D. Kaplunov, L. Y. K. and Nolde, E. V., *Dynamics of Thin Walled Elastic Bodies*, Academic press, USA, 1998.

[5] Losin, N. A., "Asymptotics of Flexural Waves in Isotropic Elastic Plates," *Journal of Applied Mechanics*, Vol. 64, 1997, pp. 336–342.

[6] Losin, N. A., "Asymptotics of Extensional Waves in Isotropic Elastic Plates," *Journal of Applied Mechanics*, Vol. 65, 1998, pp. 1042–1047.

[7] Berdichevsky, V. L., "Variational-asymptotic method of constructing a theory of shells," *PMM*, Vol. 43, No. 3, 1979, pp. 664–687.

[8] Koiter, W. T. and Mikhailov, G. K., *Theory of shells*, North-Holland Publishing Company, Amsterdam, 1980.

[9] Le, K. C., *Vibrations of Shells and Rods*, Springer, Germany, 1st ed., 1999.

[10] Leissa, A. W., "Vibration of Shells," SP 288, NASA, 1973.

[11] Noor, A. K. and Burton, W. S., "Assessment of shear deformation theories for multilayered composite plates," *Applied Mechanics Reviews*, Vol. 42, No. 1, 1989, pp. 1–13.

[12] Qatu, M. S., "Recent research advances in the dynamic behavior of shells, 1989 - 1999, Part 1: Laminated shells," *Applied Mechanics Reviews*, Vol. 55, No. 7, 2002, pp. 1989–2000.

[13] Qatu, M. S., "Recent research advances in the dynamic behavior of shells, 1989 - 1999, Part 2: Homogeneous shells," *Applied Mechanics Reviews*, Vol. 55, No. 5, 2002, pp. 415–434.

[14] Reddy, J. N., *Mechanics of Laminated Composite Plates and Shells: Theory and Analysis*, CRC Press, Boca Raton, Florida, 2nd ed., 2003.

[15] Amabili, M. and Païdoussis, M. P., "Review of studies on geometrically nonlinear vibrations and dynamics of circular cylindrical shells and panels, with and without fluid-structure interaction," *Applied Mechanics Reviews*, Vol. 56, No. 4, 2003, pp. 349–381.

[16] Le, K. C., "High frequency vibrations and wave propagation in elastic shells: variational-asymptotic approach," *International Journal of Solids and Structures*, Vol. 34, No. 30, 1997, pp. 3923–3939.

[17] R. Kienzler, H. A. and Ott, I., *Theories of plates and shells: critical review and new applications*, Springer, New York, 2004.

[18] Braga, A. M. B. and A., C. E. R., "High-frequency response of isotropic-laminated cylindrical shells modeled by a layer-wise theory," *International Journal of Solids and Structures*, Vol. 42, 2005, pp. 4278–4294.

[19] Yang, S. and Yuan, F. G., "Transient wave propagation of isotropic plates using a higher-order plate theory," *International Journal of Solids and Structures*, Vol. 42, 2005, pp. 4115–4153.

[20] Hal, B. V., *Automation and performance optimization of the wave based method for interior structural-acoustic problemss*, Ph.D. thesis, Mechanical Engineering, Katholieke Universiteit Leuven, Hevelee(Leuven), Belgium, 2004.

[21] Love, A. E. H., *A treaties on the mathematical theory of elasticity*, Dover Publications, Inc., New York, 4th ed., 1944.

[22] Gazis, D. C., "Three-dimensional investigation of the propagation of waves in hollow circular cylinders. I. Analytical foundation," *Journal of the acoustical society of america*, Vol. 31, No. 5, 1959, pp. 568–573.

[23] Gazis, D. C., "Three-dimensional investigation of the propagation of waves in hollow circular cylinders. II. Numerical Results," *Journal of the acoustical society of america*, Vol. 31, No. 5, 1959, pp. 573–578.

[24] Timoshenko, S., *Vibration problems in engineering*, D. Van Nostrand Company, Princeton, 1955.

[25] Reissner, E., "The Effect of Transverse Shear Deformation on the Bending of Elastic Plates," *Journal of Applied Mechanics*, Vol. 13, 1945, pp. A69–A77.

[26] Mindlin, R. D., "Influence of rotary inertia and shear on flexural vibrations of isotropic, elastic plates," *Journal of Applied Mechanics*, Vol. 18, 1951, pp. 31–38.

[27] Mindlin, R. D., *An Introduction to the Mathematical Theory of Vibrations of Elastic Plates*, Signal Corps Engineering Laboratories, Fort Monmouth, 1955.

[28] Kane, T. R. and Mindlin, R. D., "High-frequency extensional vibrations of plates," *Journal of Applied Mechanics*, Vol. 23, 1956, pp. 277–283.

[29] Mindlin, R. D. and Medick, M. A., "Extensional vibrations of elastic plates," *Journal of Applied Mechanics*, Vol. 26, 1959, pp. 561–569.

[30] Graff, K. F., *Wave Motion in elastic solids*, Dover Publications, Inc., New York, 1991.

[31] Lee, P. C. Y. and Nikodem, Z., "An approximate theory for high-frequency vibrations of elastic plates," *International Journal of Solids and Structures*, Vol. 8, 1972, pp. 581–612.

[32] Berdichevsky, V. L., "High-frequency long-wave vibrations of plates," *Soviet Physics Doklady*, Vol. 22, No. 4, 1977, pp. 604–606.

[33] Kvashnina, S. S., "High-frequency long-wave vibrations of elastic rods," *PMM*, Vol. 43, No. 2, 1979, pp. 335–341.

[34] Berdichevsky, V. L. and Le, K. C., "High-frequency long-wave shell vibrations," *PMM*, Vol. 44, No. 4, 1980, pp. 520–525.

[35] Kaplunov, J. D., "High-frequency stress-strain states," *Mechanics of Solids*, Vol. 25, 1990, pp. 147–157.

[36] Berdichevsky, V. L. and Le, K. C., "High-frequency vibrations of shells," *Soviet Physics-Doklady*, Vol. 27, No. 11, 1982, pp. 988–990.

[37] Le, K. C., "High-frequency longitudinal vibrations of elastic rods," *PMM*, Vol. 50, No. 3, 1986, pp. 335–341.

[38] Ryazantseva, M. Y., "Flexural vibrations of symmetrical sandwich plates," *Mechanics of Solids*, Vol. 20, 1985, pp. 153–159.

[39] Le, K. C., "High-frequency vibration of piezoelectric ceramic shells," *Soviet Physics Doklady*, Vol. 30, 1985, pp. 899–900.

[40] Le, K. C., "The theory of piezoelectric shells," *PMM*, Vol. 50, 1986, pp. 98–105.

[41] Le, K. C., "High-frequency long wave vibration of piezoelectric ceramic plates," *Soviet Physics Doklady*, Vol. 27, 1982, pp. 422–423.

[42] Berdichevsky, V. L. and Foster, D. J., "On Saint-Venant's principle in the dynamics of elastic beams," *International Journal of Solids and Structures*, Vol. 40, 2003, pp. 3293–3310.

[43] Foster, D. J. and Berdichevsky, V. L., "On Saint-Venant's principle in the two-dimensional flexural vibrations of elastic beams," *International Journal of Solids and Structures*, Vol. 41, 2004, pp. 2551–2562.

[44] Lee, B. W., *Application of Variational-Asymptotic Method to Laminated Composite Plates*, Ph.D. thesis, Aerospace Engineering, Georgia Institute of Technology, Atlanta, GA, 1993.

[45] Cesnik, C. E. S., *Cross-Sectional Analysis of Initially Twisted and Curved Composite Beams*, Ph.D. thesis, Aerospace Engineering, Georgia Institute of Technology, Atlanta, GA, 1994.

[46] Volovoi, V. V., *On End Effects in Prismatic Beams*, Ph.D. thesis, Aerospace Engineering, Georgia Institute of Technology, Atlanta, GA, 1997.

[47] Sutyrin, V. G., *Some Problems of Averaging Micro-nonhomogeneous Periodic Media*, Ph.D. thesis, Mathematics and Mechanics, Moscow University, 1984.

[48] Hodges, D. H., *Nonlinear Composite Beam Theory*, AIAA, Washington, D. C., 2006.

[49] Danielson, D. A., *Vectors and Tensors in Engineering and Physics*, Pereus Books Publishing, Cambridge, Massachusetts, 2nd ed., 1997.

[50] D. H. Hodges, A. R. A. and Danielson, D. A., "A geometrically nonlinear theory of elastic plates," *Journal of Applied Mechanics*, Vol. 60, 1993, pp. 109–116.

[51] D. H. Hodges, W. Y. and Patil, M. J., "Geometrically-exact, intrinsic theory for dynamics of moving composite plates and shells," *Proceedings of the 47th Structures, Structural Dynamics, and Materials Conference*, Newport, Rhode Island, May 2006.

[52] Libai, A. and Simmonds, J. G., *The nonlinear theory of elastic shells*, Cambridge University Press, New York, 2nd ed., 1998.

[53] Danielson, D. A. and Hodges, D. H., "Nonlinear beam kinematics by decomposition of the rotation tensor," *Journal of Applied Mechanics*, Vol. 54, No. 2, 1987, pp. 258–262.

[54] W. Yu, D. H. H. and Volovoi, V. V., "Asymptotic generalizeation of Reissner-like composite plate theory with accurate strain recovery," *International Journal of Solids and Structures*, Vol. 39, No. 20, 2002, pp. 5185–5203.

[55] Sutyrin, V. G., "Derivation of plate theory accounting asymptotically correct shear deformation," *Journal of Applied Mechanics*, Vol. 64, No. 4, 1997, pp. 905–915.

[56] W. Yu, D. H. H. and Volovoi, V. V., "Asymptotic generalizeation of Reissner-Mindlin theory: accurate three-dimensional recovery for composite shells," *Computer Methods in Applied Mechanics and Engineering*, Vol. 191, No. 44, 2002, pp. 5087–5109.

[57] W. Yu, D. H. H. and Volovoi, V. V., "Asymptotically Accurate 3-D recovery from Reissner-like Composite Plate Finite Elements," *Computers and Structures*, Vol. 81, No. 7, 2003, pp. 439–454.

[58] Hodges, D. H., "Direct solutions for Sturm-Liouville systems with Discontinuous coefficients," *AIAA Journal*, Vol. 17, No. 8, 1979, pp. 924–926.

[59] Hodges, D. H., "Orthogonal polynomials as variable-order finite element shape functions," *AIAA Journal*, Vol. 21, No. 5, May 1983, pp. 796–797.

[60] Yu, W., *Variational Asymptotic Modeling of Composite Dimensionally Reducible Structures*, Ph.D. thesis, Aerospace Engineering, Georgia Institute of Technology, 2002.

[61] Smith, I. M. and Griffiths, D. V., *Programming the Finite Element Method*, Wiley Press, 3rd ed., 1998.

VITA

Chang-Yong Lee was born on December 05, 1972, in Daebo, Republic of Korea. He received his Bachelor's degree in Applied Mathematics from Puykyong National University in February, 1997. In the United States, he began to study in the graduate program of School of Aerospace Engineering at Georgia Institute of Technology in January 2000. He received his Master of Science in Aerospace Engineering in May 2002. Continuing his graduate work at Georgia Tech, his research ultimately resulted in this Thesis.